

A Structural and Stratigraphic Interpretation of the Central Denison Trough Using Remotely Sensed Data

Master of Science Thesis for the

Earth Sciences Department, University of Queensland

By Robert J. Cornect

May 15, 1999

Supervised by Dr Rod Holcombe and Dr Chris Fielding

Statement of Sources

I hereby declare that the work presented in this thesis, to the best of my knowledge and belief, is original work, except as acknowledged in the text, and that the material has not been submitted, either in whole or in part, for a degree at this or any other university.

Robert J. Cornect May 15, 1999

ABSTRACT

Geological field mapping can be restricted by access to the mapping area and presence of outcrop. Structural field mapping has the additional problem of the masking of the underlying paleostructure of an area by surficial sediments and modification by recent tectonism of the underlying structural framework. The augmenting of traditional field mapping techniques with remotely sensed data provides additional information in areas of surficial cover or poor accessibility to map the underlying geology of an area. A thorough understanding of the geomorphology within the project area has proven to be important in distinguishing between trends that reflect the subsurface architecture and surficial cover that appears to be unrelated.

The Central Denison Trough while extensively studied still suffers to some extent from the lack of accessible outcrop and borehole data in the mapping of the areas solid geology. The rugged terrain of the Great Dividing Range, which crosses the southern portion of the study area, can hamper access to some localities.

Satellite imagery and other remotely sensed data sets were used in mapping the subsurface geology of the Central Denison Trough. A nonstandard method of normalising the thermal infrared band of the Landsat TM data covering the area was used along with vegetation-outcrop associations to suggest alterations to the existing solid geology map of the study area.

A preferred methodology for acquiring, processing and interpreting satellite data in the Denison Trough area of Queensland is presented. The synergism in using other geophysical data sets such as seismic, gravity and aeromag data in conjunction with the Landsat TM data is also explored.

Table of Contents

ABSTRACT	4
LIST OF FIGURES	8
LIST OF TABLES	8
1.0 INTRODUCTION	9
2.0 PROJECT AIM	11
Figure 2.2	
FIGURE 2.2	
3.0 GEOLOGY OF THE DENISON TROUGH	
3.1 Stratigraphy	19
3.2 Structural Features	24
4.0 PREVIOUS GEOLOGICAL STUDIES	31
5.0 PREVIOUS REMOTE SENSING STUDIES	43
6.0 DATA SETS USED IN PROJECT	43
7.0 DATA PROCESSING	44
DIFFERENCING AND STANDARDISATION	53
8.0 CONSUELO AREA PILOT STUDY	58
8.1: INTRODUCTION	58
8.2 REGIONAL GEOLOGY	58
8.3 CONCEPT	59
8.4 DATA USED IN PROJECT	61
8.5 DATA PROCESSING	62
8.6 INTERPRETATION	66
8.7 RESULTS FROM PILOT STUDY	67
REGIONAL APPLICATION	68
9.1 DIGITAL TERRAIN MODELS	70
9.2 DRAINAGE	71
9.3 CLIMATE	74
9.4 DIGITAL TERRAIN CLASSIFICATION	76
FIGURE 9.4.1 THE DIP IN DEGREES OF DIGITAL TERRAIN MODEL	77

9.5 GEOBOTANY	77
9.6 SPECTRAL AND CONTEXT CLASSIFICATION	86
10.0 REGIONAL STRATIGRAPHIC AND STRUCUTURAL INTERPRETATION	88
10.1 GROUND TRUTHING OF INITIAL INTERPRETATION	89
10.1.2 LINEAMENT ANALYSIS	93
10.3 A GENERALISED REMOTE SENSING METHODOLOGY FOR GEOLOGICAL	
IDENTIFICATION OF THE SURFACE	97
11.0 RESULTS AND CONCLUSIONS	99
BIBLIOGRAPHY	101
REFERENCES	102
GLOSSARY OF TERMS	105
APPENDIX A - ROSE DIAGRAMS AND STEREO PLOTS FROM NUMBERED OUTCR	OP114
APPENDIX B - SELECTED AIRPHOTOS FROM STUDY AREA	115
APPENDIX C - SELECTED STRUCTURAL AND VEGETATION PHOTOS OF STUDY	AREA116
APPENDIX D - WELL LOGS FROM STUDY AREA	117
APPENDIX E - SELECTED SATELLITE IMAGERY OF STUDY AREA	118
APPENDIX F - THE DENISON TROUGH REMOTE SENSING STUDY	110

List of Figures

FIGURE 3.1 AUSTRALIAN GEOLOGICAL PROVINCES, BOWEN-SYDNEY SUPER-BASIN IN YELLOW MODIFIED FROM BMR WEB PAGE IMAGE
Figure 7.6 False Colour Difference Image – AVg Band 10 – B5/7,4,6 as
B,G,R
Figure 8.3.1 Digital Terrain Model of the Central Denison Trough
FIGURE 8.5.1 TRUE COLOR IMAGE SHOWING RECTIFICATION POINTS
FIGURE 8.5.2 SPECTRAL CLASSIFICATION FROM PILOT STUDY
FIGURE 9.2.1 GEOMORPHOLOGY AND DRAINAGE MAP
FIGURE 9.3.1 PALEOGEOGRAPHY IN THE PERMIAN
FIGURE 9.1.1 DIP OF THE DIGITAL TERRAIN MODEL
FIGURE 9.5.1 SPECTRAL SIGNATURES OF VARIOUS OUTCROPPING FORMATIONS
FIGURE 9.5.2 INFRARED PHOTO OF DEVILS SIGNPOST
FIGURE 9.5.3 VISIBLE PHOTO OF DEVILS SIGNPOST
FIGURE 9.5.4 SPECTRAL SIGNATURE FROM PILOT STUDY IN CONSUELO AREA
FIGURE 10.1 FALSE COLOR IMAGE BAND 7,PC2&BAND6 AS BLUE, GREEN & RED
FIGURE 10.1.1 REIDS DOME WITH DIP AND STRIKE ROSE DIAGRAMS
FIGURE 10.1.2 LINE-8 SEISMIC LINE ACROSS REIDS DOME
FIGURE 10.1.3 LINE BMR-2 SEISMIC LINE ACROSS WARRINILLA ANTICLINE
Figure 10.1.4 Standardised Difference Image – B4/7,4,6 as B,G,R -AVg band 10
List of Tables
TABLE 1 PERMIAN ISOPACHS OF WELLS IN STUDY AREA
TABLE 2 GEOREFERENCING FOR SATELLITE IMAGE
TABLE 3 DIP AND STRIKE MEASUREMENTS FROM OUTCROP

1.0 INTRODUCTION

The Denison Trough is located approximately 700 km northwest of Brisbane in east central Queensland (Refer to Figure 1.1). Thearea is prospective for oil and gas with the main hydrocarbon bearing <u>sediments</u> being Permian in age and contained in a series of northwest-southeast and north-south trending inverted half grabens. Much of the Denison Trough is only known from boreholes with some of it's formations such as the Reids Dome Beds not actually outcropping.

Geological field mapping can be limited by access to the mapping area and availability of outcrop. Structural mapping of the underlying paleostructure is severely restricted by surficial cover and post depositional reactivation of the underlying structural framework.

When remote sensing satellites were first launched in the early seventies, geological mapping was high on the list of potential uses for these data. However over optimistic expectations for these data resulted in general disappointment with the initial images and their derived data sets. It was only after improvements in the acquisition, processing and interpretational techniques for these data sets that remote sensing came into prominence. Used today in the fields of environmental, climatic, agricultural and earth science to monitor and exploit natural resources, the field of remote sensing grows from strength to strength.

The gradual improvement in spatial, spectral and temporal resolution of the data sets is one of the key factors in its increased functionality.

The augmenting of traditional field mapping techniques with remotely sensed data sets helps to fill information gaps and peer beneath the surficial cover directly or indirectly to map the underlying geology of an area.

A thorough understanding of a project area's geomorphology has also proven important in distinguishing between purely surficial anomalies and those related to subsurface geology.

The Central Denison Trough has been extensively studied and has some exposed outcrop in the north western inverted graben area. The rugged terrain of the Great Dividing Range, which crosses the southern portion of the study area can however hamper access to some areas. Satellite imagery and other remotely sensed data sets were used to augment the mapping of the solid geology of the area. Vegetation-outcrop associations identified from previous traverses of the area (Woolley, 1943 and others) and on satellite imagery have been used to suggest alterations to the existing solid geology map.



Figure 1. Thesis AOI Location Map

The project area (see figure 1) covers a quarter scene of Landsat TM data from latitude -24.36722 to -25.24167S and longitude 147.74389 to 148.70222E. The UTM grid coordinates are 575449 to 671449 mE, 7208066 to 7304066 mN.

The projection details used for georeferencing are:

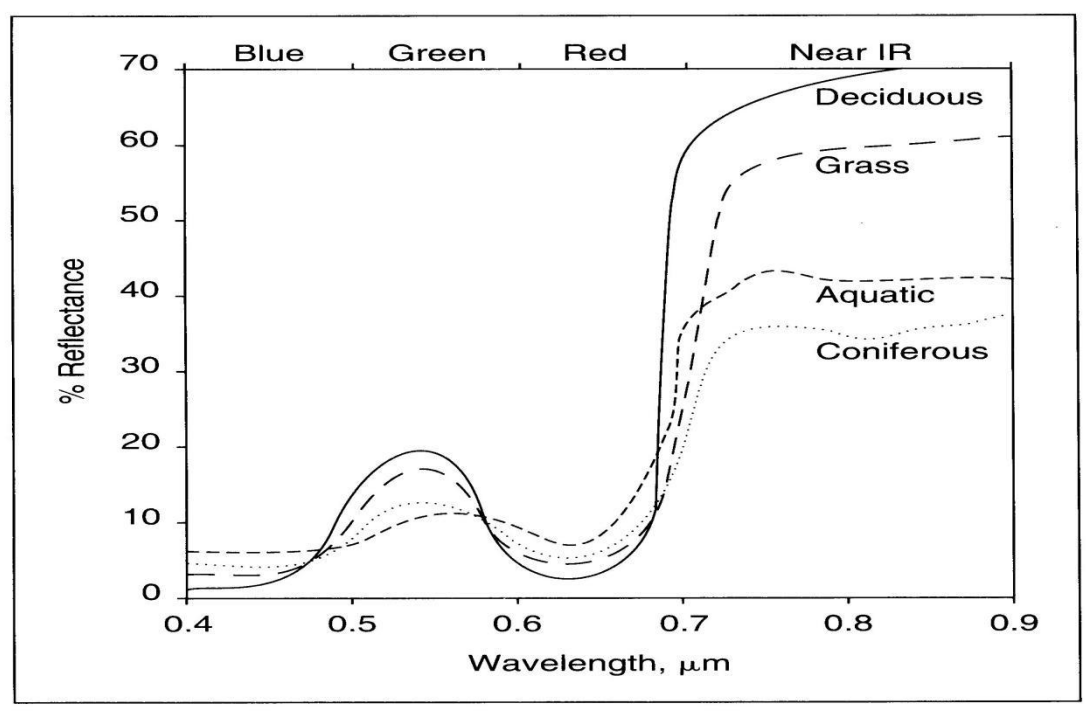
Zone 55, AGD84 Datum, UTM projection with a central meridian of 147deg E.

2.0 PROJECT AIM

With the application of satellite imagery as a primary driving force, the aim of this thesis was as follows:

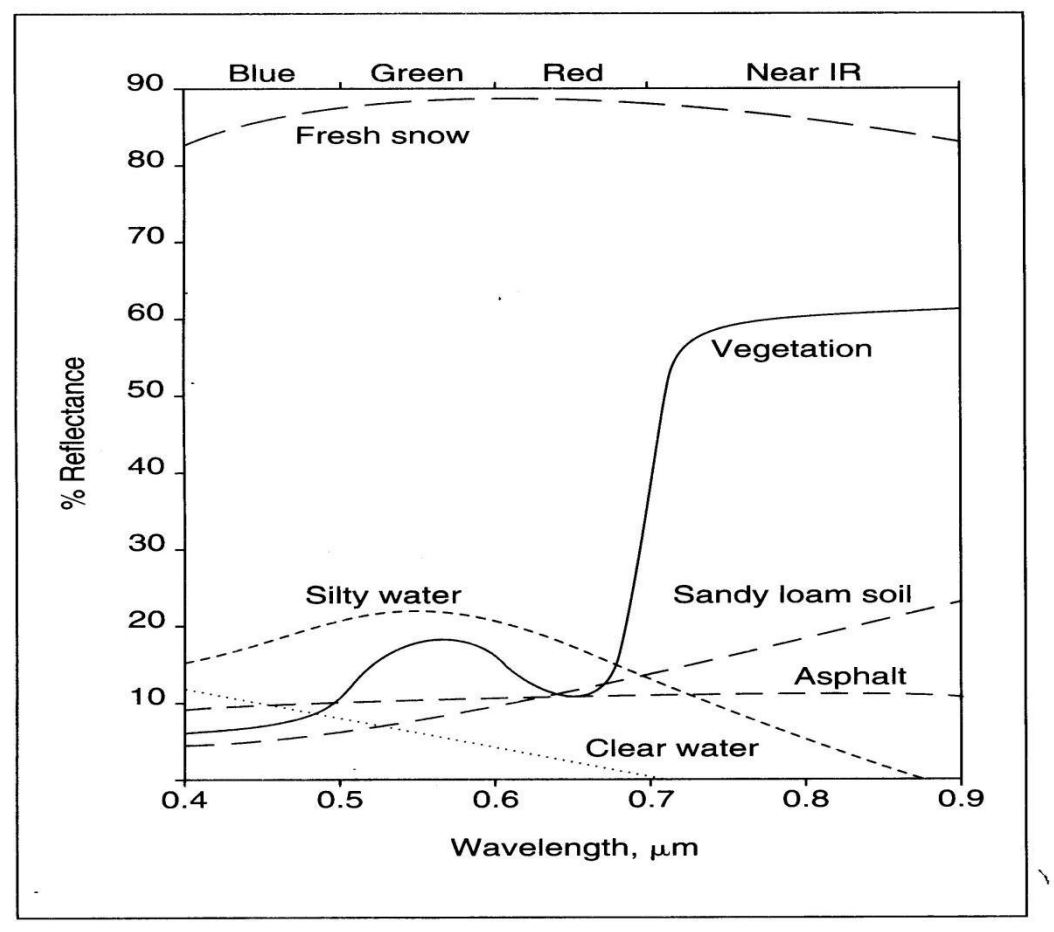
- To assess various methods and techniques of processing remotely sensed data to derive additional geological information such as rock distribution and the surface expression of the underlying structural configuration of the central Denison Trough.
- To combine pertinent results with the available subsurface data to provide an improved interpretation of the stratigraphy and structure of the central Denison Trough.
- To suggest a methodology for geological interpretation using remotely sensed data that may be applied to areas of similar geological setting.

The suitability for Landsat TM data to map variations in vegetation a rock or soil type are illustrated in the following two figures.



Average spectral resonse curves for various vegetation (modified from Avery 1992)

Figure 2.1



Average spectral resonse curves for various materials (modified from Avery 1992)

Figure 2.2

The Landsat TM data used in the study cover the range from blue through to thermal infrared in select bands or intervals. The first four bands correspond approximately to each of blue, green, red and infrared illustrated in figures 2.1 and 2.2. It can be seen from the generalized spectral profiles for various materials illustrated above, that differences or ratios between these spectral bands can be exploited to suggest the presence of one material over another. The percentage reflectance in the above profiles is indicative of the amount of incident sunlight—which is reflected from the various materials with the remainder being absorbed by the surface cover.

This study aims to broaden the application of standard mapping techniques for satellite data by including additional data sets such as digital elevation and seismic two way time in the processing routines. in It is felt that a degree of synergism in the understanding of the area resulted from this combined approach over previous studies which tended to use predominantly one or two types of data with only minor

input from other data. Oil company studies prior to drilling exploration wells such as the Dunellen –1 Well Proposal (Cornect and Stanmore, 1993) fall into this category. While fit for purpose, they can tend to rely to heavily on seismic and well data with only minor inputs from other data sets or sources.

3.0 GEOLOGY OF THE DENISON TROUGH

The Denison Trough forms part of the Bowen Basin, which joins, in the subsurface, to the Gunnedah and Sydney Basins to the south. Together they form a geological province stretching the length of the Australia from north to south (Figure 3.1). The proposed mechanisms for the origin of this super basin are varied but can be grouped into three main processes, thermal, thinning and load related (Murray, 1990). While a load related retro-arc extensional to foreland basin is currently a widely prefered model (Murray, 1985, & Baker et al, 1993), non-mutually exclusive elements of some of the other models have been incorporated into this study. In particular, elements observed in the thinning mechanism modeled on back-arc spreading (Paten, 1979, Ziolkowski & Taylor, 1985 and Hammond, 1987) have been observed in the central Denison Trough.

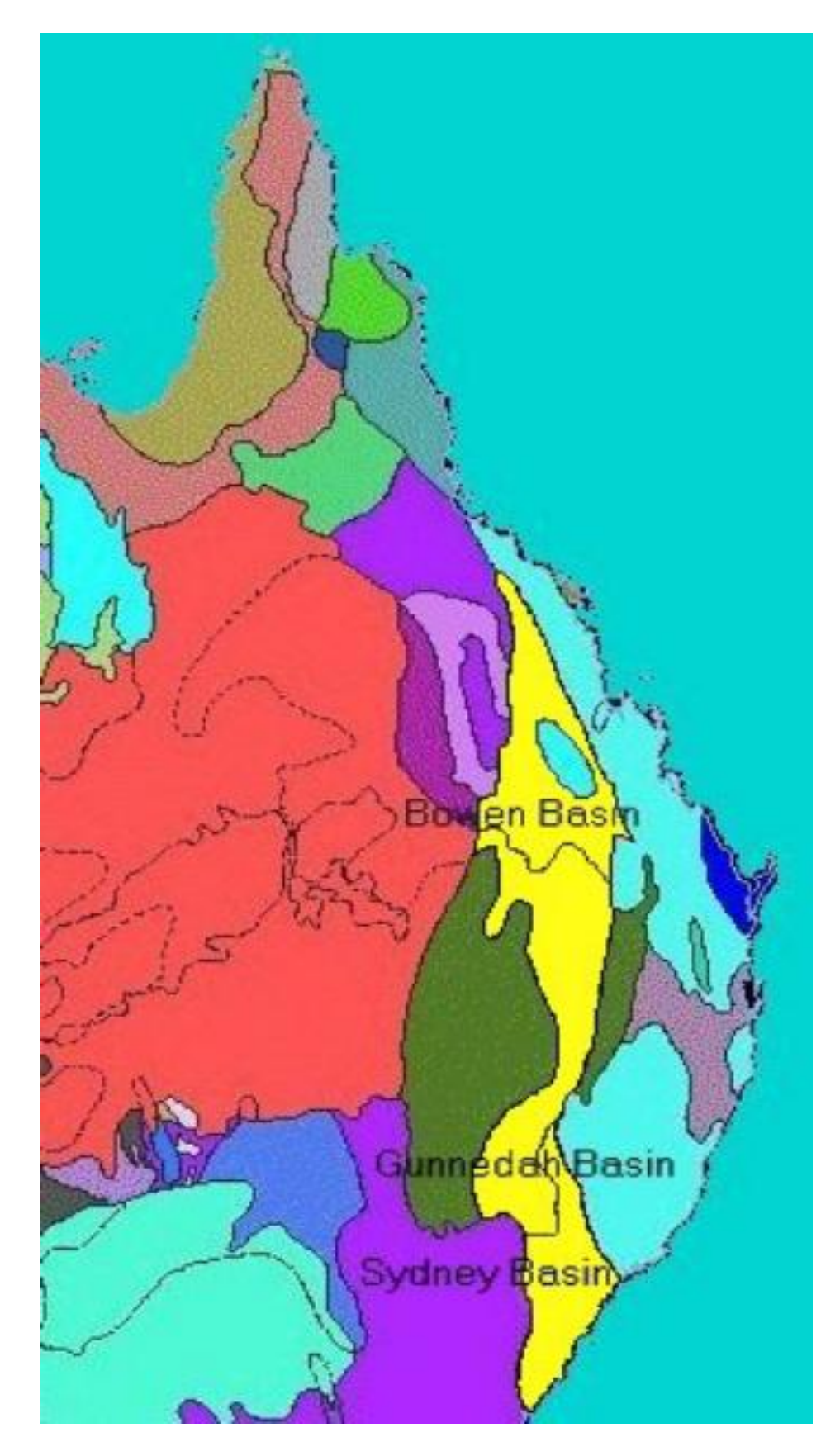


Figure 3.1 Australian Geological Provinces, Bowen-Sydney super-Basin in Yellow Modified from BMR web page image

The Retro-arc foreland basin relies on subsidence due to loading of a volcanic arc which paralleled the present day east coast of Australia (Baker & Fielding 1993).

The Back-arc model proposed by Paten, (1979) and Ziolkowski & Taylor (1985) has the Denison Trough area of the Bowen Basin formed by west dipping half grabens composed of rotated fault blocks along steep east dipping faults.

The extensional model of Hammond (1987) had extension of shallow east dipping major mid-crustal detachment faults with associated northeast trending transfer faults. These zones, termed 'transfer corridors' by Hammond (Refer to Figure 3.3), are observed as lineaments which trend northeast southwest from the Denison Trough to the present-day east coast of Australia (Hammond, 1990).

These same lineaments were observed on satellite imagery and then confirmed independently by ground truthing in this study prior to reading about Hammond's model.

The geology and structural setting of the Central Denison Trough consists of a series of NW-SE trending Permian half grabens (Refer to Figure 3.4). The half grabens are enechelon in geometry. Oblique restructuring of the area during later tectonic phases (Draper, 1985) inverted the Permian half grabens, reversing the graben bounding faults (Ziolkowski & Taylor, 1985). A possible right lateral strike slip component to the structural framework was imparted (Ziolkowski & Taylor, 1985), possibly with associated transfer zones between previously connected half grabens. The principle extensional directions are thought to be east-west and northeast-southwest (Ziolkowski & Taylor, 1985).

Elliot, 1993, based primarily on the extensive seismic coverage in the area, quotes a north-south trend for the main extentional direction with a possible 120 degree trend for the interpreted transfer faults. Five major tectonic episodes are interpreted with the predominant style being compressional. The 120 degree trend of the transfer faults are about ninety degrees to that of Hammonds trans-Queensland transfer corridors. While Elliot seemingly dismisses Hammonds results, the two directions could still co-exist as

primary and secondary strike slips directions present in a wrench fault diagram (Refer to Figure 3.2). This would be consistent with the later compressional tectonic events being oblique to the existing half graben framework (Elliot, 1993)

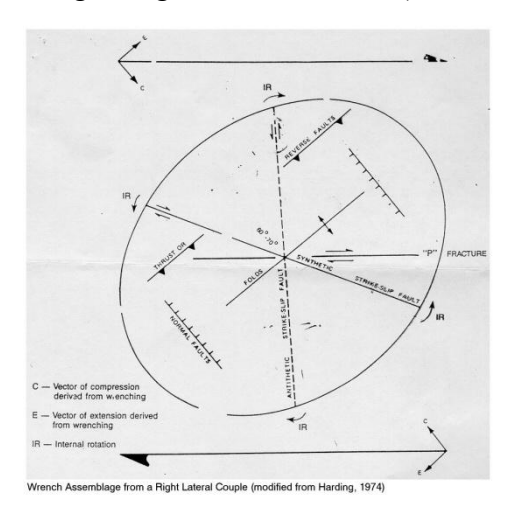


Figure 3.2 Wrench Diagram

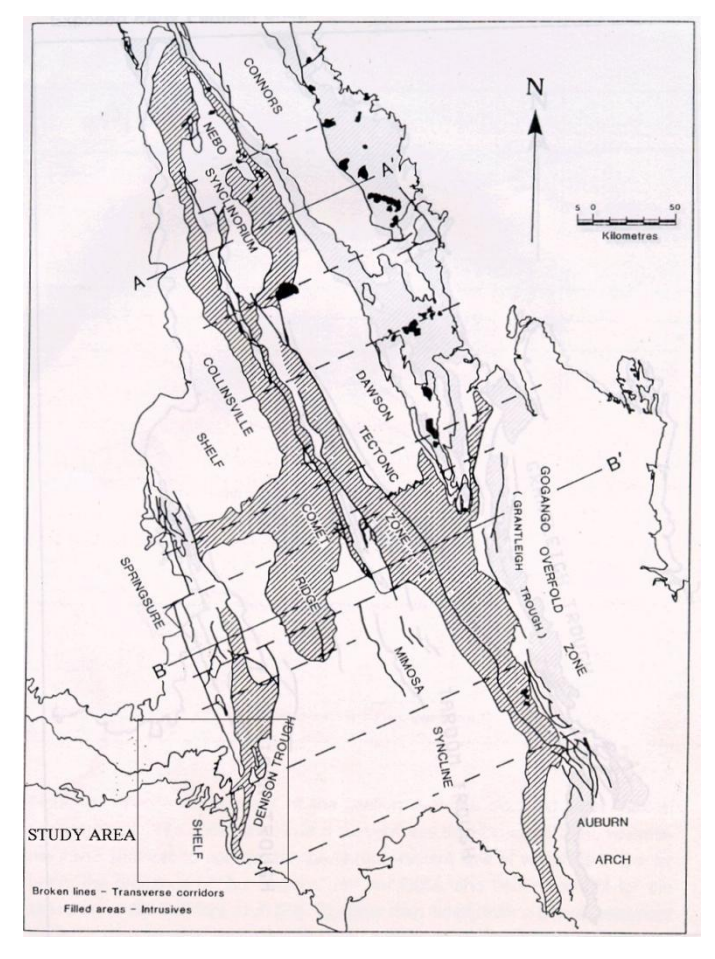


Figure 3.3 Transfer Corridors from Hammond, 1990

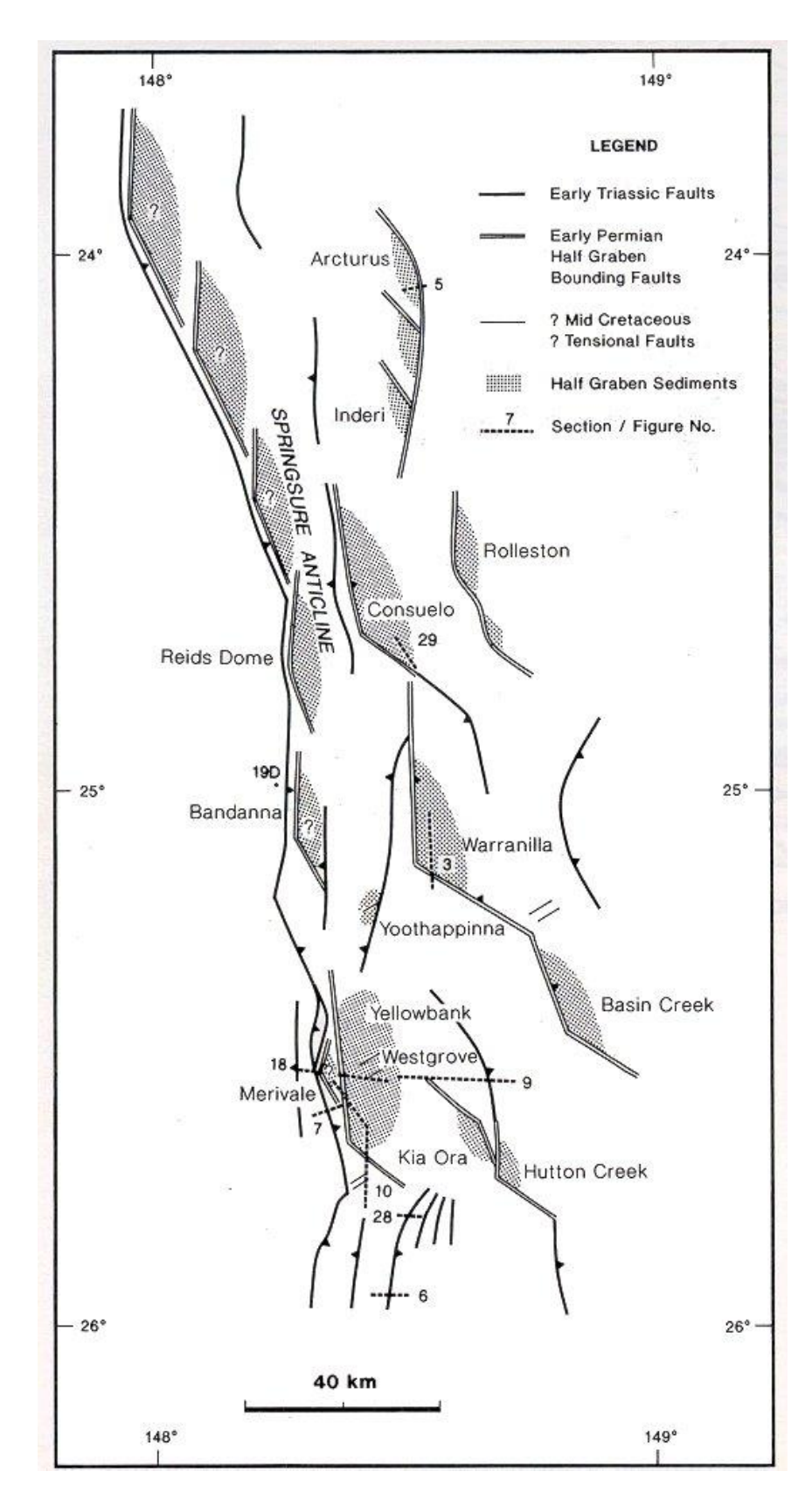


Figure 3.4 Structural Elements of the Central Denison Trough (from Elliot, 1993)

The main compressional direction is thought to come from the northeast (Ziolkowski & Taylor, 1985) and may extend across Queensland along so called transverse

corridors (Hammond, 1990). These deformation zones are interpreted to be due to deep-seated transfer faults in the basement between half grabens and other tectonic features within the Bowen Basin (Refer to Figure 3.3)).

3.1 Stratigraphy

The Permian <u>sediments</u> are unconformably underlain by Devonian-Carboniferous aged sediments of the Drummond Basin and Timbury Hill metasediments (Refer to Figure 3.1.1). The grain of these basement rocks is north-south and when extended, formed north-south trending grabens which were filled with sediment in the Permian (Ziolkowski & Taylor, 1985).

STRUCTURAL WESTERN **EASTERN FORMATION** DENISON AGE SURAT SURAT CRETACEOUS L INJUNE CREEK JURASSIC M EVERGREEN TROUBLE E L EDDYSTONE MOOLAYEMBER TRIASSIC M SHOWGROUNDS / CLEMATIS E REWAN BANDANNA L ALDEBARAN PERMIAN E REIDS DOME CARBONIFEROUS Coal Measures Non Reservoir Erosion / Non Deposition Volcanics Sands Gas

STRATIGRAPHY

Figure 3.1.1 - Stratigraphy of the Denison Trough from Stanmore, 1993

The continental derived sediments of the Reids Dome Beds, first filled the accommodation space provided by the half grabens.

Following a marine transgression, the Cattle Creek beds were laid down, smoothing out the existing topography differentially filling the existing paleo-lows.

An increase in sediment supply saw the shoreline retreat westward with the deposition of the Aldebaran Sandstone deltaic system eastward into the paleo-Pacific (Fielding et al, 1990). The sediment built out towards the then submerging volcanic arc, which extended along the present day eastern coast of Australia.

A further series of regressive pulses of sediment prograded out from the north west and from the north. This was followed by minor transgressions continuing while the Freitag Sandstone, Ingelara Shale, Catherine Sandstone, Peawaddy and Mantuan Formations were deposited.

A major marine transgression flooded the area depositing the Black Alley Shale.

Permian deposition ended with a regression which resulted in the deposition of the coal bearing Bandanna Formation.

While the individual Permian sequences varied in thickness over the study area, the total Mantuan to Aldebaran interval remained relatively constant (Refer to Table 3.1.1). This implies a relative consistency of sediment supply versus accommodation space over this interval.

Triassic, Jurassic and Cretaceous sediments conformably overly the Permian with the exception of the central areas of the inverted half grabens where unconformities can be seen to have removed significant amounts of sediment (Ziolowkowski & Taylor, 1985). The resulting angular unconformity is easily mapped by isochronal thinning on seismic data over these present day subsurface anticlines and in the truncation of the underlying section against the unconformities.

Table 1

A thin veneer of Tertiary Basalt and Quaternary Alluvium overly the Mesozoic section. The relative erosion resistance of the Tertiary Basalt, Triassic and Jurassic Sandstone's has allowed them to form the present day topographic ridges and high ground in the study area. An abundance of Tertiary aged diorite sills and dykes are present in the Reids Dome/Carnarvon Gorge area (Wolley, 1943). They predominantly trend ESE and are near vertical. This probably resulted from the same period of vulcanicity that layed down the Consuelo Tableland surrounding Carnarvon Gorge, possibly in the mid-Pliocene. Of notable exception however is the northeast trending dyke north of Bandanna and possibly at the foot of Black Alley Peak (Wolley, 1943). Rewan Hill consists of a dolerite plug and associated dykes.It is interpreted to be one of the volcanic eruption points in the area (Wolley, 1943).

The Denison Trough is bound to the west by the north-south trending Springsure Shelf. The Springsure Shelf is located immediately west of the Springsure and Sericold anticlines. (Refer to Figure 3.2). The Denison Trough is bound to the east by the NW-SE trending Comet Ridge located just off the eastern edge of the above image. The Permian sediments thin on to both of these stable Devonian Platforms.

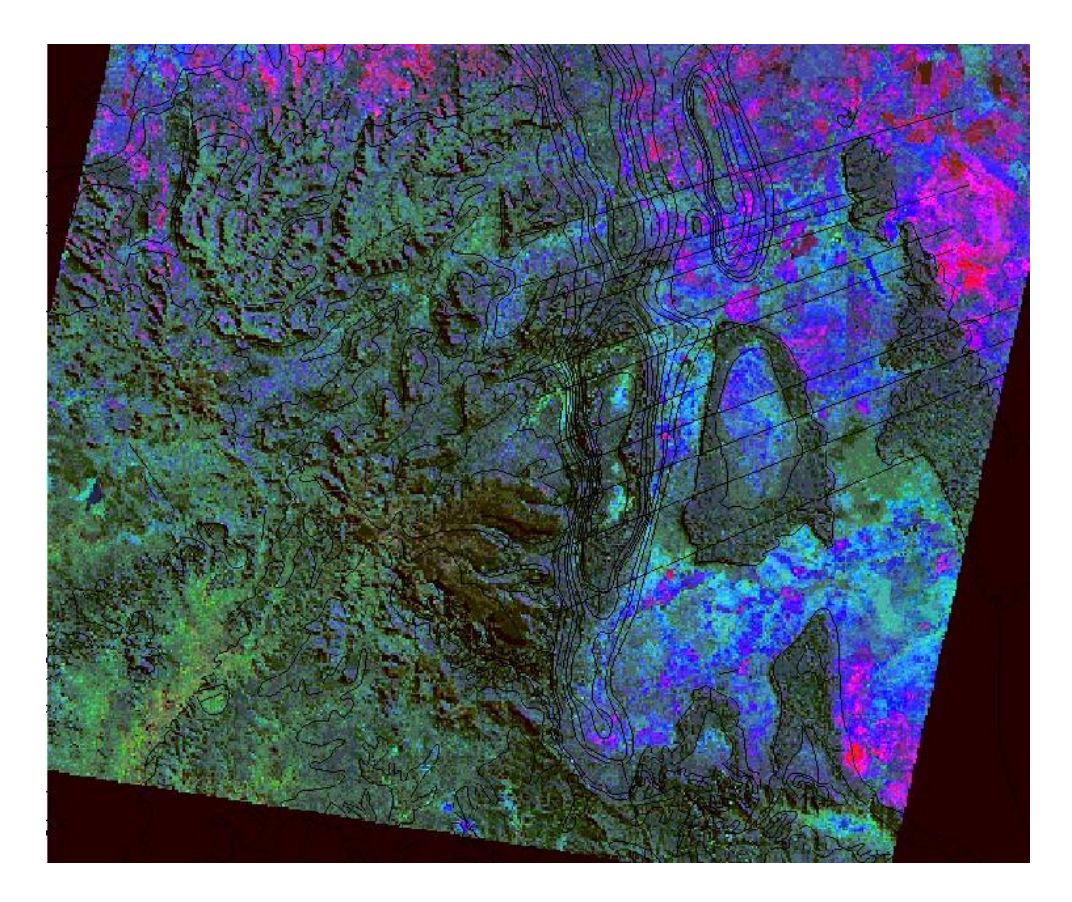


Figure 3.1.2 - Landsat TM Bands 5,7 and 6 as Blue, Green and Red with Interpreted Lineations. Vegetation shows up as green, clay based soils as blue and thermally hot areas as Red

The Denison Trough is the westernmost depocentre of the Bowen Basin. The Bowen Basin formed as a back arc extensional to foreland basin, landward of a volcanic arc on the eastern margin of the Australian plate. Back arc crustal extension occurred during the Early Permian followed by thermal subsidence and several contractional stages from the Late Permian to Tertiary. It is thought that the thermal subsidence and contractions resulted in the inversion and possible wrenching of the Permian half grabens of the Denison Trough.

Figure 3.1.2 is a false colour plot of Landsat TM data with bands 5,7,6 as Blue, Green and Red light. The Solid Geology is overlain as black vectors. The boundaries of most formations are clearly discernible. Several ENE-WSW trending lineaments have been interpreted across the study area based on corresponding offsets and associated creek development of three parallel trending structural features, the Serocold/Springsure Anticline, the Consuello/Rewan Syncline and the Nuga Nuga Syncline.

The lineaments when plotted on a <u>rose</u> diagram cluster around a 70-degree orientation. The principle half-graben extensional direction is approximately at 0 degrees.

A possible explanation for the lineaments is that they formed along pre-existing zones of weakness resulting from reactivation of transfer zones between the underlying enechelon half grabens (Hammond 1990). The interpreted transfer zones or transfer corridors are evident on air photos using creek orientations as delineation features. Examples of transfer zones can be found along Christmas Creek, Consuelo, Cattle and Mitchells/Rocky Creek. Christmas Creek cuts through the Rewan Syncline and the Nuga Nuga Syncline, while the Mitchells/Rocky, Consuelo and Cattle Creek cut through Reids Dome.

Several of the proposed lineaments were ground truth for evidence of lateral movement such as slickensides. These results are dicussed in detail in section 10.1 and 10.2.

Other evidence is seen in the <u>seismic</u> lines <u>crossing</u> these <u>zones</u> within Reids Dome which shows high angle normal faulting in the subsurface extending up to the surface. The gradient contours of the aeromagnetic map also exhibit offsets and anomalously high values oriented along the inferred zones of weakness.

3.2 Structural Features

Reids Dome

Reid's Dome is a late <u>breached</u> inverted Permian aged half graben (Refer to Figure 3.2.1). The development of cracks and keystone faulting in the crest of the arched strata after inversion, allowed the development of obsequent then subsequent streams to erode out the core of the anticline. This resulted in the present day topographic reversal with the previous anticlinal crest forming a valley in between the preserved limbs. Possible later compressional deformations caused a series of enechelon movements cutting trough the dome, which allowed <u>subsequent</u> creeks to cut through the feature along these zones of weakness.



Figure 3.2.1 - Airphoto of northern end of Reids Dome showing possible Transfer corridor /Shear zone

Rewan Syncline

The triangular shaped Rewan Syncline is bounded by the preserved limbs of the relatively resistant Clematis Sandstone (Refer to Figure 3.2.2). The floor of the bowl shaped feature is comprised of Triassic aged Rewan Formation continental red beds.



Figure 3.2.2 – Airphoto of Rewan Syncline

Nuga Nuga Syncline

The Triassic aged Nuga Nuga Syncline trends north south on the eastern edge of the study area (Refer to Figure 3.2.3). It outcrops against Clematis Sandstone and is dissected by Christmas Creek in the middle and is bound to the south by the small Nuga Nuga Lake. The feature is a positive topographic high rising several hundred meters above the flat surrounding plains.

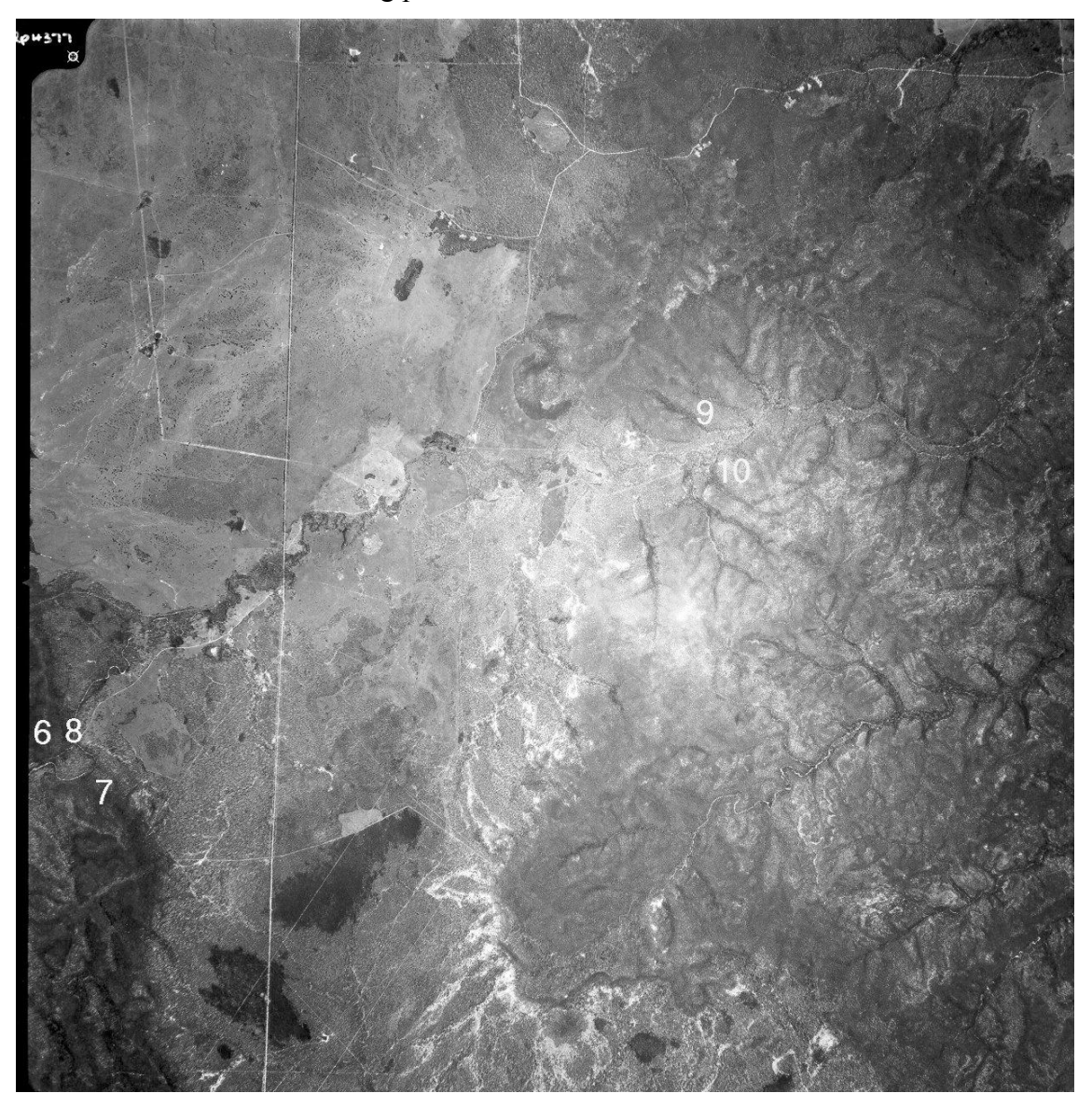


Figure 3.2.3 – Airphoto of Nuga Nuga Syncline with Numbered Outcrops from Ground Truthing Field Trip

Mt Inglis

Mt Inglis is a Permian aged domal anticline located at the intersection of the NNW-SSE trending Sprinsure Anticline and north-south oriented Serocold Anticline containing Reids Dome (Refer to Figure 3.2.4). The core of the dome is comprised of outcropping Aldebaran Formation and is flanked by preserved limbs of the Catherine Sandstone and Mantuan Formation.

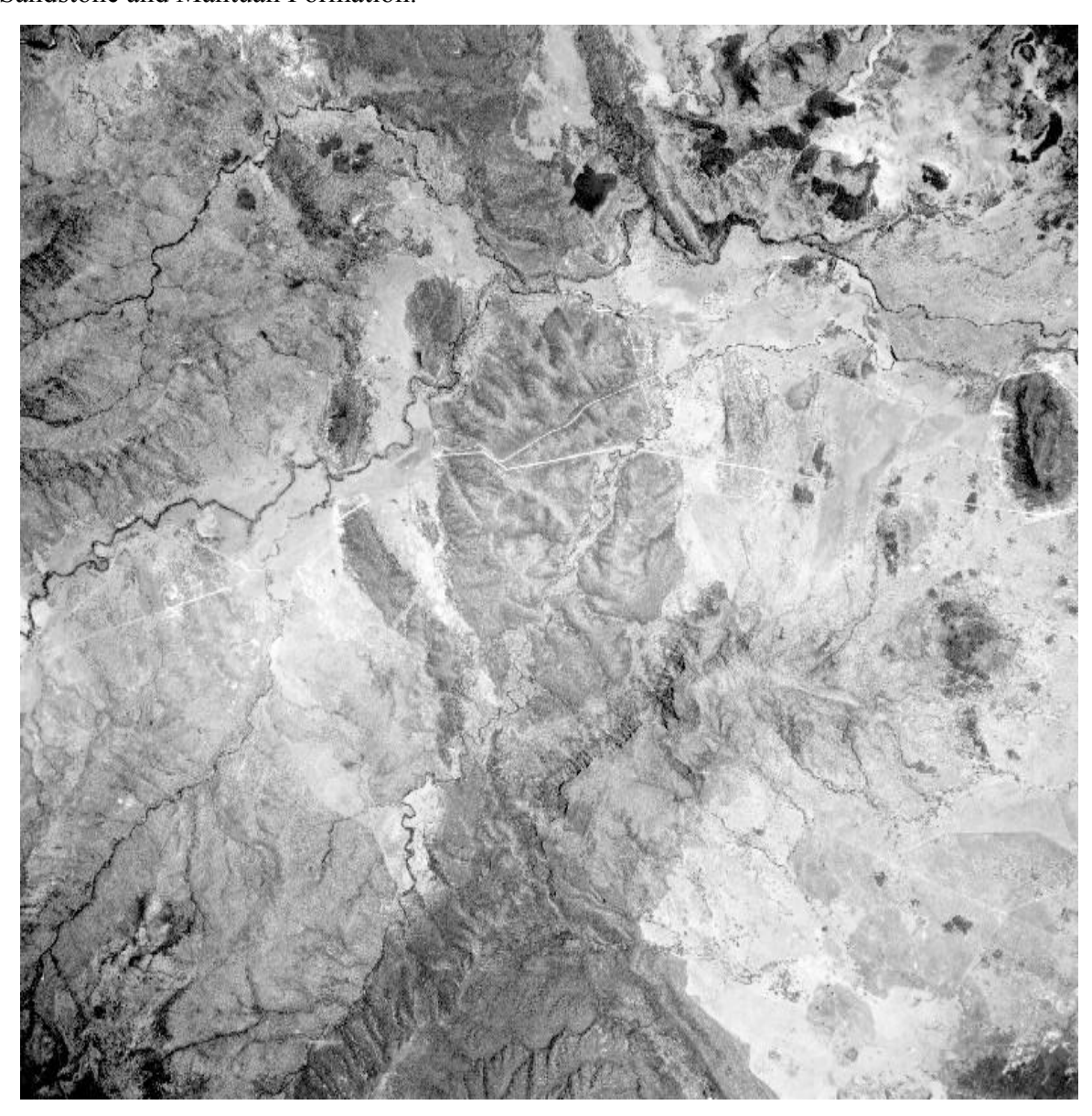


Figure 3.2.4 – Airphoto of Mt Inglis Dome

The geology of the Mt Inglis Dome is covered in detail by McLoughlin, 1988. It is also an undrilled potential Permian aged gas field sitting on trend with the sub-economic Reids Dome gas field.

Consuelo Anticline

The NNW-SSE trending Consuelo Anticline is comprised of an outcropping Aldebaran Formation core and alternating Permian aged sandstone and siltstone formations on the flanks (Figure 3.2.5). It is bounded by the Consuello Creek to the south, the Meteor Creek to the north and is bisected by Sandy Creek and Peawaddy Creek in the middle. Several hydrocarbon exploration wells were drilled on the structure with out any signs of encouragement. This was probably due to breaching of the reservoir sands by unconformities and late stage—faulting

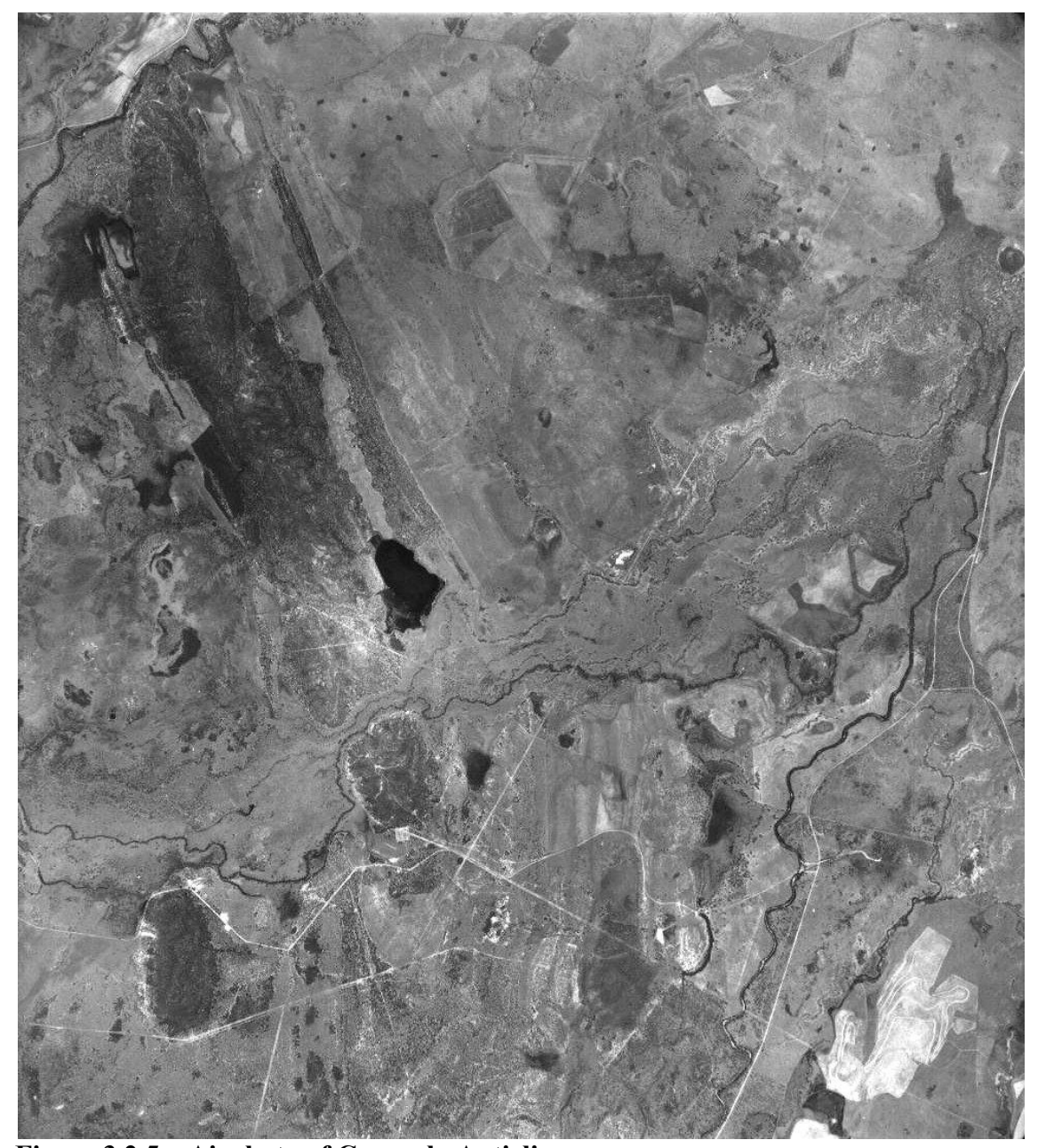


Figure 3.2.5 – Airphoto of Consuelo Anticline

Consuelo TableLand

The flat-topped Consuello Tableland is located on the western side of the study area within the Great Dividing Range and is comprised of horizontal layered Tertiary aged basalts. The feature has distinctive vegetation to that of the surrounding landscape and is easily recogonised on airphotos and satellite imagery (Refer to Figure 3.9). The horizontal layering is most likely due to a volcanic lava flows which spilled out on to the surrounding plainsof the Tertiary, possibly preferentially filling topographic lows with additional thickness of the what was to become erosion resistant basalt.



3D View of Carnarvon Corge and Consuelo Tableland from the South East Landsat TM Bands 1,2&3 as B,G&R Draped over Digital Terrain Model

Figure 3.2.6

Carnarvon Gorge

The Carnarvon Gorge cuts it way into the Consuello Tableland forming a series of a dendritic creek systems that feed into the Carnarvon Creek. The gorge has eroded through several hundred metres of Jurassic and Triassic aged sandstone formations. The erosion has resulted in the formation of spectacular terraced cliffs from the Moolayember Member canyon floor to the Tertiary aged basalt tableland. The Carnarvon Gorge and the basalt tableland are easily spotted on satellite imagery due to its relative flatness, the dark tonal character of it's ground cover and the sinuous shape of the gorge (Refer to Figure 3.2.6 and 3.2.7).



Looking East Down Carnarvon Gorge from Battleship Spur

Figure 3.2.7 - Carnarvon Gorge

4.0 PREVIOUS GEOLOGICAL STUDIES

The Denison Trough has been studied extensively over the years from 1926 on horseback by Jensen through to the present day where studies are carried out from four wheel drives utilising the latest of electronic gear both on and above the ground. One of the early pioneer geologists of the area was Reid (1930's) whose name lends itself to the Reids Dome Formation and Anticline.

Publications and thesis of the area include Woolley (1943), Crespin (1945), Campbell (1953), Mollan et al. (1964), Power (1966), Jensen (1968), Evans (1969), Dickens & Malone (1973), Price (1976), Rigby & Hekel (1977), de Jersey (1979), Paten et al. (1979), Jackson et al. (1980), Palmeri (1983, Wilkinson (1982), Wood (1984), Ziolkowski and Taylor (1985). More recently, McLoughlin (1988), Fielding et al (1990), Baker (1991), Kassan and Fielding (1991), Elliott (1993), Stanmore (1993) and many others.

Wooley's 1943 geological report on the Carnarvon Gorge area for Shell Qld Development Pty Ltd while general in nature was a comprehensive survey covering most aspects of the geology, geomorphology and even touching on the geobotany of the area. Wooley was one of the first geologist to document the geobotanical association between certain trees and selected outcrops in the area. While his geological surveys' primary aim appears to have been an economic reconnaissance, the bulk of his concepts and conclusions remain largely unchanged today and his ideas can be seen echoed in many of the more recent studies (Elliot, 1973).

Elliot in 1973 reviewed the Permian stratigraphy and geobotanical associations of the Springsure Area including most of the current study area.

Ziolkowski and Taylor in 1985 while working for CSR Petroleum which operated the hydrocarbon exploration in the area, produced a landmark structural paper describing the wrench tectonism active in the area. Their paper relied heavily on seismic data combined with geological mapping and is extensively quoted as a structural reference for the Denison Trough and Bowen Basin.

The structural history and Permian stratigraphy of the Mt Inglis Dome was covered in detail by McLoughlin, 1988. The geology of the Mt Inglis Dome and it's context to the surrounding area is described.

Fielding et al in 1990 reviewed in detail the depositional history and paleogeography of the Permian and Triassic sediments of the eastern Australia. The data is presented as a series of paleogeographic maps encomposing the Bowen Basin and eastern Australia. The maps have been used extensively and modified in places by further studies in the area. Fielding in this paper and with Baker in 1993 promotes the formation of the Bowen Basin as part of a Complex Back-Arc Extensional to Foreland Basin system which is perhaps the most widely accepted of the models for the areas tectonic origin.

Elliot in 1993, reviewed the tectonic history of eastern Australia reviewing the nature of the tectonic episodes and stressing the similar structural histories of the Bowen, Gunnedah and Sydney basins. Elliot promotes the super basin concept linking the three basins at their inception at the start of the Permian and comments on the relative significance of each event stressing the importance of the mid-Triassic compressive episode.

Stanmore and Cornect (1993) attempted to predict the depositional environment of a seismic anomaly, the <u>Dunellen Mound</u>, based on shingled progrades interpreted as a paleoslope.

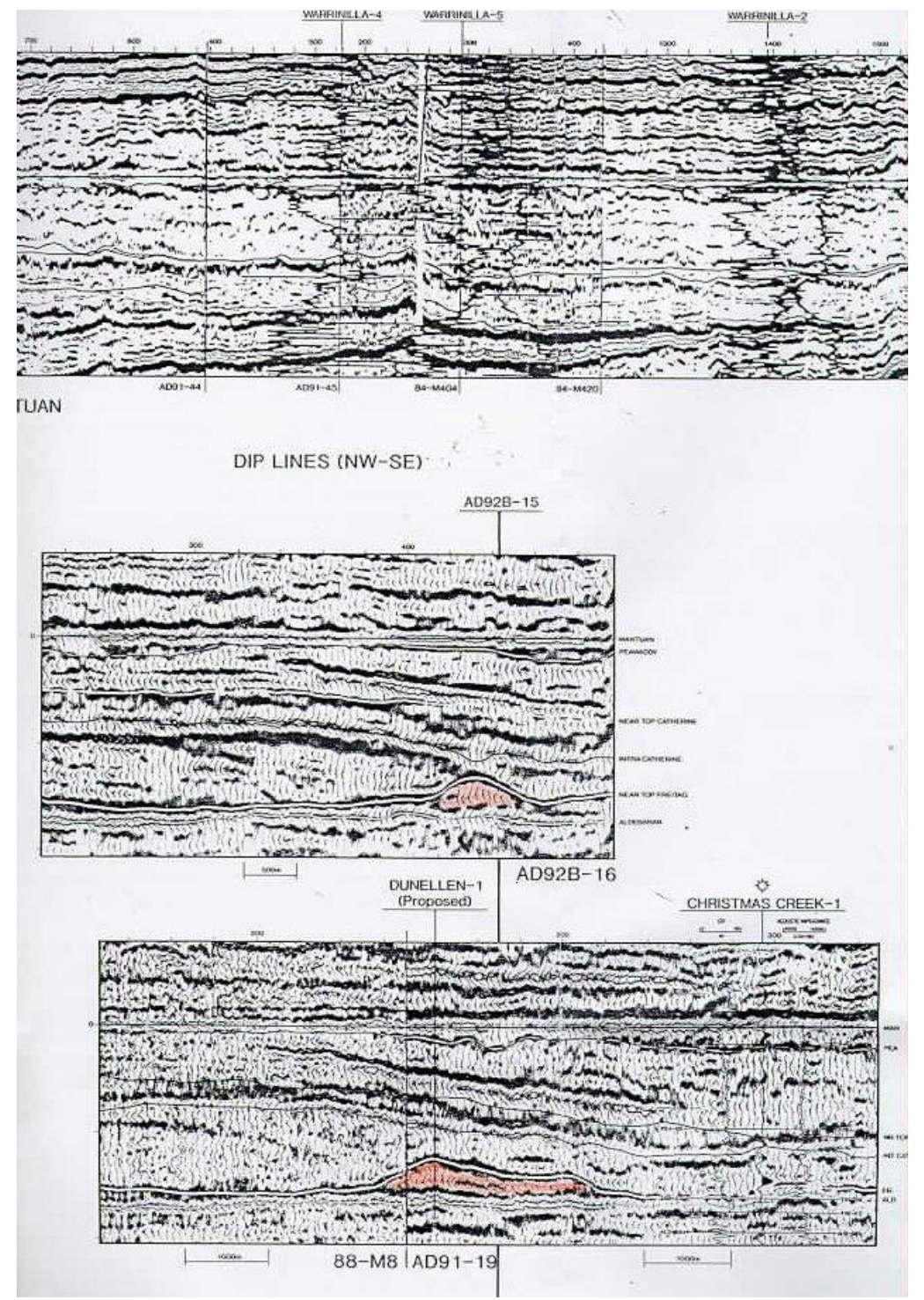


FIGURE 4.1 DATUMED SEISMIC ACROSS DUNELLEN MOUND

The well resulted in the drilling of a low velocity claystone encased in higher velocity siltstone (Dunellen-1). While the anticipated sandstone lithology for the mound was not encountered, the result did not necessarily negate the interpreted depositional setting for the mound, but might merely have shown the siltstone prone nature of the sediment supply in the area.

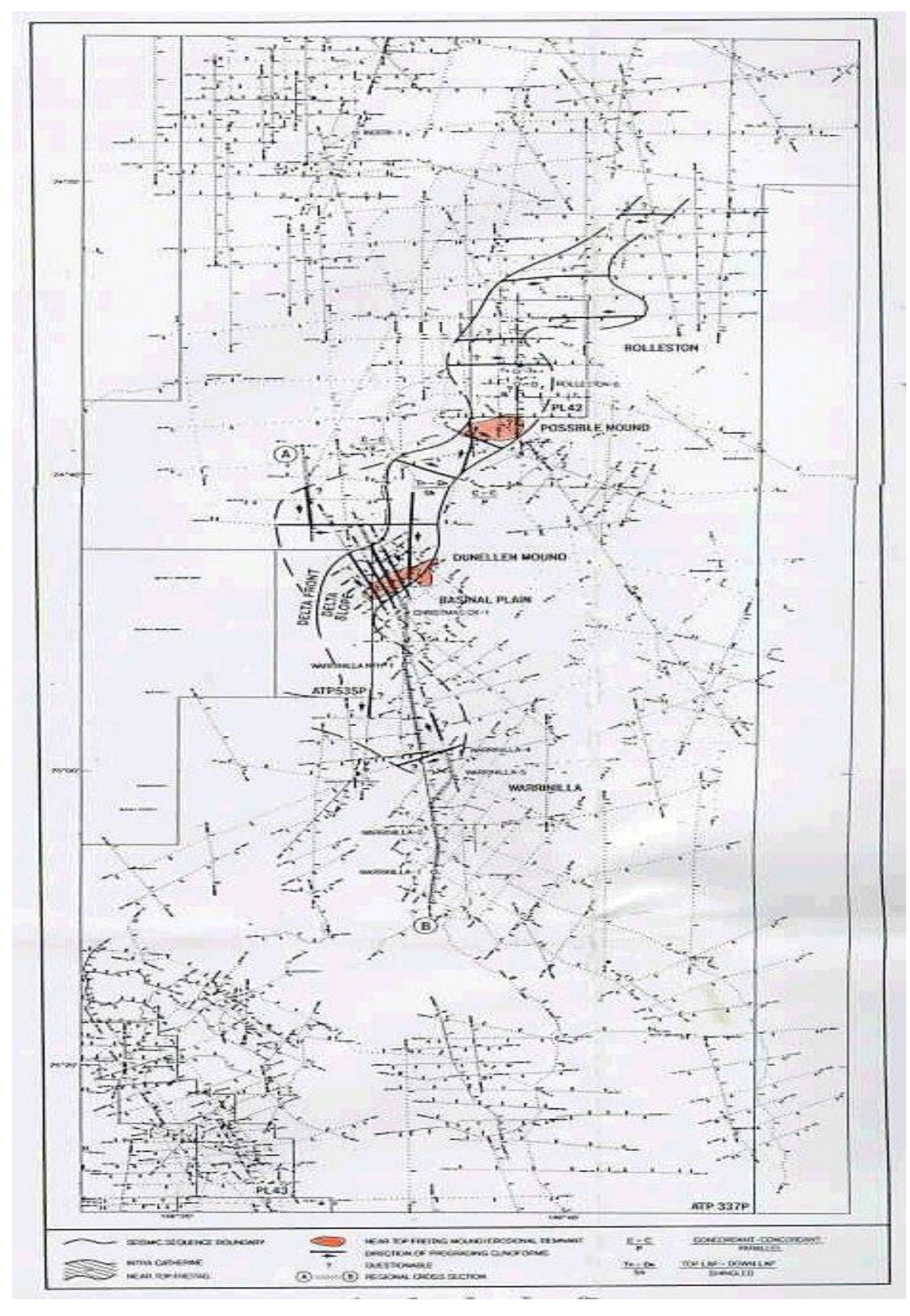


FIGURE 4.2 SEISMIC STRATIGRAPHY MAP FOR CATHERINE SANDSTONE/INGELARA SHALE (R CORNECT, 1993 FOR SANTOS LTD)

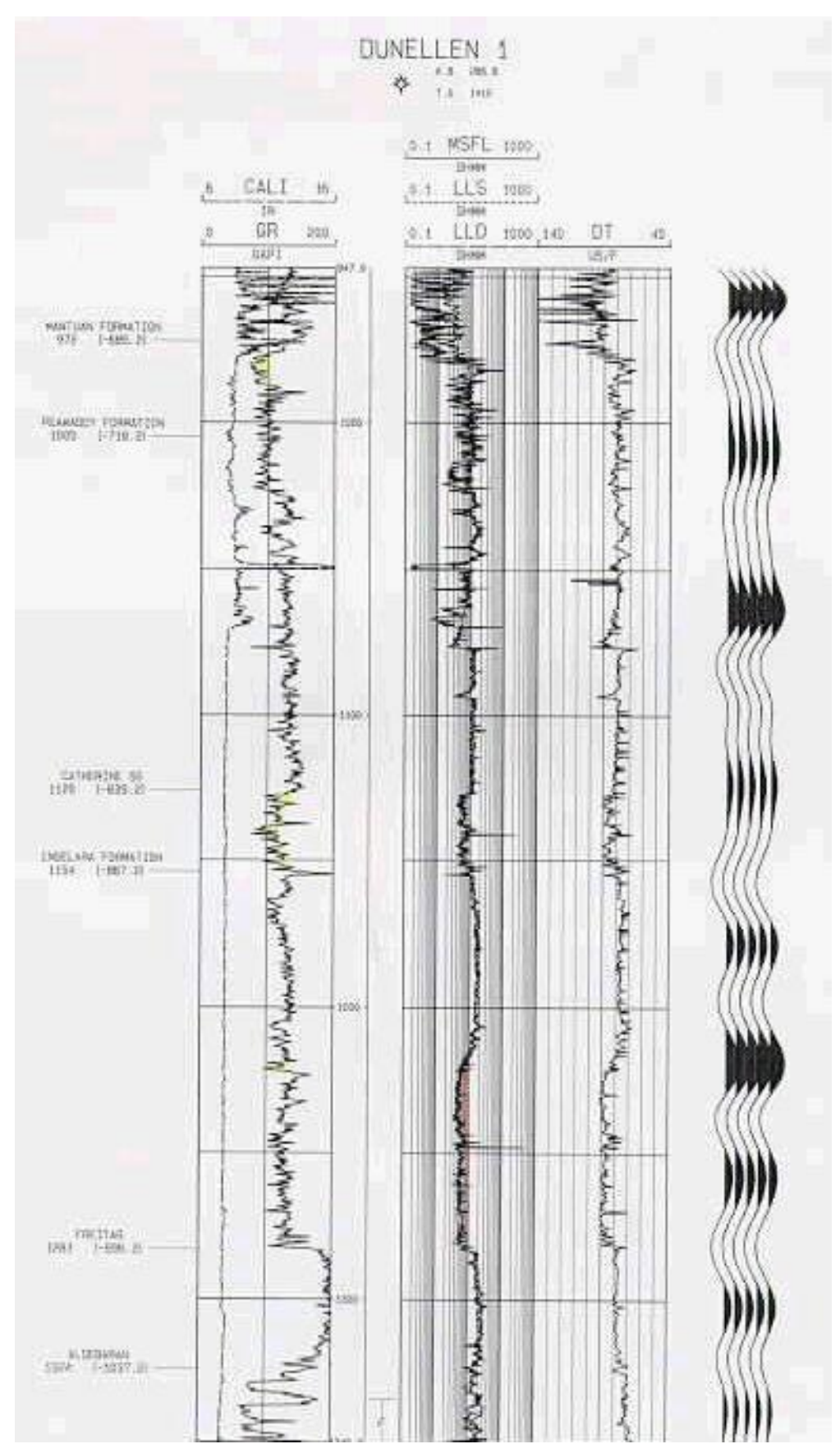
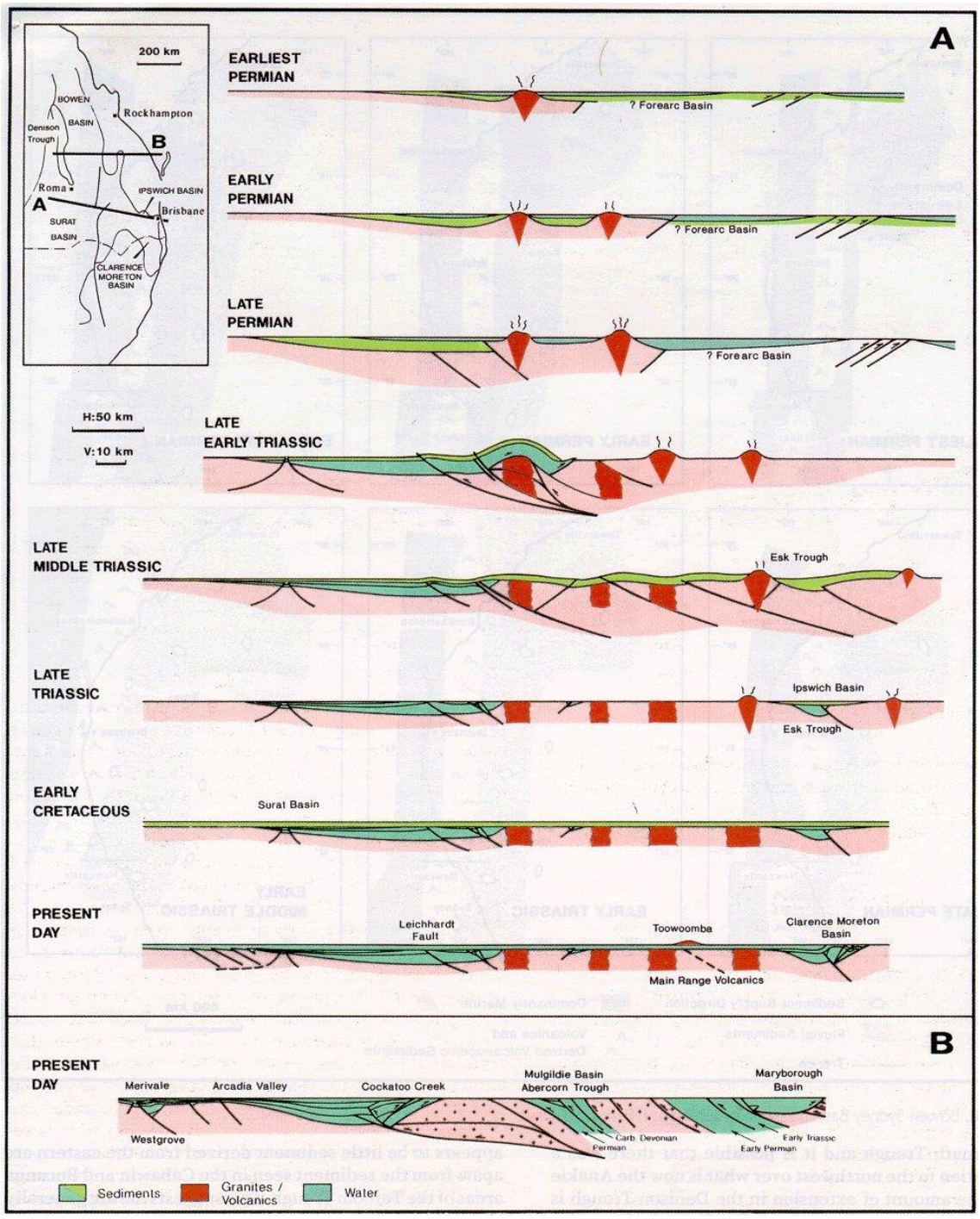


FIGURE 4.3 DUNELLEN-1 WELL LOGS AND SYNTHETIC TRACE

The Seismic Stratigraphic approach might therefore still be useful in decreasing the reservoir risk of other undrilled features along this trend such as within the <u>Rolleston</u> Gas Field to the north of Dunellen-1.In the Rolleston Gas Field, hydrocarbon bearing



sandstone has been encountered within the same formation as the mound.

Figure 4.4 Proposed tectonic history of eastern Australia by Elliot, 1993 based regional BMR seismic lines

Geological study of The Central Denison Trough is actively being carried out today by Fielding et al through the University of Queensland, and geologists at Santos Ltd and the Oil company of Australia who operate the hydrocarbon exploration in the area.

5.0 PREVIOUS REMOTE SENSING STUDIES

Previous Remote Sensing Studies of the central Denison Trough have mainly involved airphoto geological interpretations (l'Ons, 1984) or paper based regional scale lineament interpretation on transparent overlay. Apart from regional studies by government agencies (Hammond, CSIRO 1988), which may have included the Denison Trough, or studies of a more cursory nature, this study is thought to be the first detailed digital based remote sensing study of the central Denison Trough.

6.0 DATA SETS USED IN PROJECT

The bulk of the effort has concentrated on obtaining, processing and interpreting satellite data. The 30m by 30m pixel size of the Landsat imagery was deemed good enough to delineate the outcropping formations which because of the low dips in the Consuelo area covered 100 plus metres in a horizontal dip direction. This relates to at least four pixels width which is more than enough to see on an image providing there is a difference in reflective properties with it's neighbouring areas.

The geophysical data included in the project were:

Seismic Time Structure Map of the Mantuan and Aldebaran Horizons, Digitised and gridded Total Magnetic Field Aeromagnetic Map and Bouger Gravity Maps covering the study area.

The Mantuan Seismic Horizon, which corresponds to the top of the Mantuan Formation, was initially selected because of its significance as a Permian reservoir rock and its continuity over the study area. The amount of absent Mantuan coverage

due to erosion however resulted in the deeper more preserved Aldebaran Formation being selected.

The Department of Mines and Energy (Queensland), gravity and aeromagnetic maps were included to focus on the underlying basement structure of the region. It was expected that any unrecognised half grabens or postulated inter-grabenal transfer faults might show up on these data sets

The Digital Terrain Model (DTM) was included because of the different erosional properties of the rocks involved in the study. The masking Tertiary volcanics, the ridge-forming Clematis Sandstone and siltstone based formations (Ingelara, and Peawaddy) all have distinct topographic expressions.

7.0 DATA PROCESSING

The satellite images used in this study underwent a basic processing stream recommended by Taylor (1991). The processing consisted of a contrast stretch, 2 - 98%. The contrast stretch was not sufficient to minimise differential atmospheric absorption and albedo or topographic effect. It was decided to correct for this using a combination of dark pixel subtraction and ratioing.

Processing Stream

Dark Pixel Subtraction to compensate for differential atmospheric absorption in different satellite bands. The dark pixel subtraction is accomplished by checking each individual band for it's darkest or lowest density value pixel, and subtracting this number from all other pixels in that channel. The darkest pixel is assumed to be a shadow that should be black which would have a density value of zero. Its deviation from zero is the result of quantum scattering by light photons in the atmosphere, which is greater at the higher wavelengths or the blue end of the spectrum.

Contrast Stretch to increase the dynamic range of the image and partially compensate for albedo effect.

Ratioing to create the NDVI and FE Oxide band and clay a content ratio etc. Most ratios involve the simple dividing of each pixel of one band by its corresponding pixel in another band. Sometimes with a scaling factor such as 127 added or in the case of the NDVI ratio, a normalising procedure is carried out as follows;

$$NDVI = (Band 4 - Band 3) / (Band 4 + Band 3)$$

Spectral Classification to obtain areas of similarity in all four bands. A spectral classification of a data set involves the cross plotting of each corresponding pixel value for the different data bands so that a statistical cluster analysis can group the image into a specified number of like classes. An n dimensional number represents each pixel with n corresponding to the number of channels or data bands in the classification. In this way the image can be broken up into areas of similar spectral signature which hopefully corresponds to the same ground cover (i.e. forest, urban, water etc).

Context or Spatial Classification is carried out to obtain areas of similar context with respect to neighbouring pixels, i.e. using a 5x5 pixel area. A context or spatial classification takes a spectrally classified image and repeats the cluster analysis process but in one dimension (i.e. only one input image not n) also taking into account a user specified number of pixels surrounding the cell being operated on. Where the spectral classification might have identified all cells containing vegetation, the context classification will further divide these into pixels with vegetation next to a road or a lake.

Supervised and Unsupervised Classifications In the later it is left up to the computer to perform a purely statistical analysis of the image. The classes are then identified by maps or ground truthing (inspection). In a supervised classification an unsupervised classification is followed up by assigning particular classes signatures and instucting the computer to find more of the them.

Supervised classifications are viewed by many purists to be unduly biasing what should be a purely statistical process and is therefore given less air time in this study. Correspondingly, only one of the five areas underwent a supervised classification.

The main use of the supervised classification was generate band specific statistics which could be plotted up in exel on an outcrop specific basis. The step was used to higrade certain bands for later more directed processing such as principle component analysis.

Rectification to a georeferenced image with DTM and vector data, which involved the selection of 8 to 10 control points. A nearest neighbour sampling approach was used instead of a bilinear one in order to preserve the spectral uniqueness of the Landsat TM image. Nearest neighbour sampling simply assigns the value of the nearest pixel to the desired new pixel location rather than extrapolating the values from the four nearest (bilinear) or nine surrounding pixels (cubic spline). This also had the added advantage of allowing it to distinguish the roads more clearly because of less smearing from neighbouring pixels.

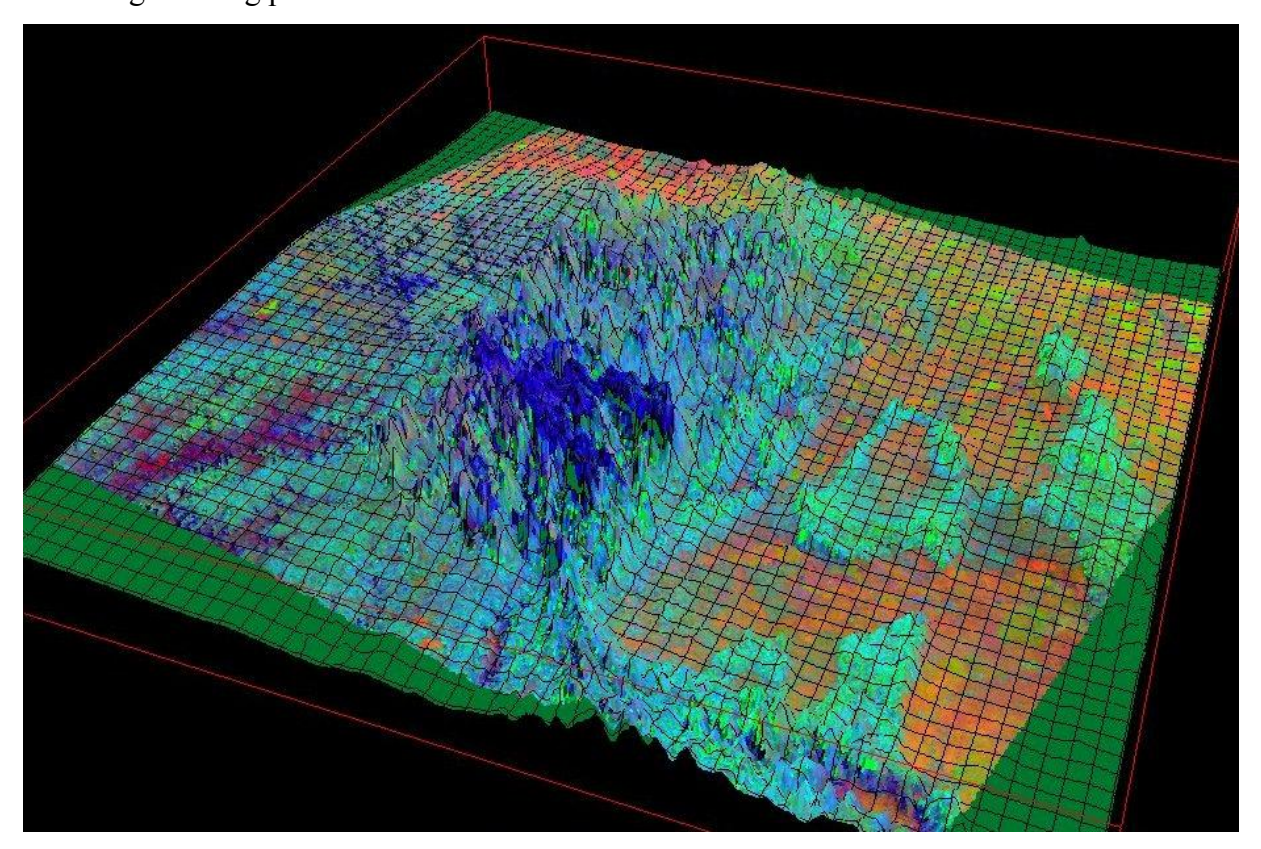


FIGURE 7..1 FALSE COLOR IMAGE OF BANDS 5,7 ANDSTANDARDISED BAND 6 (USING AVERAGE OF NON THERMAL BANDS IN AND NDVI RATIO) AS BLUE, GREEN AND RED, DRAPED OVER DIGITAL TERRAIN MODEL.

Creating a 3-D Drape over the Digital Terrain Model for improved visualisation of each area. Topographic information for the area was merged from digitised maps and

an Auslig 250 x 250m digital data set. The data was regridded at 30 x 30m and formed band 8 of the data set. The DTM (Band 8) was also used in initial classifications and directed principle component analysis wit limited success.

Performing Principle Component Analysis Principal Component Analysis of multiband data reorganises the data along axis of maximum variation. The first axis is called the first principal component (PC 1) and it can contain up to 90% of the multiband sets information. Each successive band has its axis at 90 degrees to the previous and contains slightly less information. Typically, only three Principal Components are required to display up the 99 % of the total data even if it is a 7 band Landsat TM data set. This is because of the high correlation between bands, probably due to the presence of topographic or albedo effects in all bands.

The false colour image in figure 7.2 has Principal Components 1, 2, 3 displayed as blue, green and red light. Principal Component 1 typically displays the surface roughness/texture of an area, which can be the dominating feature of an image set (Refer to Figure 7.2). PC's 2, 3 and 4, usually contain information about the vegetation or geology.

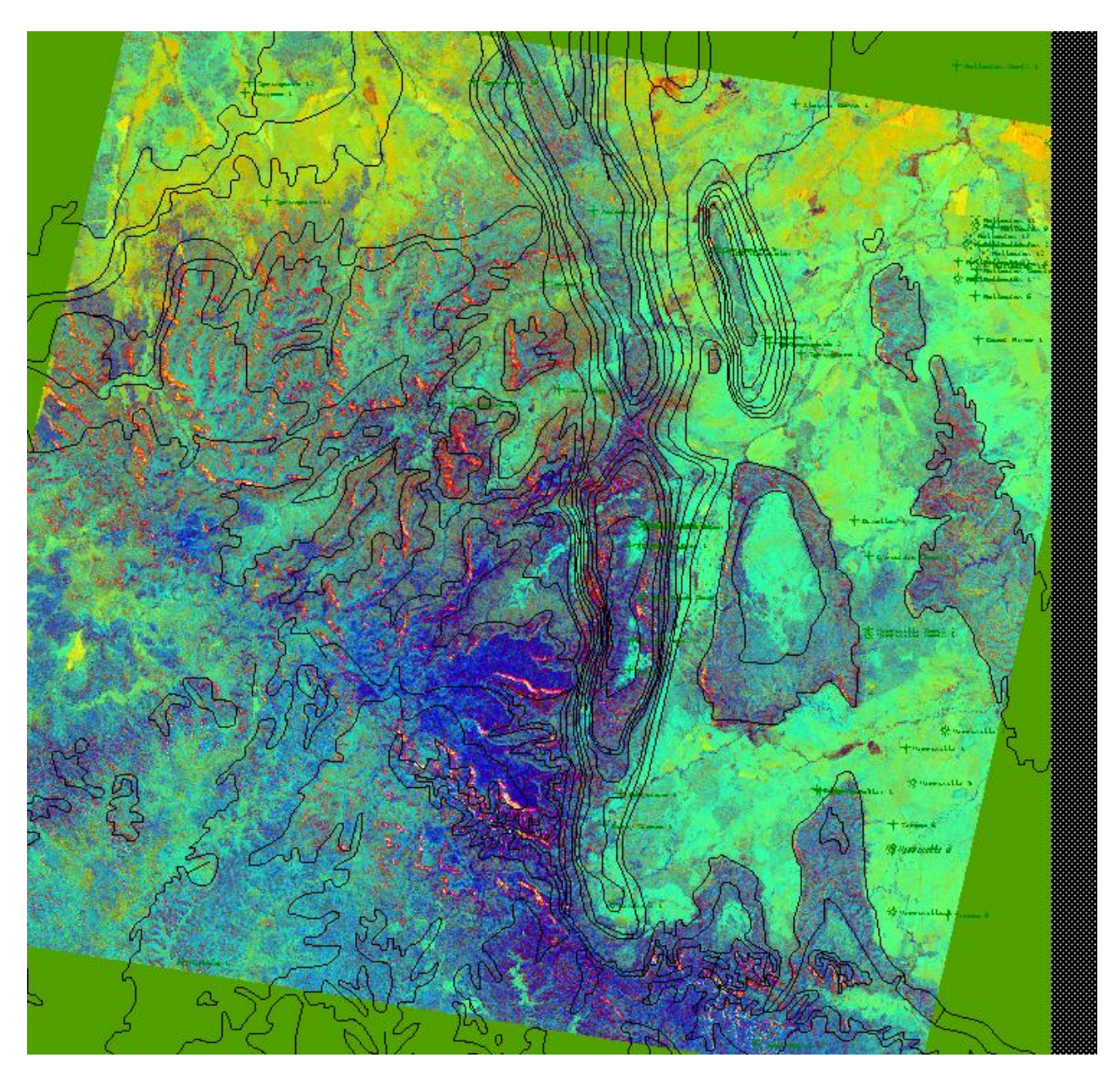


Figure 7.2 - Pseudo colour Image of Principal Components 1,2 and 3 as Blue, Green and Red.

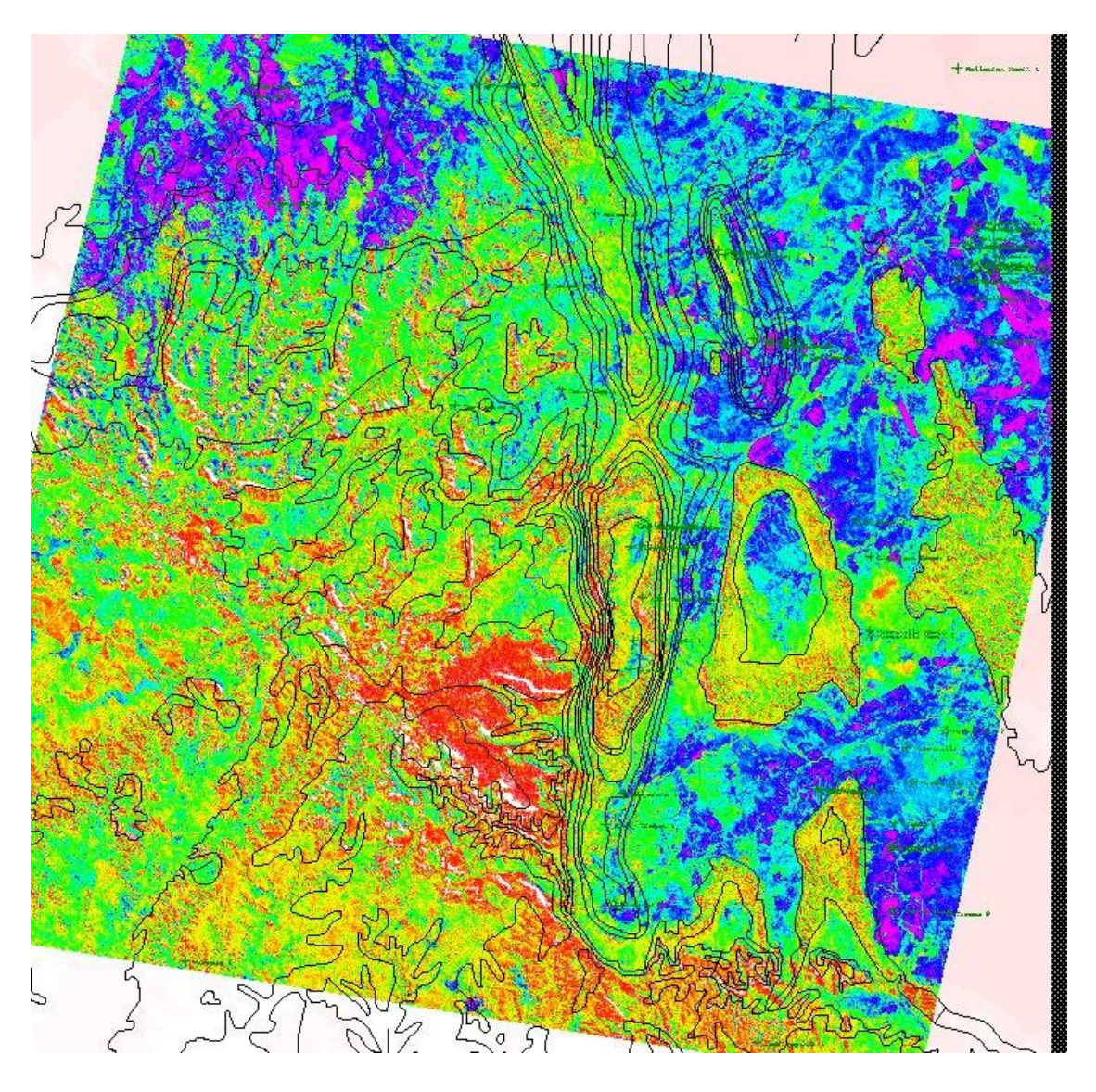


Figure 7.3 Pseudo Color of PC 1 for Landsat Bands 1-7 & DTM

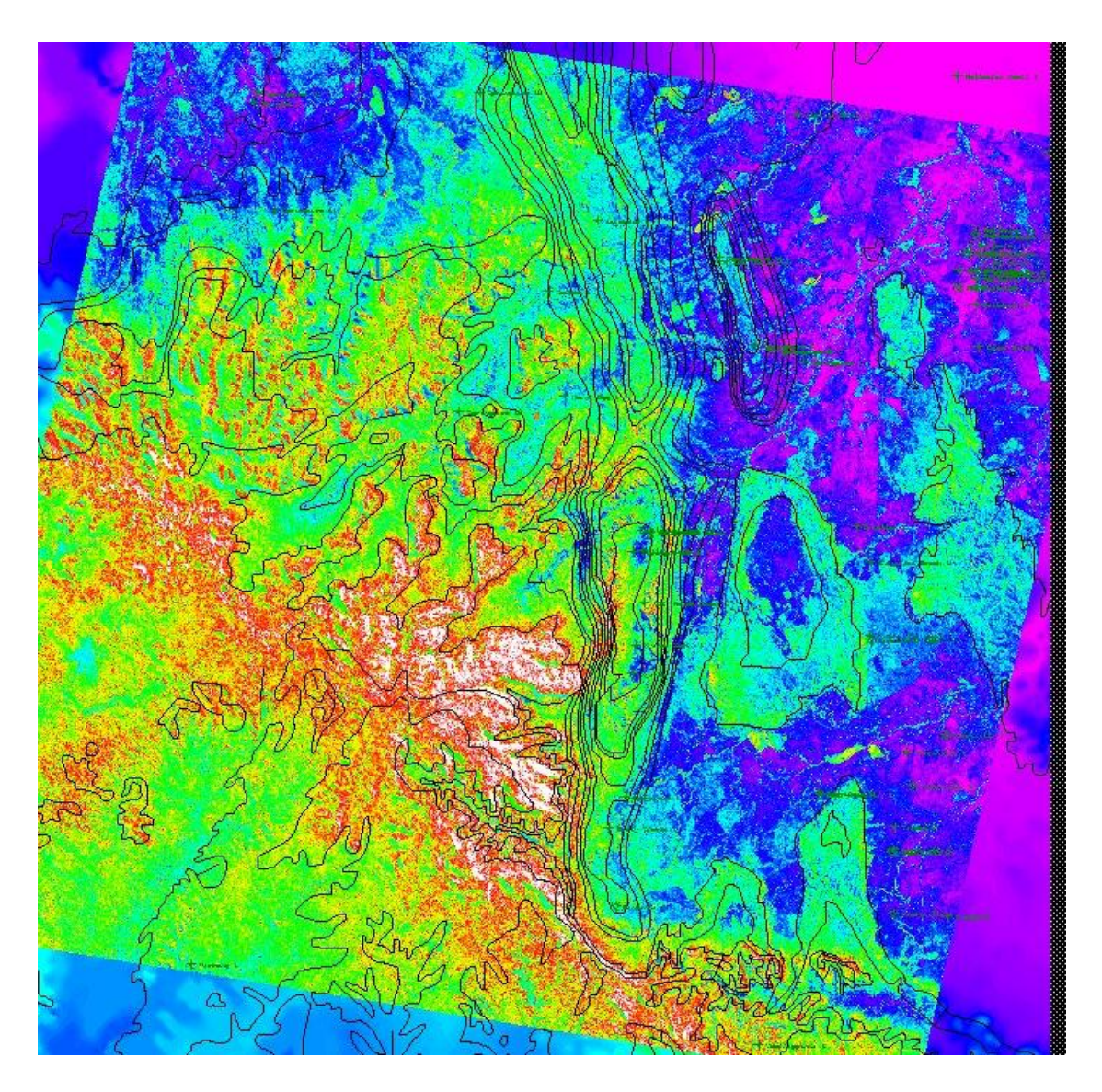


Figure 7.4 Pseudo Color of PC 2 for Landsat Bands 1-7 & DTM

From other studies in Australia (Taylor, 1991) it has been shown that the second principal component (PC 2) can represents variations in the soil's mineral composition or vegetation. In Taylors 1991 study in central Australia, it was found to distinguish between iron rich soils and leached soils or bare ground (Taylor, 1991). This might also be the case here as is evident by the strong eigen vector loading shown for PC2 over most of the formations (Refer to Figure 9.5.4).

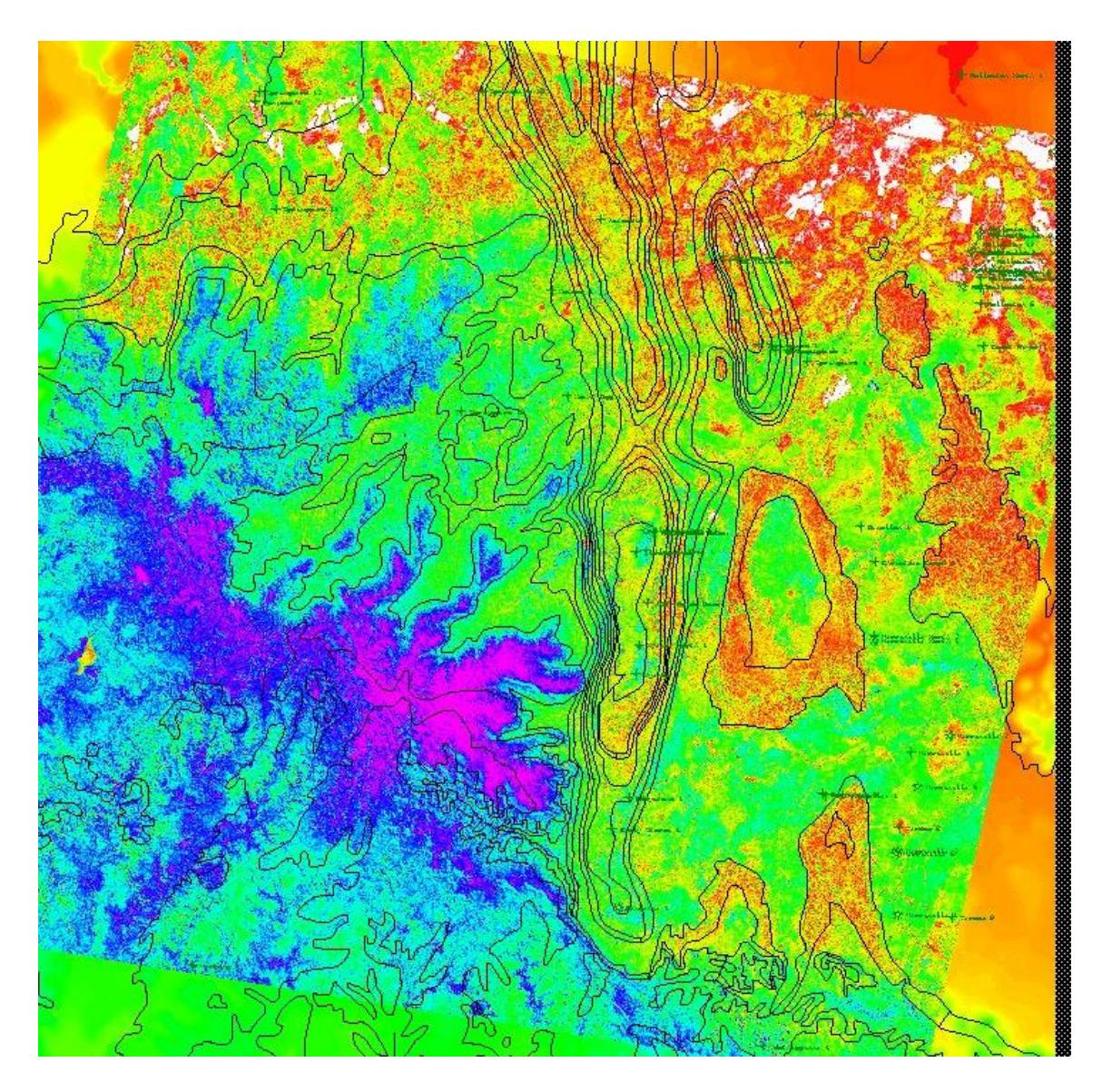


Figure 7.5 Pseudo Color of PC 3 for Landsat Bands 1-7 & DTM

The third principal component (PC 3), displayed as red light has been known to contain largely vegetation cover variation (Taylor, 1985). However this does not appear to be the case in the study area where the bulk of the geometrically significant variation appears to be in PC 2.

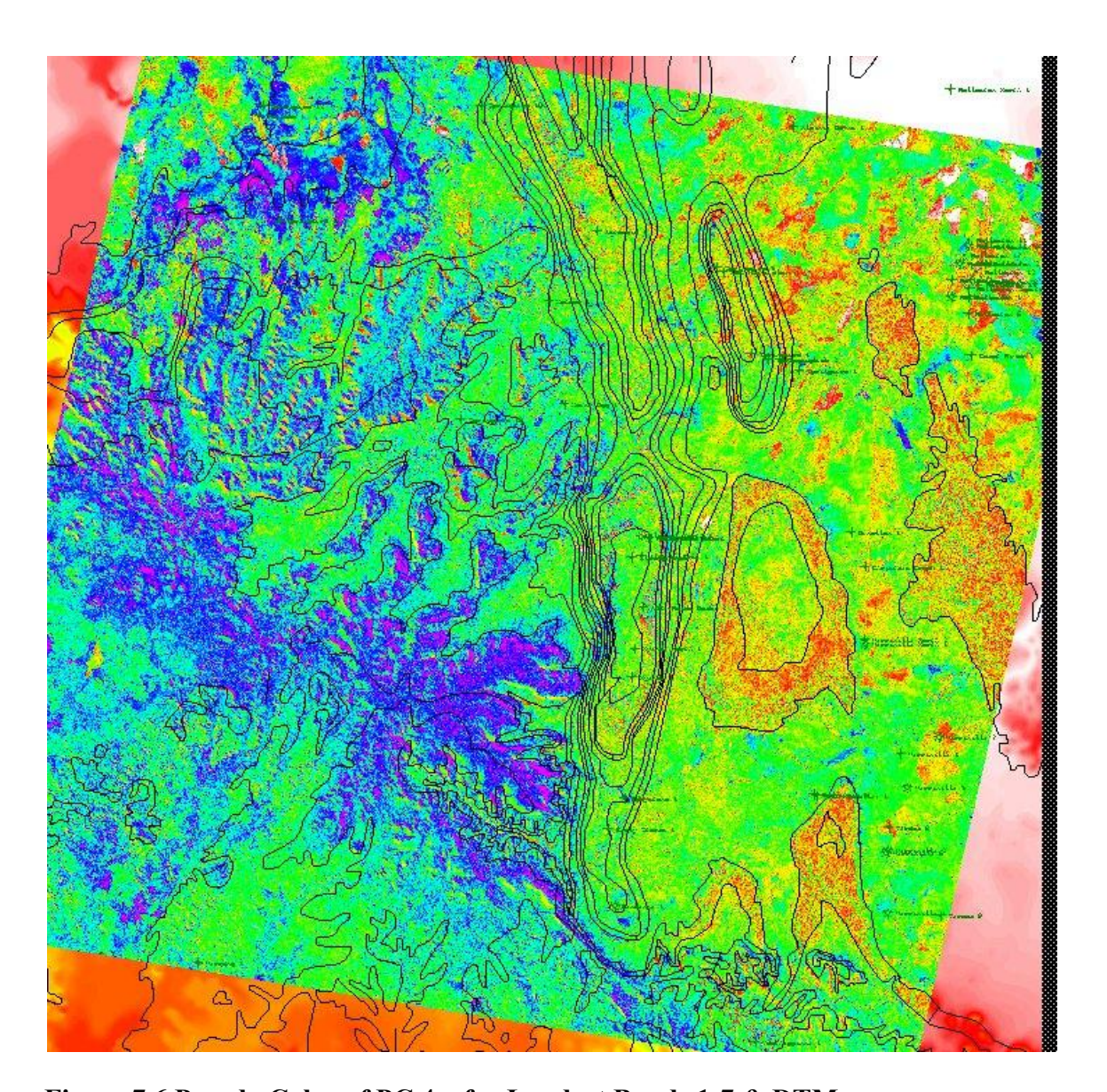


Figure 7.6 Pseudo Color of PC 4 for Landsat Bands 1-7 & DTM

The fourth principal component, PC 4, seems to contain a lot more noise than the other principal components and subsequently was not used in the mapping.

Principle Components of TM 9377 captured in 1993 during the dry season

DIFFERENCING AND STANDARDISATION

The usually unused thermal infrared band 6 was incorporated into the mapping to great effect by standardising it to the average of bands 1 to 7 without 6. This was accomplished using an NDVI ratio with band 6 and the average band. This is thought to have the effect of increasing the normally 120x120m resolution of band 6 to 30x30m

in a similar way that combining of 30m Landsat data with 10m SPOT to results in a combined 10x10m product. It is also hoped that the ratioing minimises any contamination in the thermal emitted band by the reflected IR bands. This last effect is yet to be proven however.

Difference images were also generated on the data set by subtracting each band from the average band in an attempt to standardise the data to the average of the non thermal bands and to possibly double the dynamic range of the imagery. This should also allow a better comparison with these images with any work done on altter vintage or image

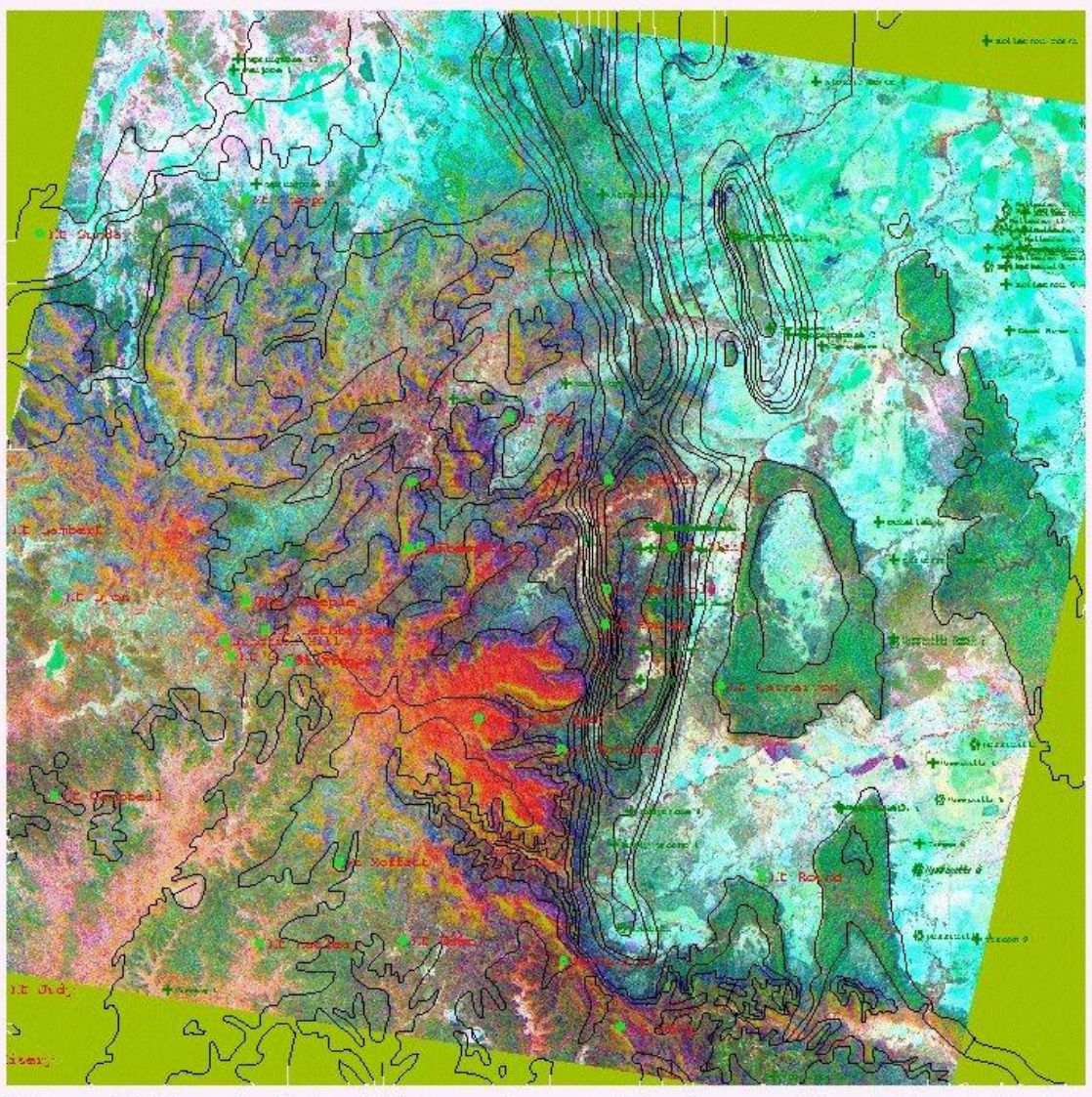


Figure 7.7 Pseudo Color Difference Image - The Average Band 10 - each of Band 5/7, 4 & 6 as Blue, Green & Red.

Blue=>Clay Rich, Green=> Veg, Red=>Thermally Hot

from a different area.

8.0 CONSUELO AREA PILOT STUDY

8.1: INTRODUCTION

The Consuelo Area Pilot Study was undertaken for the GN888 Image Engineering courseat the University of Queensland. It formed the first part of an overall project to build a remotely sensed digital database for the greater Denison Trough area. The main objective in building the database was to combine all pertinent geophysical and geological data onto the one Geographical Information System (GIS) in order to evaluate and change where necessary the structural and stratigraphic interpretation of the Denison Trough sediments. It was hoped that the project would enhance the understanding of the geological make-up of the area and high grade with respect to hydrocarbon potential some areas over others. The secondary aim of the project was to evaluate the usefulness of satellite imagery for hydrocarbon exploration in the project area. This pilot study was to be carried out over a small but well exposed part of the study. If the methodology would work anywhere, it would work here. This allowed the proving of the method prior to spending large amounts of time and money on a bigger area and then getting useless or ambiguous results.

8.2 REGIONAL GEOLOGY

The pilot study area within the Denison Trough was located approximately 700km northwest of Brisbane and 30km southwest of Roleston and fell mainly within the Authority to Prospect 337P. The main hydrocarbon bearing sediments are Permian in age and are contained in a series of inverted northwest to southeast trending enechelon half grabens. The unconformably underlying basement rocks are comprised of Devonian aged Drummond Basin and Timbury Hills metasediments. The Bowen Basin Triassic sediments conformably over lie the Denison Trough inverted half grabens. Almost all of the Jurassic and Cretaceous sediments have been eroded from the area except in the south of the region.

A thin veneer of tertiary and quaternary aged rocks covers the Triassic sediments. Within the tertiary are the Minerva Volcanics, which are present in abundance in the form of surface and subsurface basalt sills. Their higher resistance to erosion than

that of the Jurassic and Triassic sandstones and siltstones have resulted in the present day topography of basalt capped ridges rising several hundred metres above eroded creek beds. The Triassic aged Clematis Sandstone was probably the next most erosion resistant formation and forms a series of high ridges outlining the now eroded inverted half grabens and outlining or capping the old inter-grabenal horst blocks exposed present day. The northern edge of the Rewan Syncline is one such example and can be seen as a high topographic ridge in the bottom right hand corner of the pilot area.

8.3 CONCEPT

The Department of Minerals and Energy's (DME) 1:500,000 Bowen Basin solid geology map was purchased in digital form for use as a template in assessing any revisions to the solid geology vector file. The Consuelo and Springsure Anticline area had been mapped extensively using conventional geological and geophysical techniques combined with air photography analysis. However, it had not been mapped using satellite imagery and a digital terrain model (DTM) in conjunction with conventional methods. It was felt that the combination of all individual data sets on the one GIS database might result in a synergistic interpretation and possibly lead to modifications of the existing solid geology map.

To that end, the Department of Minerals and Energy's (DME) 1:500,000 Bowen Basin solid geology map was purchased in digital form for use as a template in assessing any revisions to the existing interpretation.

The inclusion of Landsat imagery with its vegetation sensitive infrared bands was felt to be instrumental to the revised interpretation (Refer to Figure 2.1 and 2.2).

The bulk of the effort in conjunction with GN888 concentrated on obtaining, processing and interpreting satellite data. The 30m by 30m pixel size of the Landsat imagery was deemed good enough to delineate the outcropping formations which because of the low dips in the Consuelo area, covered 100 plus metres in a horizontal dip direction. Phase two of the project initially called for augmenting the spatial

resolution by combining the Landsat data with 10m monochromatic SPOT imagery. It was decided to prove the viability of the method first before incurring any additional data acquisition costs. However, funding was cut short and phase two was never carried out.

The geophysical data selected for inclusion in the project was the seismic derived Time Structure Maps of the Mantuan and Aldebaran Formations, the digitised and grided DME Regional Total Magnetic Field Aeromag Map and Bouger Gravity Maps covering the study area. The Mantuan and Aldebaran Formations were selected because of the good continuity of the events regionally and their significance as main reservoir rocks for the permit area.

The DME's gravity and aeromagnetic maps were included to focus on the underlying basement structure of the region. In particular, it was expected that unrecognised half grabens or postulated inter-grabenal transfer faults might show up on these data sets. However, their regional nature and greater grid spacing than that of the other data sets proved to be only of minor use in the pilot area. The DME data was felt to be suited for regional structural work when the project was extended outside the pilot study area.

The topography or DTM (Refer to Figure 8.3.1) is important because of the different erosional properties of the rocks involved. For example, the resistant Tertiary aged volcanics, the ridge forming Clematis Sandstone and the highly erosive nature of the predominantly siltstone based sediments such as the Ingelara, Black Alley Shale and Peawaddy formations. Put in a little bit more explanation as to why this is useful/important. Using the DTM, you can readily identify lithologies and weathering patterns based on lithologies. The inclusion of Landsat imagery with its vegetation sensitive infrared bands was felt to be instrumental to the revised interpretation.

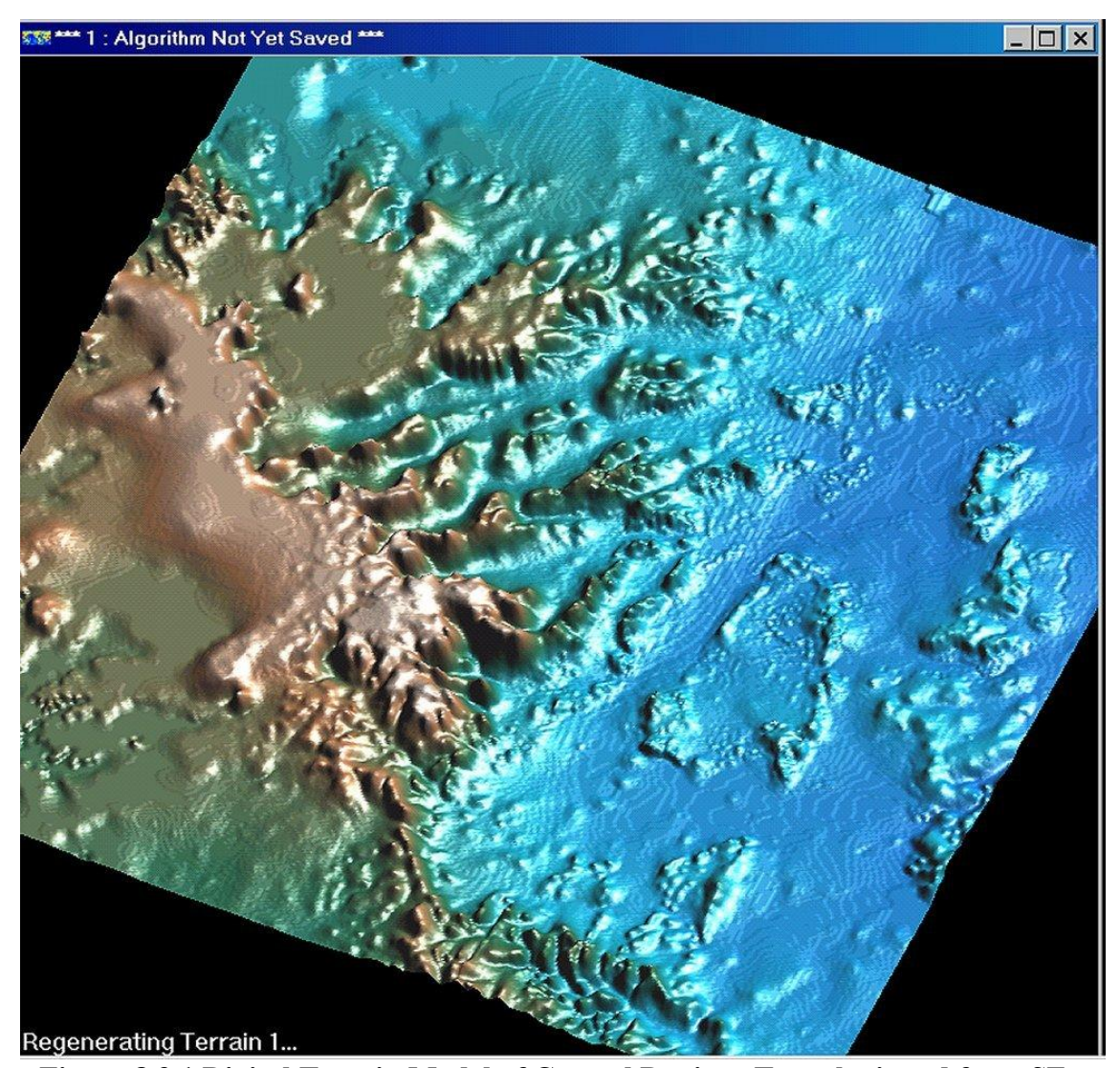


Figure 8.3.1 Digital Terrain Model of Central Denison Trough viewed from SE

8.4 DATA USED IN PROJECT

The bulk of the effort to date and in conjunction with GN888 has concentrated on obtaining processing and interpreting satellite data. The 30m by 30m pixel size of the Landsat imagery was deemed good enough to delineate the outcropping formations which because of the low dips in the Consuelo area covered 100 plus metres in a horizontal dip direction.

However phase two of the project will call for augmenting the spatial resolution by combining the Landsat data with 10m monochromatic SPOT imagery. It was decided to prove the viability of the method first before incurring any additional data acquisition costs.

The geophysical data selected for inclusion in the project was the seismic derived Time Structure Map of the Mantuan and Aldebaran horizons the digitised and gridded DME Regional Total Magnetic Field Aeromagnetic Map and Bouger Gravity Maps covering the study area. The Mantuan Horizon was originally but was replaced by the Aldebaran horison because it did not out crop within the study as much as the younger formation and because of it's significance as one of the main Permian reservoir rocks for the permit area.

The DME's gravity and aeromag maps were included to focus on the underlying basement structure of the region. In particular, it was expected that any unrecognised half grabens or postulated inter-grabenal transfer faults might show up on these data sets. However, their more regional nature and greater grid spacing than that of the other data sets proved to be only of minor use in the pilot area but were of more use in the more regional full study area project which followed.

The DTM was felt to be important because of the different erosional properties of the rocks involved especially that of the masking tertiary volcanics, the ridge forming Clematis Sandstone and the highly erosive nature of the predominantly siltstone based rock types such as the Ingelara, Black Alley and Peawaddy formations.

8.5 DATA PROCESSING

Except for the satellite imagery, the other data sets were either obtained in digital form or were digitised and gridded. The additional step of calculating the first horizontal derivative for the aeromagnetic and gravity maps were also performed although at this stage only as separate dz/dx and dz/dy maps. The ideal situation would be to end up with only one omni-directional derivative map. This method was latter found to be available in the ER-Mapper software package.

Rectification

The bulk of the processing effort centred on getting the Landsat imagery rectified to allow combining with the other data sets. Rectification points were digitised from a

cadastral topographic map and eventually were field acquired with a Magellan 1000 GPS unit. Fourteen control points, mostly at road intersections and road/creek crossings, were surveyed in from which the best eight were selected for rectification of the Landsat Bands. A detailed analysis between the mapped coordinates and the GPS points is included on the attached spreadsheet (Table 2).

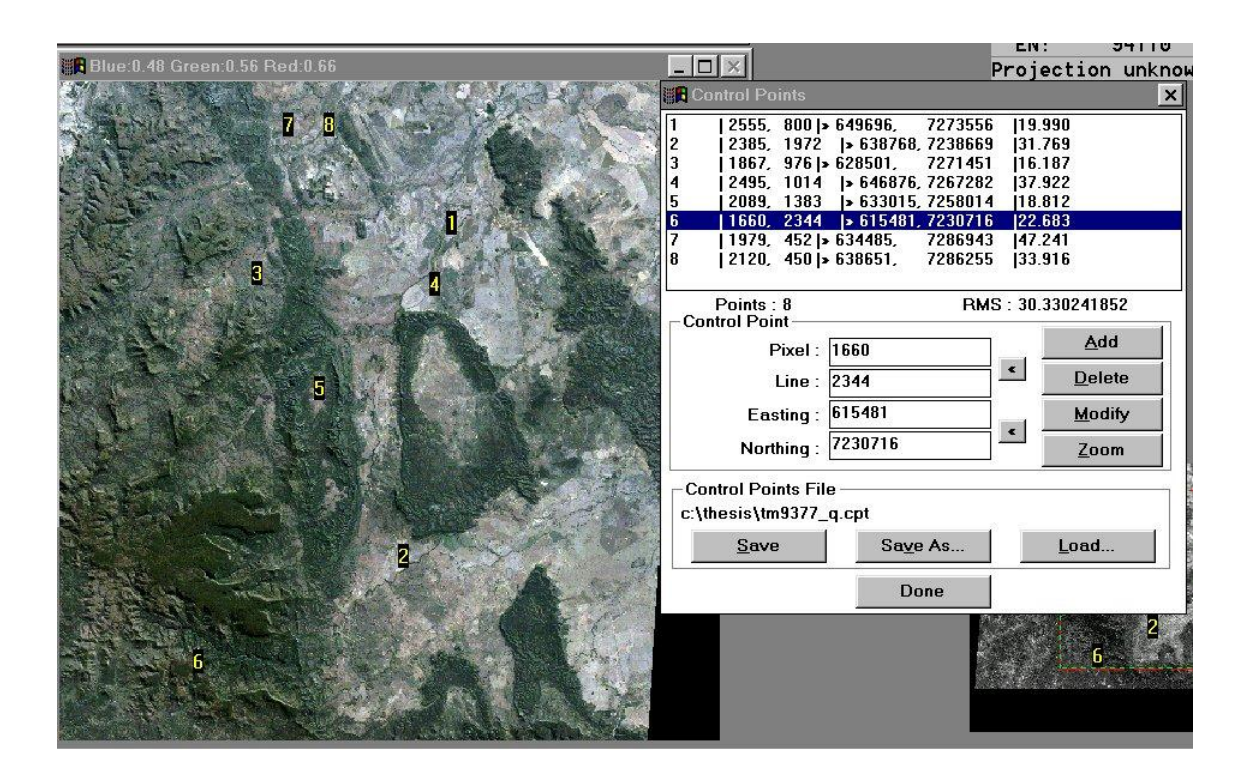


Figure 8.5.1 True color image showing rectification points for Landsat image

From three to five readings (each an average of fifty readings and the utilising of at least two different sets of four satellites), was adequate to get the control point within about 50m horizontal distance and 30m in elevation to that of the topographic map. This equates to about 1 and half pixels and was felt to be within operational parameters and comparable to the maps probable accuracy. To that end, it was decided to use the GPS points for the QIPS rectification program. The rectification points are listed in Table 2 and are shown in figure 8.5.1 when they were later used, with the addition of a few more points, to rectify the image over the whole study area.

Contrast Stretch

Each band of satellite data was contrast stretched from 2% to 98% in order to use the full dynamic range of the imagery over the 256 levels available for 8 bit data (2 to the power of 8 levels). The data below 2% of the maximum reflectance value was

NAME	PIX	LINE	TOP	O MAP	LONG		EAST	NORTH	LAT	18.4m/.0	LONG	16.9m/.0	xPDO	SATS	xSiQu	ELEV	StDev	TIME	DATE		COMMENTS
RQ1 SUB RAW	781 2631	226 626	24	35.97	148	30.63	652927	7278549	24 24 24	36.01 36.02 36.01	148	30.62 30.62 30.60		04260205 04260205 04260205		172 217 289		14:50	941013 941013 941013	CONT	INT DEV HWY&REWAN RD 12m NTH of int
									24	36.03 36.03	148	30.62	3.5	04260205	9996	213 180	25.6	15:10	941013	50AVG	50 reading avg
									24 24 24	36.03 36.05 36.00	148 148	30.60	4.2 4.2	05170624 14182731 14182731 14182731	9994 9996	170 415	25.0 36.5 17.4 25.5	08:11 08:21	941016 941016	50AVG 50AVG	
						AVG	652908	7278453	24	36.02	148	30.61		14182731	9996	235	25.5	08:31	941016	50AVG	
						AVGcor MAPdif PIXdif	652908 19	7278445 104 3	24	36.03 -0.06	148	30.62 0.01			MAPeh	6					
							652861 652907 652819	7278501 7278549 7278470							1270						GROUND TRUTHING REPEAT READINGS
							652829 652887 652892	7278496							2748 2748 0057			10:11	971231 971231 971231	CONT	
						AVG DIFF	652866 -42	7278453 7278453 8							0057			10:11	971231	CONT	
RQ3 SUB RAW	786 2636	300 698	24	37.36	148	30.62	652882	7275984	24 24	37.02 37.00	148 148	30.50	2.7	05060924 05060924	9879 9879	250 272	14.3 19.5	18:09 18:19	941015 941015	50AVG 50AVG	INT DEV HWY&SM RD WST 6m NTH of INT
						AVG AVGcor	652671 652671	7276628 7276628	24 24	37.01 37.01		30.50				261	16.9				
			-			MAPdif PIXdif	211 7	-644 -21							MAPek	-32 229					
RQ4 SUB RAW	905 2755	856		40.14	148	32.12 32.16	655355 655423		24	40.12 40.09 40.10	148	32.11 32.12	3.5	05061724 05061724 05061724	9996	303 167	16.4	18:36	941015 941015 941015	50AVG	INT DEV HWY& VESTA RD AT INTERSECTION
	CADAS	LKAL		40.14	140	32.10	037423	7270024	24 24	40.11 40.12	148 148	32.11 32.11	2.5	18142728 18142728	9098 9695	253 230	31.0 22.2	08:40	941016 941016	50AVG	(<u>)</u>
						AVG	655347	7270882 7270882	24	40.11	148	32.12		18022728	9996	236		09:00	941016	50AVG	
						AVGcor MAPdif PIXdif	655347 8 0	7270882 -58 -2	24	40.11	148	32.12			MAPeh	-5 229					
RQS SUB RAW	705 2555	400 800	24	38.68	148		649734	7273581	24 24	38.66 38.70	148 148	28.77 28.76	3.0	02071926 02071926	9000	254 235	19.1	12:24	941015	50AVG	INT REWAN RD& MT OGG RD AT INTERSECTION
	CADAS	TRAL	24	28.67	148	28.67 DIFF	649566 168	7273694 -113	24	38.71 38.70 38.68	148	28.77	3.0	02071926	9999 9959	189 235 189	20.8	16:17	941015	50AVG 50AVG	
						AVG	649727	7273563	24	38.69	148	28.77		04051624	9909	220		10:27	941015	SUAVG	
						AVGcor MAPdif PIXdif	649727 7 0	7273563 18	24	38.69	148	28.77			ELVdif MAPek	5 225					
							649786 649752 649762	7273610 7273423 7273434							75910 75910			7:21 7:21	971228 971231 971231	CONT	AUSS4 UTM GROUND TRUTHING REPEAT READING
						AVG DIFF	649767 39	7273489 -74													
RQ7	2383	1978		57.66	148		638837		24	57.71 57.72	148 148 148	22.54 22.56	3.7	16182731 16182731		290 364	1	10:46 10:51	941015 941015	CONT	NTH INT REWAN RD&WYSEBY RD 5m STH OF INTERSECTION
			24	57.83 -0.17	148	-0.01	638851 -14	314	24	57.70	148	22.54	3.7	02071619 02071619		290		11:01	941015 941015	CONT	
						AVG AVGcor MAPdif	638888 638888 -51	7238575 7238581 77	24	57.71 57.70	148 148	22.55 22.55	3.7		ELVdif	294	0.0				
						PIXdif	-2 638833 638855	7238598 7238617							MAPek	310			971230	CONT	GROUND TRUTHING REPEAT
			1				638817 638840	7238519 7238575							002 002	179		14:56 14:56	971230 971230	CONT	READING
3						AVG DIFF	638836 -51	7238577 -3							1						
RQ7B			24	51.13	148	22.22	638454	7250716	24	51.09 51.10	148	22.21 22.22		02071619 02071619		276 343		11:25 11:30	941015 941015	CONT	INT REWAN RD&SEROCOLD DRVW. AT INTERSECTION
						AVG AVGcor MAPdif	638446 638446	7250780 7250780	24 24	51.10 51.10	148 148	22.22 22.22	0.0		ELVdif	310 -30	0.0				
						PIXdif	0	-2			_				MAPeh	280					
RQ7C			24	46.73	148		640254		24	46.75 46.75	148	23.24	2.8	07181926 07181926		249	2 2	11:40	941015	CONT	INT REWAN RD&ALDINGA DRV WA AT INTERSECTION
						AVG AVGcor MAPdif	640246 640246 8	7258783 7258783 37	24	46.75 46.75	148	23.24	2.8		ELVdif	262	0.0				
RQ9	17	578	24	39.95	148	PIXdif 16.18	628473	7271450	24	39.94	140	16 20	21	07002627	MAPeh		162	12.43	041015	50 AVC	MT OGG PRADDY CRY AT MT ING
	1867 CADAS	978	100	39.93 0.02	148	16.28	628642	7271485	24	39.93 39.92	148	16.19 16.20	3.2	07092627 07092627 07092627	9999 9798	336 404	24.7	13:52 14:02	941015 941015	50AVG 50AVG	MT OGG RD&DRY CRK AT MT ING 30m WEST OF CREEK BED
				0.02		-0.10 AVG AVGcor	628501 628471	7271487 7271487	24 24 24	39.93 39.93		16.20 16.18	3.2			381	18.5				
			8			MAPdif PIXdif	0	-37 -1			1 8				ELVdif MAPek	310	2 1				
RQ16	647 2497	613 1013	24	42.07	148	27.16	646935	7267372	24 24 24	42.09 42.08 42.09	148	27.14 27.17 27.16	3.4 3.4 3.4	02071926 02071926 02071926 02071926	9996 9995	212 161 222		12:03	941015	20AVG 40AVG	INT REWAN RD& DIRT RD EAST AT INTERSECTION
									24 24	42.10 42.11	148 148	27.19 27.20	3.3	02071926 02071926		296 349		12:13	941015	CONT	SAT 02 URA 30, 52deg, 176degT
			9			AVG AVGcor	646955 646955	7267328 7267328 44	24 24	42.09 42.09	148 148	27.17 27.17	3.4		VY 1/46	248	0.0				
						MAPdif PIXdif	-20 -1	1							ELVdif MAPek	240					
RQ11B			24	31.92	148	22.12	638640	7286175	24 24 24	31.85 31.86 31.92	148 148 148	22.14 22.15 22.09	4.4 4.4 4.4	14221929 14221929 14221929	9999 9989 9999	217 241 277	22.4 30.8 31.7	06:47 06:57 07:07	941016 941016 941016	50AVG 50AVG	PROJ OF SPRINGWOOD RD&CREEK AT INTERSECTION
						AVG AVGcor	638651 638651	7286255 7286255	24	31.88 31.88	148	22.13 22.13				245	28.3				
						MAPdif PIXdif	-11 0	-80 -3		-1.00					ELVdif MAPeh	260					
RQ11C			24	31.43	148	22.74	639695	7287069	24	31.45 31.47	148	22.73	3.9	14192229	9999	257 264	23.3	07:20 07:30	941016	50AVG	INT SPRINGWOOD RD&FENCE WES AT INTERSECTION
						AVG	639695	7287014		31.46	148	22.74		14192229	9999	358 293		07/40	941016	30AVG	
						AVGcor MAPdif PIXdif	639695 0	7287014 55 2	24	31.46	148	22.74			ELVdif MAPels	-33					
RQ13	239	985 1385	24	47.18	148	18.98	633083	7258040	24		148										REID'S DOME NOT RECORDED
RQ15			25	2.08	148	8.68	615481	7230716	25 25	2.08	148 148	8.72 8.73		02071926 02071926		885 998					BATTLESHIP SPUR LOOKOUT
									25 25 25	2.09	148 148 148	8.74 8.75		02071926 02071926 02071926		991 1094		13:00 13:05	941014 941014	CONT	
				3		AVG AVGcor	615574	7230688 7230688	24 24	2.10 2.10	148 148	8.74 8.74				992	0.0				
						MAPdif	-93 -3	1							HAPek MAPek						
RQ16			24	38.26	148	25.3	643888	7274418	24 24 24	38.38 38.31 38.30	148	25.19 25.18 25.17	3.4 3.4 3.2	02040726 02040726 04260212	9799 7199 9759	245 204 255	31.2 30.6 14.9	13:02 13:12 14:35	941015 941015 941015	50AVG 50AVG	INT MT OGG RDÆNTH TRACK 8KM FROM REWAN RD
						AVG	643685	7274298	24	38.33	148	25.18	3.1	04260212	9539	174	14.4	14:45	941015	50AVG	
						AVGcor MAPdif	643685 203		24	38.33		25.18			ELVdif	41	10.2				
RQ17			24	38.12	148	PIXdif 20.39	635607	7274760		38.09	148	20.38	4.2	04072602	MAPek 9997	260	12.3	13:22	941015	50AVG	INT MT OGG RD&CREEK WITH TR
									24 24 24	38.10 38.11 38.08	148 148	20.40 20.39 20.39	5.3	04072602 07260927 07260927	9998 9999				941015 941015 941015		
						AVG AVGcor	635607 635607	7274806	24	38.10 38.10	148	20.39					11.9				
						AVGcor MAPdif PIXdif	0 0	7274806 -46 -2	24	38.10	148	20.39			ELVdif MAPek	-30 280					
RQ20							654179 654211	7237060 7237094	24	58.42 58.42	148	31.68			.0;	249			971230 971230	CONT	DEVELOPMENT/CARNARVON RD GROUND TRUTHING NEW RQ PT
						AVG	654193	7237094 7237048 7237117 7237080	24		148 148		E		01	245 179 035		14:38 14:38	971230 971230	CONT	
RQ21							654767	7256369	24	47.96 47.96		31.82			4	271 104		9:08	971230 971230	CONT	DEV RD, CHRISTMAS CRK BRDG GROUND TRUTHING NEW RQ PT
_							654725	7256444 7256392 7256472 7256419	-1	*****	440	24.62			01	180		14:12	971230 971230 971230	CONT	THE PARTY OF THE P

TABLE 2 Georeferencing points for satellite image

assigned the value 0 and the data above 98%, 255. The data falling in between these values were stretched proportionately in a similar manner to an Automatic Gain Control filter in seismic processing.

Band Ratios And Classification

The seven rectified bands were put through an unsupervised spectral classification followed by a context classification, each of sixtyfour classes. The resulting image was plotted out and a transparent overlay of the geology was created to check for correlation with the image. The correlation was found to good enough to feel that there was merit in extending the project to cover the whole of the study area.

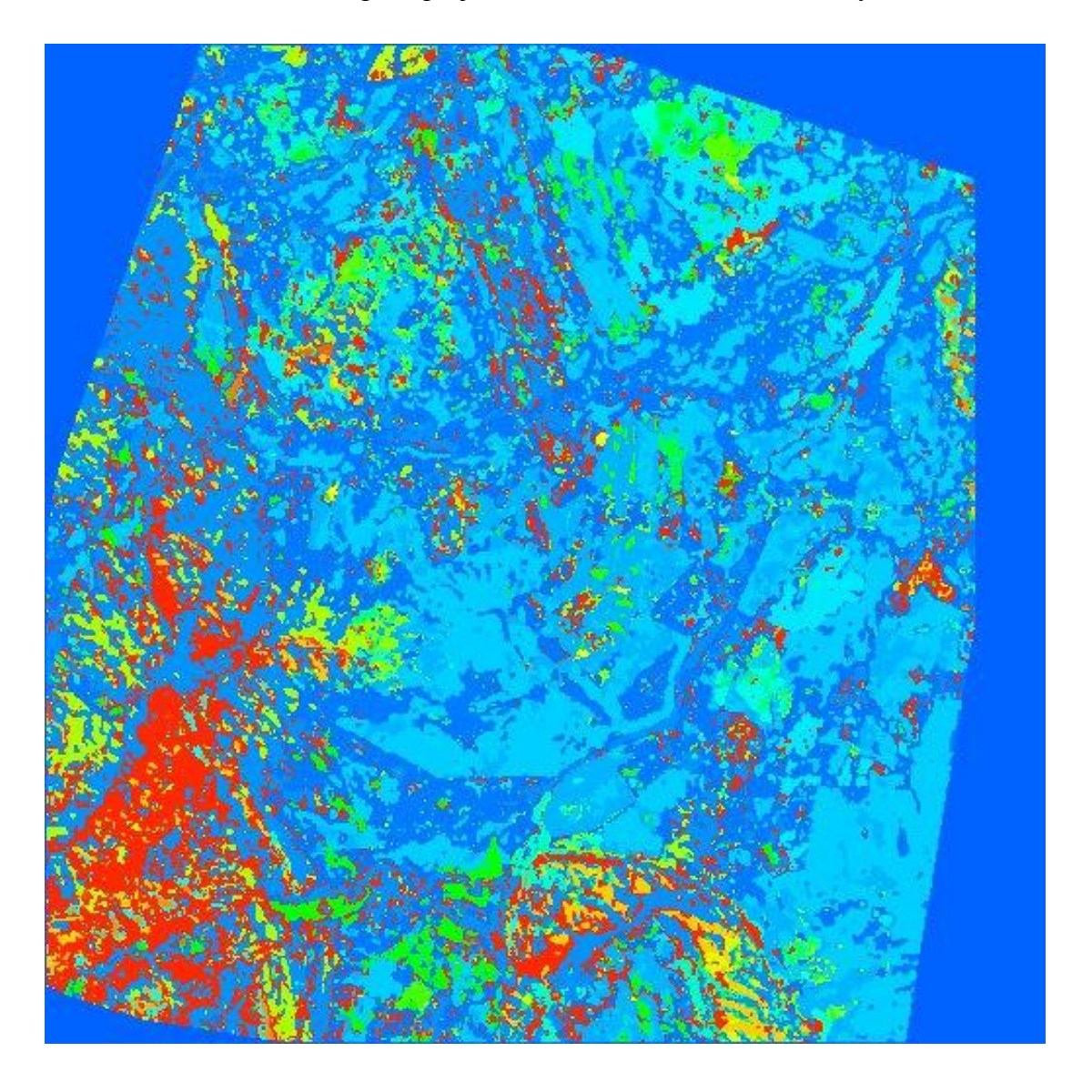


Figure 8.5.2 Spectral Classification from Pilot Study

A Normalised Difference Vegetation Index (NDVI) image using bands 4 and 3 as well as two other ratios, Bands 5/2 and 5/7 were calculated for their vegetation and soil sensitivity.

8.6 INTERPRETATION

The NDVI is meant to be useful in measuring biomass and differentiating between stressed and non-stressed vegetation. The band 5/2 ratio is useful in distinguishing different vegetal types while ratio 5/7 is sensitive to different clay rich formations because of clay's absorption in band 7 and high reflectance in band 5.

It was felt that they would be useful in the classifications although the possibility of duplication of information if the individual bands were also used in the same classification was also taken into account. In addition to the ratios, it is also planned to generate an optimum difference index to help select the three most different bands for inclusion in a Principal Component Analysis. The decorrelating nature of the Principal Component Analysis however omits the image's use from a spectral classification standpoint.

In identifying the ground control points on the satellite image, three colour images using bands 3,2,4 and bands 1,2,7 for red, green and blue were found to show the road and creek crossings the best. While the main body of the processing was accomplished within the QIPS processing package, the TerraScan Windows based software package proved useful in selecting the ground control points, subset generation and general data handling. Some of the data has also been loaded into ERMapper. However the early release of the package while promising to be extremely versatile in combining all the data sets, resulted in slower progress than initially hoped and as a result was not used for this thee pilot study. The latter releases of the software proved much more user friendly and the package eventually became the predominant one being used.

At the completion of the GN888 pilot study the initial unsupervised classifications (see figures 8.5.2) revealed banding with and overall geometry similar to that of the surface outcrop map. An important addition to the classifications was to be the inclusion of the DTM because of the erosion resistant nature of the basalt ridges and some of the sandstones in the area.

The gravity and aeromagnetic data sets were not overly useful in the classifications of the pilot area due to their regional nature in grid size and variation. Initial interpretation of the first derivative maps showed boundaries which line up with existing mapped faults on seismic and have a general shape to the some of the currently interpreted basement structure in the area. As with any digital project, half the work was in getting the data loaded into the software packages Such was the case with the non satellite data in this study due to differences in data formats.

8.7 RESULTS FROM PILOT STUDY

The pilot study in the Consuelo anticline area showed that the initial concept of mapping the geology using satellite imagery to distinguish between different formation specific tree types was a helpful technique. This was largely due to the high reflectance of vegetation in the infrared bands contained in the imagery (Refer to Figure 2.1 and 2.2) and the different spectral signatures of the various formation specific tree types in the study area. These findings provided impetus to apply the methodology to the remainder of the area.

9.0 GEOMORPHOLOGY AND

REGIONAL APPLICATION

Australia can be divided into three broad geomorphic provinces, The Western Plateau, The Central Lowland and The Eastern Highlands. The Denison trough is located in the Eastern Highlands along the Great Dividing Range (Refer to Figure 3.1).

The geomorphology of the Denison Trough is varied and includes several different landform types. The elevation of the study area varies between 100 and 1000+meters.

Over the years, the classification of streams and drainage systems has followed four main sets of criteria:

- 1) The cycle of erosion system composed of three stages, Youth, Maturity and Old age as described by Davis (1898).
- 2) The structural control classification system comprised of consequent, subsequent, obsequent and super imposed streams as described by Powell (1875) and Davis (1898).
- 3) The present day morphological classification system of straight, meandering, braided and anastomosing rivers based on streamenergy. This system is probably the most widely used of the four especially in geology possibly because of it's direct relevence to sedimentary process.
- 4) The Process-Response classification system, which relates the discharge and sediment type to channel morphology.

This last system is gradually becoming more popular with the advent of scale sediment models, computer simulations of active systems and the honing of analytical measurement techniques.

The landscape of the study area was divided into the following geomorphic systems based on work by Mollan (1969):

A Dissected Tableland; the Buckland <u>Tableland</u>, a high peneplaned basalt plateau of volcanic origin within the Great Dividing Range. The tableland is interspersed by valleys with steep sided scree covered slopes;

Small Plateau, Mesas and <u>Buttes</u>; With white sandstone and cliffs and <u>volcanics</u>. In some cases sinuous gorges have been cut by streams;

Hogback <u>ridges</u>, cuestas and scarps; sometimes dissected by transverse streams and creeks. Reids Dome is a good example of this type;

Undulating Country; With low relief <u>scarps</u> and ridges broken by mature profile streams and creeks; and Rolling Downs; Flat silty and eroded basaltic soil valley floors and downs.

The great dividing ranges located in the <u>south</u> of the study area separates streams that run north into the Fitzroy River and south into the Darling River (Refer to Figure 8.3.1). The streams and creeks tend to be perennial, however many dried up during the previous drought of the early 1990s.

The source of the Carnarvon <u>Creek</u> is filtered through several hundred meters of Jurassic aged sandstone.

Erosion

Several depositional hiatus and periods of uplift followed by erosion have acted upon the sediments comprising the present day geomorphic surface of the Central Denison Trough. The most significant in terms of sediment removed in the study area is interpreted to have occurred in the mid-Cretaceous.

Another major period of uplift in the area occurred in the Tertiary in conjunction with the formation of the Buckland Volcanic Tableland. Evidence of laterization and other duricrusts (Mollan et al, 1969) possibly associated with the Tertiary volcanics has also been observed in the area.

Human Impact

The study area is mainly agricultural in nature with cattle and sheep stations common. Tourism and hydrocarbon exploration/exploitation also play a part in the area with the Carnarvon National Park and several gas fields and pipelines present. Suggest splitting this last bit up - talk about the tourist stuff separately from the industry stuff. The fertile basaltic soil in the north and east of the study area forms the basis for a thriving agricultural industry growing everything from cotton to cantaloupe.

This far inland however, water is crucial to the area. The farmers always looking for new water supplies commonly approach seismic uphole drilling crews. During the past drought, several farmers without permanent water or bores faced extreme hardships.

Several dams and other irrigation projects have been carried out in the area over the years in an attempt to maintain a consistancy of water supply and to help the water intensive cotton industry in the Emerald area at the northern end of the Denison Trough. If a recent planned dam goes ahead, it will essentially flood the northeastern corner of the study area and will necessitate the shifting of the entire town of Rolleston. All of which will surely leave its mark on the geomorphology of the area.

9.1 DIGITAL TERRAIN MODELS

In rugged areas such as the Central Denison Trough, the type and severity of the terrain is all important in the land use and the erosional process that go on year to year. It was felt that any study of the project area geomorphology should include some modeling of the topography. 3D models were constructed for the study area by digitizing the elevation contours from good quality topographic maps and merged with a regional AUSLIG DTM data set. The contours were then gridded to a cell size similar to the satellite imagery and georeferenced to form an additional band of data.

In this way, the various images could be draped over the terrain and viewed from different prospectives and vertical exaggerations.

Figure 8.3.1 is a view of the study area viewed from the southeast. The highest elevation is in excess of 1000m dropping to 180 masl for the lowest elevation.

9.2 DRAINAGE

Wolley (1942) described the drainage system of the central Denison Trough as superimposition on a folded series of variable erosion resistant strata exhibiting capture and local rejuvenation.

The creeks in the area tend to flow down the regional slopes in broad low relief valleys. Changes in the slope gradient are usually accommodated by changes in the depth and channel shape of the fluvial valleys. Streams and rivers attempt to obtain equilibrium with the landscape by eroding their way down to base level or if coastal, sea level given sufficient time, sediment source and water.

As the slope of the valley floor or the quantity and size of the transported sediment increases, the geometry of a stream tends to change from straight to meandering and then braided. Whether a stream becomes braided or anastomosing depends on if it has eroded into bedrock (anastomosing) or whether it is of a purely depositional form (braided). Need to change this sentence - why have you written it? Why does it mean to your study?

During the <u>meandering</u> phase, a study of the Mississippi River has shown that the meander loops tend to work their way down stream.

The timing of a river or related structural event can some times be deduced by whether the drainage surcumvents or follows the contours of a topographic feature or whether it cuts straight through it. The later usually indicates an older river and

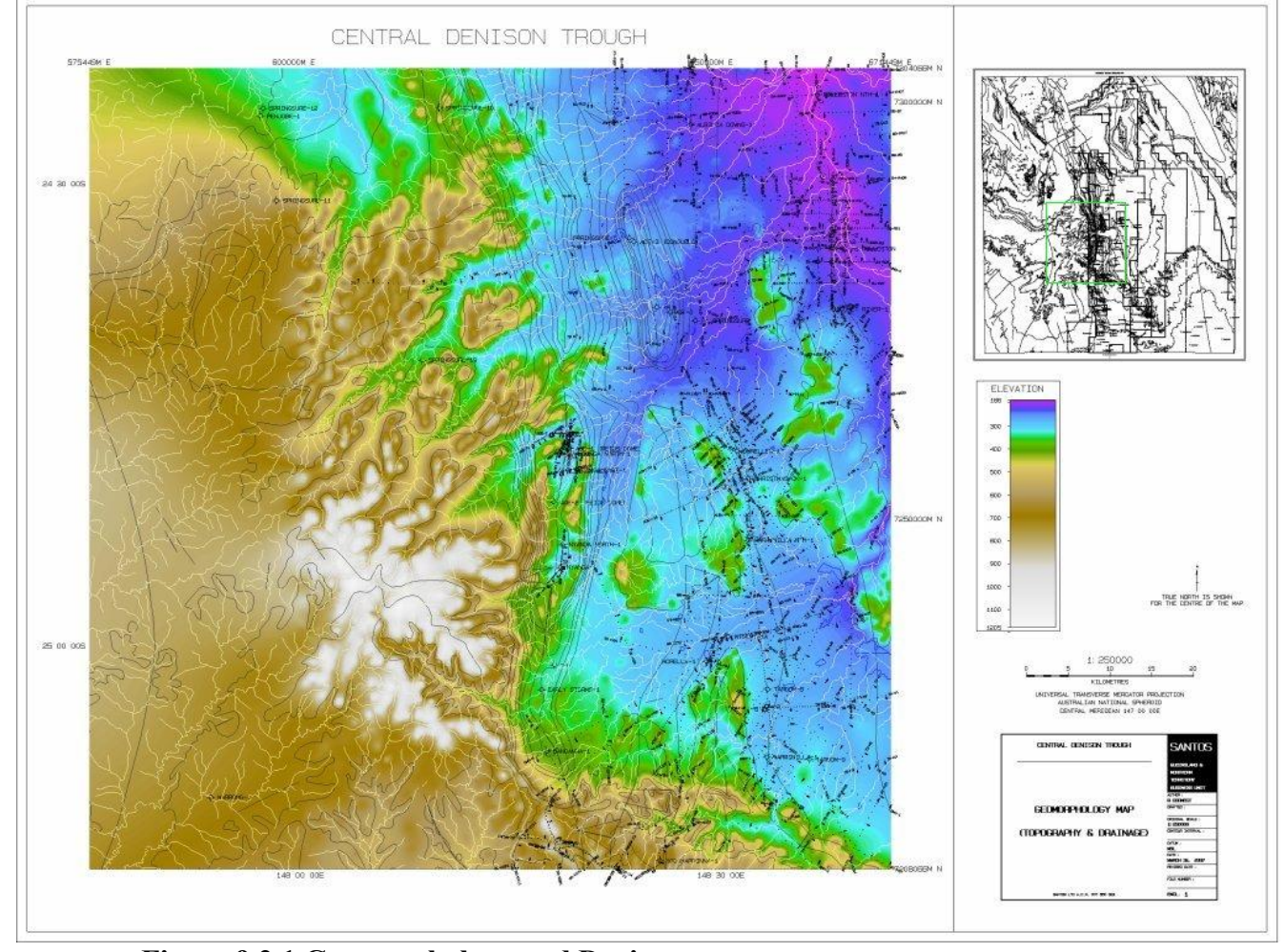


Figure 9.2.1 Geomorphology and Drainage map

structure. Reactivation of the structure or breaching/collapsing of domes can however confuse the issue.

Anomalous stream deflection (high angle) or localised pattern change can often indicate an obscured or buried basement warp feature. These drainage patterns are called structurally controlled streams and can be divided into four main types:

- 1)Locally perturbed drainage pattern; a change in pattern from that of the regional.
- 2) Abrupt changes in drainage pattern; sometimes resulting from an older prexisting stream crossing a buried or reactivated structure.
- 3)Local stream deflection; upon crossing or surcumventing a hidden <u>basement</u> warp feature.
- 4)Localised change in drainage density; can be caused by jointing or a change in slope.

The drainage patterns in the study area vary from dendritic on the scarp slopes between the basalt and sandstone capped ridges (western area) to meandering and anastomosing on the silty plains and valley floors. Possible buried basement warp features or transverse/tear faults are indicated by sudden right angle shifts in the creeks or the join of creek tributaries to the main streams at high angles.

The Study Area was divided into 6 drainage basins. Stream orders were marked and bifurcation ratios for each basin were calculated. However no significant conclusions could be drawn from the ratios other than the drainage pattern containing the most obviously reactivated of the structures, Reids <u>Dome</u>, had the highest 1st to 2nd order ratio, 10:1. This compared to drainage cell <u>3</u>, which had the lowest ratio, 4:1, and contained a large portion of silty valley floor landform.

Additional study is required before any concrete assertions could be made utilising the ratios in this area. A more useful technique may be to create a stream density map by assigning a value of the number of streams per unit grid cell (eg 1 x 1 km) and contouring up the results. This might highlight highly erosive and thereby softer/siltier host rock or steeper slope areas and allow some conclusions to be made.

The drainage cells could also be classified by processing their sinusoidal location data through a Fast Fourier Transform in a similar manner to a seismic trace. This would allow a frequency-based classification in cycles per kilometre realm to take place. The high angle deflection of creeks passing over buried basement warp structures could show up as a particular high frequency peak in the resulting Amplitude versus Frequency plots of the streams. This study however has not yet been carried out.

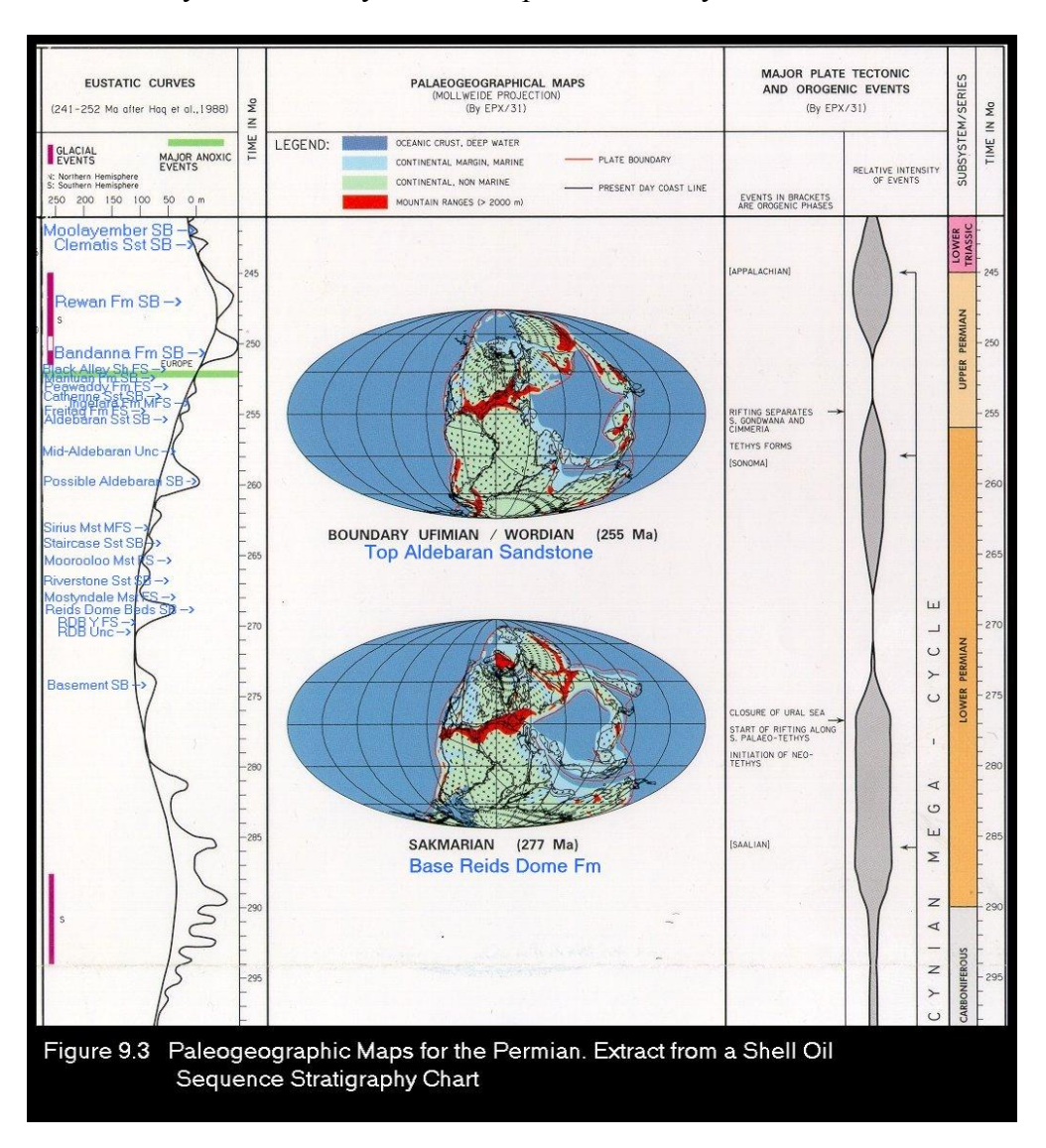
9.3 CLIMATE

The climate of the central Denison Trough ranges from subtropical for the Carnarvon Gorge to temperate for the rest of the area. It's relative elevation, which exceeds a 1000m in places due to its position within the Great Dividing Range. The area has a

dry season between July and October and a rainy season between December and April. Average rainfall for the area is about 66 cm a year with slightly more falling in the western rather than the eastern parts. The study area is located within the band across Australia which is usually swept cloud free due to the prevailing westerly tradewinds.

The study area is just recently coming out of a near decade long drought caused by the El Nina effect which has it's start in the middle of the pacific.

A more detailed climatic study could attempt to recreate the prevailing wind directions of the study area by plotting the continents paleogeographic position trough time and assume a similar latitude based tradewind band and coastal weather patterns as today. This is beyond the scope of this study however.



The paleogeographic setting of Australia during the Permian is shown in Figure 9.3 which is an extract from a Shell Oil Ltd Sequence Stratigraphic Chart. It can be seen from the paleo-reconstructions that The Denison Trough and indeed all of Australia was located farther south than it is present day. Corroberating evidence for this is found in the presence of cold climate drop stones in the Permian aged Ingelara Shale in the Denison Trough (Elliot, 1973).

9.4 DIGITAL TERRAIN CLASSIFICATION

The terrain over the study area was classified using mathematical products derived from the Digital Terrain Model (DTM).

Taking the first horizontal derivative of the DTM in both the X (west-east) and Y (north-south) directions calculated the slope of the terrain. These two images were then merged to approximate the slope in an omnidirectional case.

The curvature or convexity of the terrain was calculated in a similar manner by taking the second derivatives of the DTM and merging.

The Dip Angle was calculated from the DTM using a simple trigonometric routine. The four images, DTM, Slope, Convexity and Dip were then put through a spectral classification which assigned similar values to highly correlatable pixel locations between images.

The spectral classification was put through a context classification which further compared the surrounding 5x5 pixels in it's cluster analysis. It is felt that this image resulted in an approximate classification of the landscape in terms of dip, slope, convexity and elevation. Additional work beyond the scope of this project is required to further test the validity of this methodology and to fine tune the process.

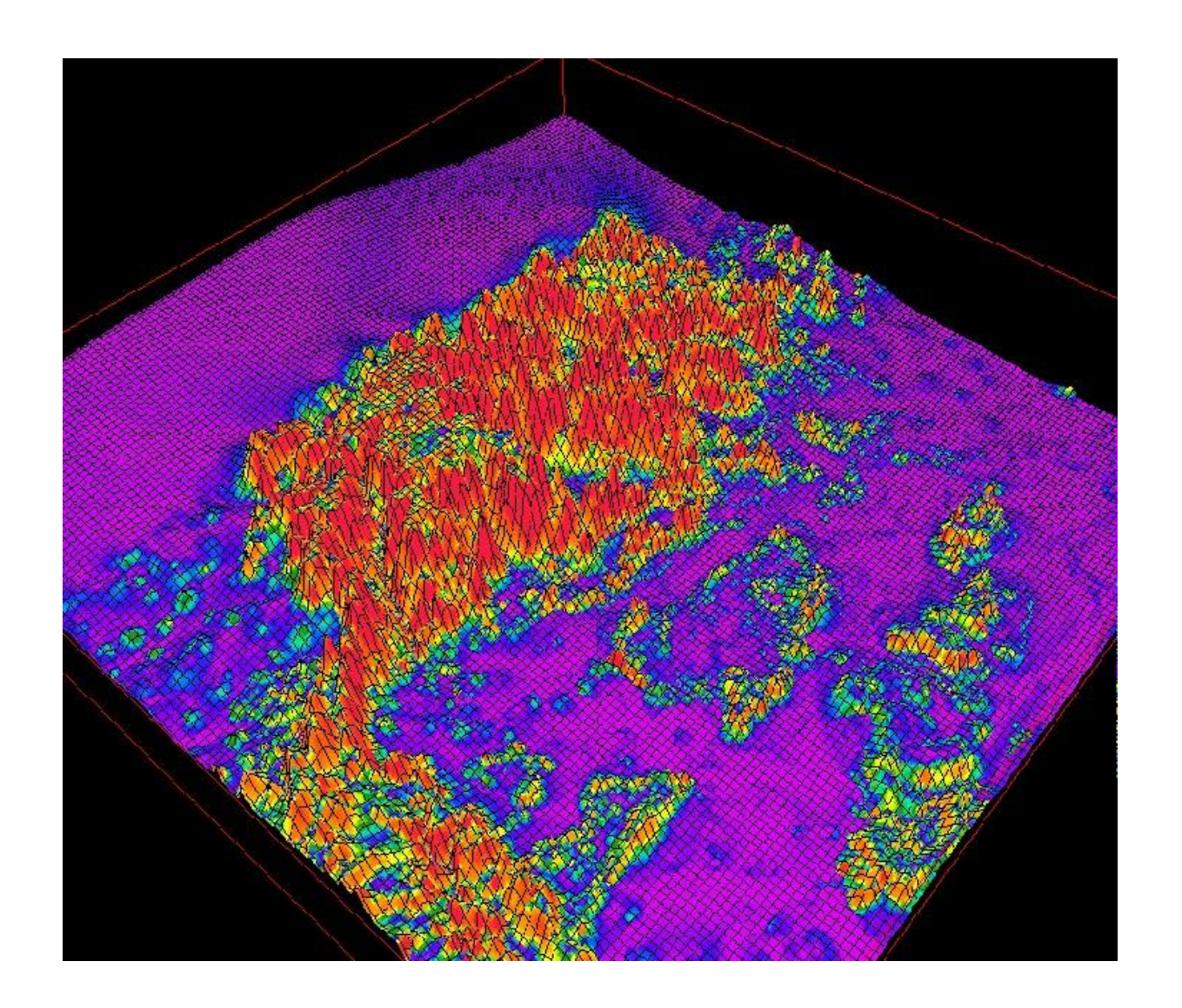


FIGURE 9.4.1 THE DIP IN DEGREES OF DIGITAL TERRAIN MODEL

9.5 GEOBOTANY

Previous study (Wolley 1943, Elliot et al, 1973) of the area had identified the association of certain tree types with particular outcropping formations. The geobotanical association is strong enough in parts of the study area to allow geological mapping based on tree type and ground cover when outcrop is absent or intermitant. The change from one vegetation type to another in the study area was observed by Wolley to be quite sudden.

A more recent study compiled by the department of Environment and Heritage in 1991-94 detailed the vegetation cover in the Carnarvon Gorge area in the form of a map "Park Map, Carnarvon National Park, Carnarvon Gorge Section". The source of the map is based on field traverses and aerial photographic interpretation by Paul Young et al, 1985.

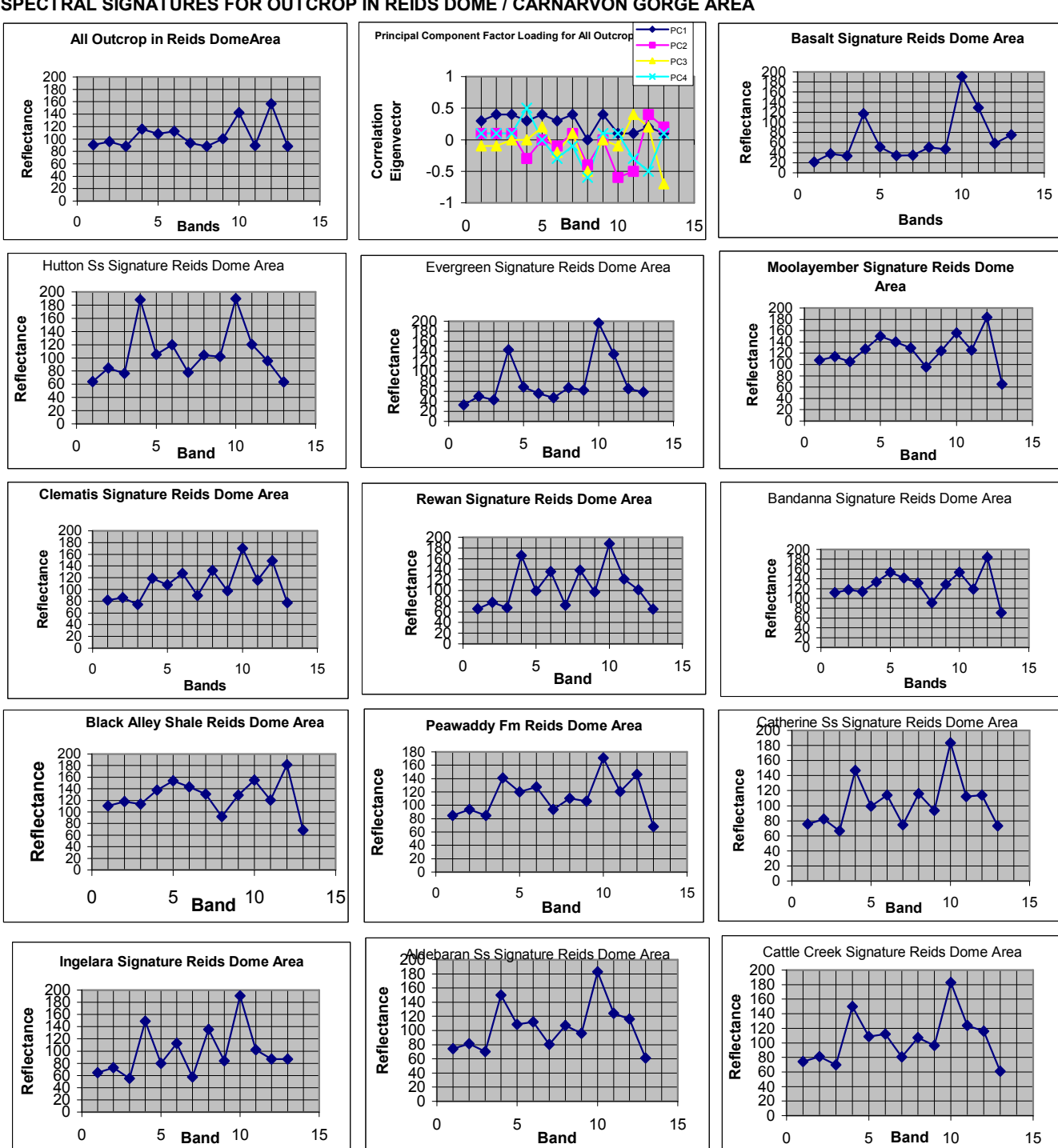
These geobotanical associations and observations were in part what stemmed the idea to map the geology of the area using vegetation "sensitive" satellite imagery. In particular, the infrared bands 4 and 5 of Landsat TM data detect vegetation as pixels having large reflectance values. While only band 2 of the visible bands (green light) is positively sensitive to vegetation, the negative sensitivity of band 3 (red light) is used in a ratio with either band 4 or 5 to quantify vegetation vigor. Usually expressed in the form of a normalised differential vegetation index, NDVI, high values (light tones) of the ratio represent healthy vegetation. The common form of the ratio used in this study is expressed as follows;

NDVI = (band 4 - band 3)/(band 4 + band 3)

Tertiary Basalt

The vegetation of the Tertiary aged basalt Consuello Tableland is tall grassy/shrubby open forest of silvertop stringybark (Eucalyptus *laevpinea*) with some Sydney blue gum (Eucalyptus *saligna*). The Eucalyptus saligna as described by Cronin, can be grows to 20-55m in height with trunk up to 2.5m in diameter. These trees possess a

SPECTRAL SIGNATURES FOR OUTCROP IN REIDS DOME / CARNARVON GORGE AREA



Landsat TM Bands 1-7 Band 8 = Normalised Band 6

Band 9 = Avg of Bands 1 to 5&7

Band 10 = NDVI

Band 11 = PC1

Band 12 = PC2

Band 13 = PC3

Figure 9.5.1

smooth grey to bluish-grey lower bark, which roughens towards the base. More importantly, as seen from above on satellite imagery, a sparse spreading crown is covered in thin shiny dark green leaves. It's preferred habitat is heavy deep soil in wet sclerophyll forests of the coastal regions and lower slopes.

The Consuelo Tableland is very distinctive on airphotos and the thermal infrared band (channel 6) by it's dark tone and flat appearance. The darker low emittance of the thermal band might be due to the heat absorbing qualities of the basalt having a thermal capacity of 0.2 compared to 0.35 for moist clay soils or 0.24 for sandy soils (Refer to Table 9.5 Thermal Properties of Materials). This is supported in the basalt spectral signature from this area which shows a low mean reflectance of 28 (out of a 0-255 range) for band 6 and similar or lower values for the three visible bands (see Appendix G and Figure 9.5.1). It also shows a peak of 120 in band 4 and 191 for the NDVI band.

Moolayember Formation

The vegetation growing on the Moolayember formation in the Carnarvon Gorge is varied. Young et al describes it as comprised predominantly of tall grassy open forest of Turpentine (Syncarpia glomulifera), Grey Gum (Eucalyptus longirostrata), Sydney Blue Gum, Spotted Gum (Eucalyptus Maculata), White Mahogany (Eucalyptus acmenoides), Swamp Mahogany (Lophostemon suaveolons) and by the creeks, Cabbage Palms (Livistona nitida). The predominate feature in the Moolayember Formation's spectral signature is a peak in the infrared band 5 which can partially be attributed to it's sensitivity to vegetaion and to clay content in the soil (see Figure 9.5.1).

An attempt to detail the infrared response of the vegetation was made by shooting matching pairs of visible and infrared photos during the 1997 field trip. Figures 9.5.2 and 9.5.3 show one such pair looking north from Boolimba Bluff towards the Devils signpost. The greater sensitivity and higher contrast is evident in the infra-red photo over the visible shot. The infrared image was shot using black and white infra-red film through an infrared filter which blocks out most visible light (below .7 um wavelength). This corresponds to blocking out Landsat TM bands 1, 2 and 3. With the



Figure 9.5.2 Infrared Photo of Devils Signpost from Boolimba Bluff

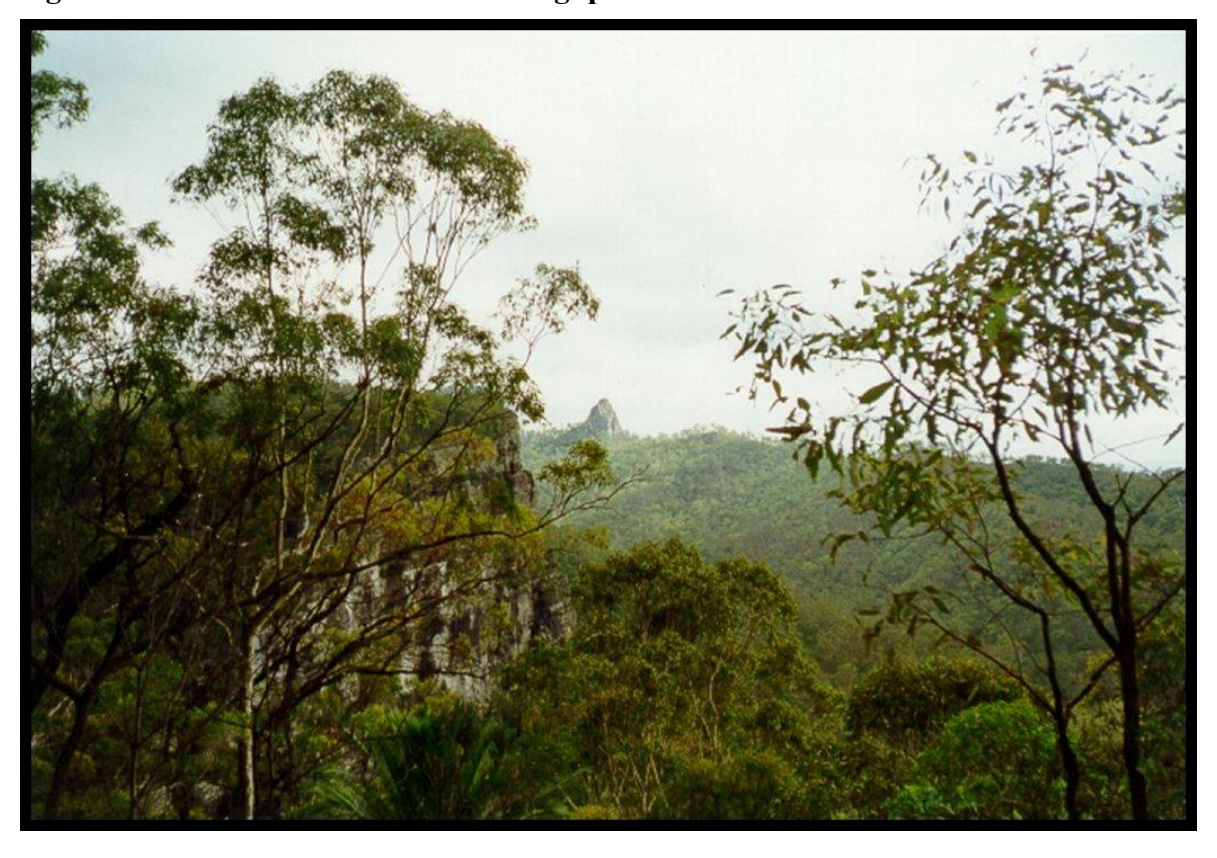


Figure 9.5.3 Visible Photo of Devils Signpost from Boolimba Bluff

sensitivity of the film dropping off above .9 micrometers, the light gathered should approximate a combination of band 4 and 5. The visible photo was shot using 200 ASA film from the same location. The high reflectance of the vegetation is obvious in the bright white appearance of the vegetation compared to the pitch black lack of reflectance from the Precipice Sandstone cliff face. This is dispite the cliffs appearing white in the visible photo amongst a back ground of medium toned green vegetation. It's also interesting to note the greater contrast on the infrared shot between the light colored Spotted gum and the dark trunked Iron bark in the foreground compared to that in the visible photo. The Devils signpost is a Precipice Sandstone erosional remnant overlying the steeply dipping Moolayember Formation.

Aldebaran Sandstone

The Yellow Box <u>orange</u> barked gum tree (Eucalyptus melliodora) distinguishes the Aldebaran Formation from most Permian aged formations (Elliot 1973) in the study area. However contrary to previous observations, the orange barked eucalypt was also observed on Mantuan Formation and Catherine Sandstone outcrop on the eastern flank of Reids Dome (present study) and is probably merely sandstone selective as opposed to Aldebaran and Freitag Formation selective. The orange bark probably doesn't help in the final analysis as it's mainly the leafy crowns of the trees that are seen from the vertical overhead satellite imagery. The visible-infrared photo pair of figures 7.

The spectral signature for the Aldebaran shows a strong peak in band 4 with an absorption low in band 3. This results in an even stronger peak for the NDVI band 11 (displayed as band 10 on graph as the DTM band 8 was left out of the statistics) which is a ratio of the two. The strong absorption in band 7 might mean that a new ratio of band 4 over band 7 might help in distinguishing the Aldebaran formation.

The Eucalyptus Melliodora is a medium sized tree growing 10-30 m in height. It prefers better quality soils in woodlands and open forest mainly on lower western slopes and tablelands. The sandstones in the study area might provide some trace element that improves the soil favouring these orange bark gums

Freitag Formation

Relatively open tree cover of white trunked spotted gum (Eucalyptus maculata) with some black trunked Iron barks (Eucalyptus depranophylla) are the most prevalent over the Freitag Sandstone outcrop. The Eucalyptus maculata can grow up to 50 m and has a dense crown with a smooth and grey and yellow spotted bark. It is generally found in taller open forests prefering sandy soils. Very little grass undergrowth is observed over the siltier areas (Elliot, 1973).

A spectral signature was not created for the Freitag Formation as it was not included in the DME's digital template used to create the supervised classification which the intraband statistics were calculated for.

Ingelara Formation

A black trunked Iron Bark (Eucalyptus siderophloia) dominates the Ingelara Siltstone outcrop where present. The outcrop tends to be sparsely wooded. It's ease of erosion results in very little preserved outcrop compared to the more sandstone prone formations. A thick ground cover of burrs and spear grass is also present above this formation.

The spectral signature of the Ingelara in the Reids Dome area has a strong absorption low in bands 3 and 7 with a strong peak at band 4 and 10 (NDVI). The low at band 7 could be due to clay/siltstone prone nature of the formation. Clay minerals exhibit strong absorption in band 7 and high reflectance in the band 5 part of the spectrum. This signature differs significantly from the Ingelara spectrum generated for the pilot study in the Consuelo Anticline area (Figure 9.5.2). This could be due to lack of atmospheric correction and paucity of values in the earlier study compared to the most recent one or due to significantly different grown cover in the two areas. The latter was not observed in traversing the two areas so it is felt to be a data processing difference. This highlights the importance of properly processing imagery prior to generating signatures.

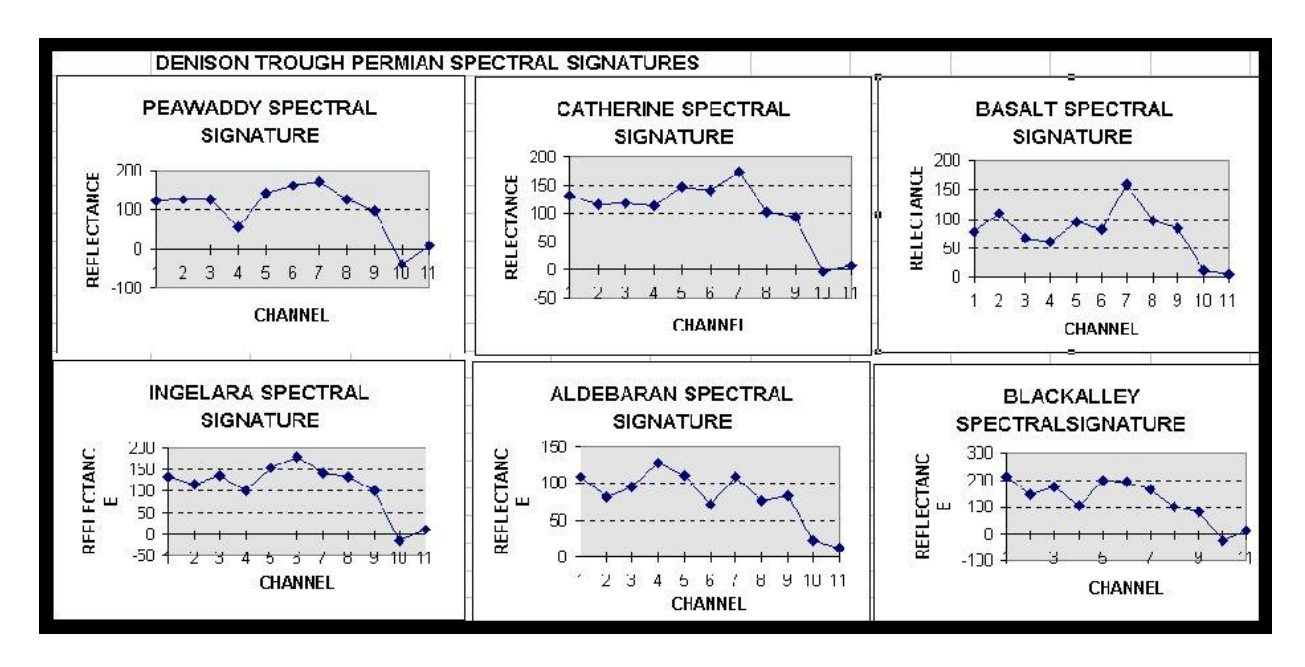


Figure 9.5.4 Uncorrected Spectral Signatures from the Consuelo Area Pilot Study

9.6 SPECTRAL AND CONTEXT CLASSIFICATION

Spectral Classification

A spectral classification of a data set involves the cross plotting of each corresponding pixel value for the different data bands so that a statistical cluster analysis can group the image into a specified number of like classes. Each pixel is represented by an n dimensional number with n corresponding to the number of channels or data bands in the classification. In this way, the image can be broken up into areas of similar spectral signature, which corresponds, to the same ground cover (ie forest, urban, water etc).

Spatial Classification

A context or spatial classification takes this method one step further by taking a spectrally classified image and repeating the process but in one dimension (ie only one input image not n) also taking into account a user specified number of pixels surrounding the cell being operated on. Where the spectral classification might have identified all cells containing vegetation, the context classification will further divide these into pixels with vegetation next to a road or a lake.

Supervised and Unsupervised

Classifications can be either supervised or unsupervised. In the latter, it is left up to the computer to perform a purely statistical analysis of the image. The classes are then identified by maps or ground truthing. In a supervised classification, an unsupervised classification is followed up by assigning particular class signatures and instucting the programme to locate the same signatures throughout the image.

Supervised classifications are viewed by many purists to be unduly biasing what should be a purely statistical process and are therefore given less airtime in this study. Correspondingly, only one of the five areas underwent a supervised classification.

Multitemporal Classification

As the name implies, a multitemporal classification involves the use of a repeat data set in a classification as if they were simply additional data bands. This method while more expensive is ideal for change detection in an area. It also allows for the use of much lower order components when processing the image trough a principal component analysis. This classification technique was not performed however due to the project only having the one vintage of data and is included here for completeness sake only.

The seven bands of the Landsat TM data was rectified then along with the DTM processed through a spectral classification. The spectral classification through a cluster analysis identified areas of high correlation between the eight data channels. Each pixel was grouped into similar classes which were then colour coded and draped over the DTM to aid in the visualisation and identification of the classes with surface features such as outcropping formations, topographic features and similar vegetation/landusage.

The spectral classification was passed through a context classification, which performed a texture classification on the image. This essentially toke into account the surrounding pixels in a sliding five by five matrix and assigned similar density values to each pixel accordingly. This image was also colour coded and draped over the DTM like the spectral classification.

10.0 REGIONAL STRATIGRAPHIC AND STRUCUTURAL INTERPRETATION

A digital version of the Queensland Government Department of Mines and Energy's (DME) solid geology map for Queensland was used as a template over the processed and rectified imagery. The digitising of the finer detail hard copy version of the DME's Solid Geology Map resulted in a smoothed, lower resolution product, which lacked the detail of previous field mapping and photo geologic interpretations of the area.

While the main body of the image processing was originally accomplished using the QIPS processing package, the TerraScan Windows based software package proved useful in selecting the ground control points, subset generation and general data handling. Towards the end of the study however, a more user friendly versions of the ER-Mapper software saw the image processing move to it as the sole processing package due to the depth and flexiblity of the software.

The data was loaded into MapInfo and overlain with the solid geology vector template. The solid geology vector set was altered based on the underlying higher detail imagery.

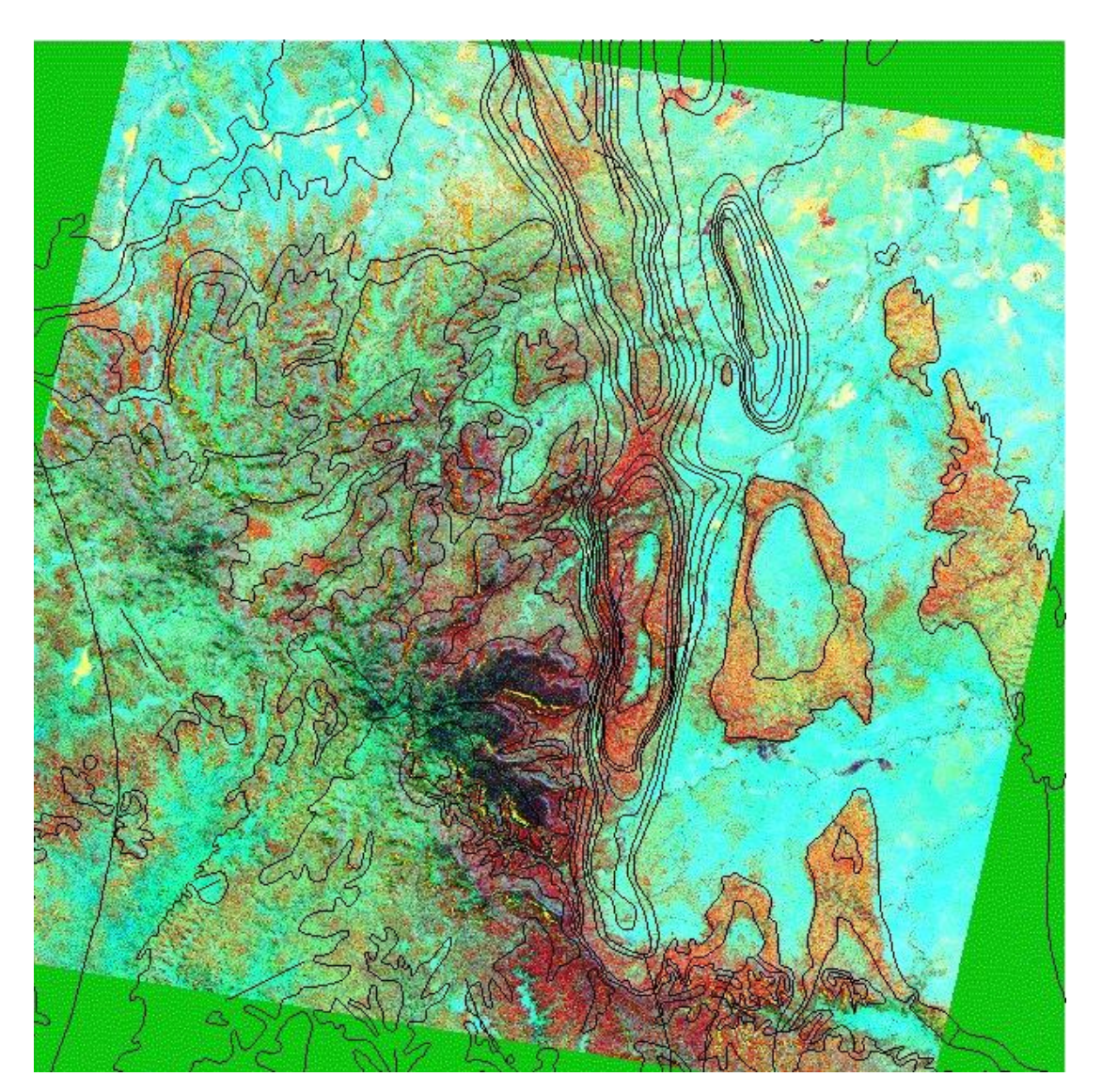


FIGURE 10.1 FALSE COLOR IMAGE OF BAND 7,PC2&6 AS BLUE,GREEN&RED WITH SOLID GEOLOGY VECTOR OVERLAY

The gravity and aeromagnetic data sets were not useful in the spectral and context classifications. Interpretation of the first derivative maps show boundaries which line up with some existing mapped faults on seismic and have a general shape to the some of the currently interpreted basement structure in the area. As with any digital project, most of the work involved simply getting the data loaded into the various software packages due to differences in data format.

10.1 GROUND TRUTHING OF INITIAL INTERPRETATION

The term ground truthing means to investigate and confirm in the field, lineaments or interpreted ground cover types made from imagery interpretation. Several rounds

of ground truthing took place throughout the course of the study. Yearly visits were made to the study area from 1992 to 1996 for the collection of geophysical seismic surveys, geological field trips or the drilling of hydrocarbon exploration wells (Turkey Creek-1& 2, 1993,94 and Dunellen-1, 1994). Two main ground truthing trips to the study area were carried out.

The first took place early during the pilot study when the ground control points were collected using a GPS unit. While it took place over three days, it was mainly road based with the exception of a day long hike up Carnarvon Gorge to Battleship Spur to GPS the apex of this basalt ridge. The vegetation associations of previous studies (Elliot, 1973 et al) with particular outcrops were confirmed.

The second and more significant of the two visits took place in 1997/98 over four days. It's purpose was to ground truth lineaments interpreted from the first pass interpretation of the area and to look for evidence of transverse faulting. It was originally hoped that the presence of slickensides might confirm this. However after visiting the first Mantuan Formation outcrop on the eastern side of Reids Dome it was decided to try and indirectly detect the lateral movement by taking dip and strike measurements (utilising dip and strike measurements). It was felt that any original slickensides would probably been eroded away especially if they were related to later creek formation.

Structural measurements were made on outcrops crossing streams that formed along zones of possible transverse movement.

The majority of the rest of the trip involved the taking of dips and strike measurements along the entire east west length of one of the more continuous lineaments (Refer to Table 3 and Figure 10.1.1).



Figure 10.1.1 Reids Dome with Rose Diagrams from measured Dip & Strike
Possibly showing left lateral movement across Consuelo Creek on both the
Mantuan and Cattle Creek outcrops

The field trip also involved a close investigation of the geobotanic association trying to identify the tree types and associate them with different lithologies/outcrops/formations. In conjunction with the geobotanic association, it was decided to experimented with infrared photography hoping to enhance differences with vegetation. Along all traverses we looked for evidence of structural deformation which might have bore fruit in the sighting of a possible flower structure on the northern side of Christmas Creek just east of Rewan Syncline. If it is authentic it is indirect evidence of wrench tectonics post the Rewan sediments it occurred in.

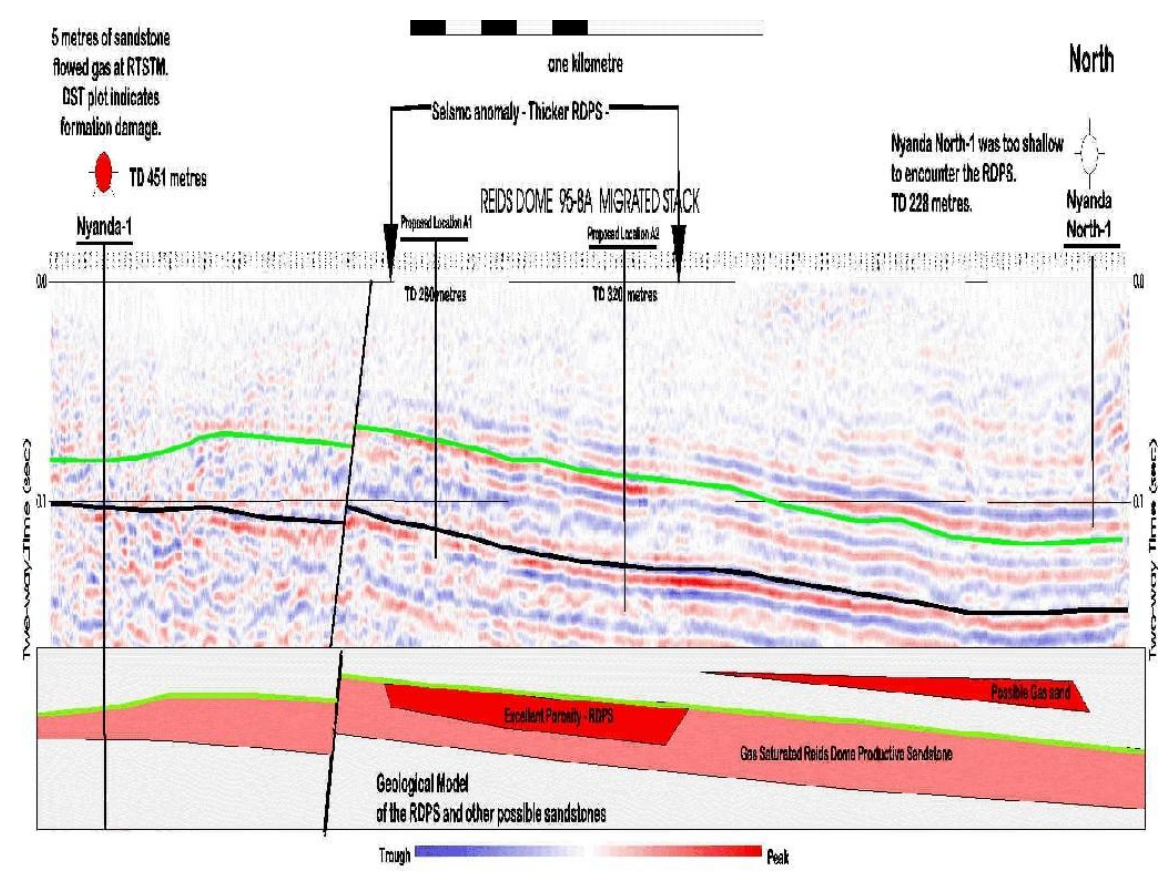


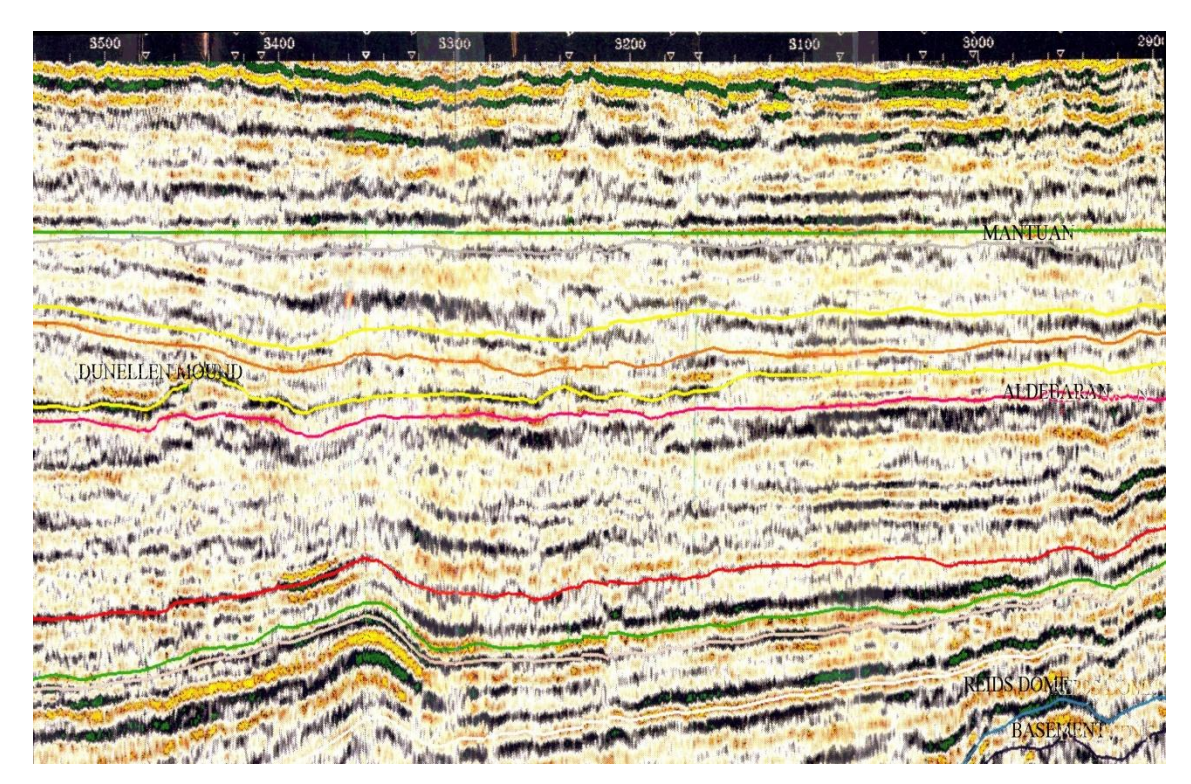
FIGURE 10.1.2 LINE-8, A NORTH-SOUTH SEISMIC LINE ACROSS RIEDS DOME AND LINEAMENT "C" SHOWING NEAR VERTICAL POSSIBLE WRENCH FAULTING EXTENDING TO THE SURFACE (FROM INTERPRETATION BY RON PREFONTAINE for VIC Petroleum, 1997)

The abundance of 2D seismic in the area also has many examples of interpreted high angle normal block faulting which may have significant wrench components to them.

Figures 10.1.2 and 10.1.3 are possible seismic examples in the study area.

In addition to the lineament work, anomalous signatures on the imagery were investigated and in some instances, confirming the presence of crops amongst pasture or wooded areas.

Many of the ground control points were resurveyed using a GPS to confirm the previous measurements used in the rectification of the satellite imagery table.



NORTH SOUTH FIGURE 10.1.3 LINE BMR-2, **NORTH SOUTH** LINE **ACROSS** WARRINILLA ANTICLINE AND LINEAMENT "C: SHOWING POSSIBLE HIGH ANGLE BASEMENT FAULTING. LINE DATUMED ON MANTUAN **FORMATION (INTERPRETATION** BY R CORNECT **FOR PETROLEUM)**

10.1.2 LINEAMENT ANALYSIS

A lineament analysis was performed on the imagery and the interpreted lineaments were exported into the Georient Structural software package to create rose diagrams.

One of the more continuous features, nominally termed Lineament C, starts at the eastern edge of the basalt tableland and extends across Reids Dome trending ENE following Cattle Creek in part. It then continues across to the triangular shaped

IP	DIP DIR	OUTCROP		Easting	Northing	Readin
28	90		STH of Consuelo Crk on Seismic Line			
16		Mantuan				
26	90					
27	53					
27	63		NTH of Consuelo Crk			
26		Mantuan				
54	200		Joint			
30	52					
24	64					
60	274		Joint			
18	116	11	NTH of Cattle Crk by Rd, Orange Brk & Spotted Gum	635694	7248351	
18	86	Mantuan		635448	7248255	
17	108			635502	7248215	
17	102			635485	7248224	
18	86		Photo IR of possible offset	635447	7248172	
90	335		Joint	635447	7248172	
38	142		Possible Transfer Fault with offset & drainage valley	635529	7248031	
90	190		Joint	635529		
20	56		o o n c	635529		
18	86		Near Cattle Crk	000020	1240001	
90	32		Joint			
25	86		STH of Cattle Crk near crk			
			STH OF CALLIE CIK HEAF CIK	G2EEE4	7247600	
18		Mantuan		635554	7247600	
20	68			205222	7017710	
22	85		Orange Bark Gum, Photo of thinnly bed SS	635229	7247746	
16	93		Other & Community Code	00555	704700-	
20	102		Sth of Consuelo Crk	635502	7247638	
24		Cattle Crk	Catherine SS,Sth of Consuelo Crk,IR,IronBrk&Spotted Gum			
20	106		Orange Brk, Bioturbated zone?			
70	326		Joint			
26	106					
26	92		About 400m from Crk at Near Highest pt on Outcrop			
24	96		Catherine SS, Nth of Consuelo Crk,Eastern ledge			
60	78		Joint			
26	50					
26	50					
26	68					
74	66		Joint			
26	50		2nd ledge, Pebble lag			
26	68		Highest pt up Outcrop and from Crk			
58	44		Joint			
24	44		oon.	1		
80	152		Joint with photo of displaced joint			
28	88		Cont. With prioto of displaced joint.	-		
28	82 202			-		
70						
74	44		Western Reids Dome Catherine Out Crop			
136		Catherine				
136	24					
22	80		Joint			
94	74		East Rewan Syncline, Clematis Sandstone,250m Nth of Crk			
74		Clematis Ss	Joint			
74	14					
68	46		Photo of X-Bedding			
78	82		Joint			
60	20					
98	12					
94	80		Joint			
70	14					
56	9		E Rewan Syncline, Sth Christmas Crk, Clematis Ss			
	14					
82	. 350					
82 56	8	Clematis Ss				
56	6 14	Clematis Ss	Iron Bark			
56 86	14	Clematis Ss	Iron Bark			
56 86 74	14 14	Clematis Ss	Iron Bark 400m Sth of Crk			
56 86 74 294	14 14 10	Clematis Ss	Iron Bark 400m Sth of Crk Possible Flower Structure in Christmas Crk, Top of FS			
56 86 74 294 105	14 14 10 89	Clematis Ss 8 Rewan	Iron Bark 400m Sth of Crk			
56 86 74 294 105 62	14 14 10 89 14	Clematis Ss 8 Rewan	Iron Bark 400m Sth of Crk Possible Flower Structure in Christmas Crk, Top of FS Joint			
56 86 74 294 105 62 4	14 14 10 89 14 32	Clematis Ss 8 Rewan	Iron Bark 400m Sth of Crk Possible Flower Structure in Christmas Crk, Top of FS Joint Bottom of FS			
56 86 74 294 105 62 4 88	14 14 10 89 14 32 6	Rewan	Iron Bark 400m Sth of Crk Possible Flower Structure in Christmas Crk, Top of FS Joint Bottom of FS Nuga Nuga Syncline, Nth of Christmas Crk, 400m frm Crk			
56 86 74 294 105 62 4 88 28	14 14 10 89 14 32 6	Rewan 9 Clematis Ss	Iron Bark 400m Sth of Crk Possible Flower Structure in Christmas Crk, Top of FS Joint Bottom of FS Nuga Nuga Syncline, Nth of Christmas Crk, 400m frm Crk Joint			
56 86 74 294 105 62 4 88 28 56	14 14 10 89 14 32 6 78 78	8 Rewan 9 Clematis Ss	Iron Bark 400m Sth of Crk Possible Flower Structure in Christmas Crk, Top of FS Joint Bottom of FS Nuga Nuga Syncline, Nth of Christmas Crk, 400m frm Crk Joint Photo of Joint			
56 86 74 294 105 62 4 88 28 56	14 14 10 89 14 32 6 78 78	Rewan 9 Clematis Ss	Iron Bark 400m Sth of Crk Possible Flower Structure in Christmas Crk, Top of FS Joint Bottom of FS Nuga Nuga Syncline, Nth of Christmas Crk, 400m frm Crk Joint			
56 86 74 294 105 62 4 88 28 56 102 30	14 14 10 89 14 32 6 78 78 11	Rewan 9 Clematis Ss	Iron Bark 400m Sth of Crk Possible Flower Structure in Christmas Crk, Top of FS Joint Bottom of FS Nuga Nuga Syncline, Nth of Christmas Crk, 400m frm Crk Joint Photo of Joint	660053	7258260	
56 86 74 294 105 62 4 88 28 56 102 30 10	14 14 10 89 14 32 6 78 78 11 9	Rewan 9 Clematis Ss	Iron Bark 400m Sth of Crk Possible Flower Structure in Christmas Crk, Top of FS Joint Bottom of FS Nuga Nuga Syncline, Nth of Christmas Crk, 400m frm Crk Joint Photo of Joint Photo of Out Crop	660053	7258260	1 1
56 86 74 294 105 62 4 88 28 56 102 30 10 84	14 14 10 89 14 32 6 78 78 11 9	Rewan 9 Clematis Ss	Iron Bark 400m Sth of Crk Possible Flower Structure in Christmas Crk, Top of FS Joint Bottom of FS Nuga Nuga Syncline, Nth of Christmas Crk, 400m frm Crk Joint Photo of Joint Photo of Out Crop 100m frm Crk	660053	7258260	
56 86 74 294 105 62 4 88 28 56 102 30 10	14 14 10 89 14 32 6 78 78 11 9	Rewan 9 Clematis Ss	Iron Bark 400m Sth of Crk Possible Flower Structure in Christmas Crk, Top of FS Joint Bottom of FS Nuga Nuga Syncline, Nth of Christmas Crk, 400m frm Crk Joint Photo of Joint Photo of Out Crop	660053	7258260	1 1
56 86 74 294 105 62 4 88 28 56 102 30 10 84	14 14 10 89 14 32 6 78 78 11 9	Rewan 9 Clematis Ss	Iron Bark 400m Sth of Crk Possible Flower Structure in Christmas Crk, Top of FS Joint Bottom of FS Nuga Nuga Syncline, Nth of Christmas Crk, 400m frm Crk Joint Photo of Joint Photo of Out Crop 100m frm Crk Sth of Crk, 100m	660053	7258260	
56 86 74 294 105 62 4 88 28 56 102 30 10 84	14 14 10 89 14 32 6 78 78 11 9 13 9	Rewan 9 Clematis Ss 10 Clematis Ss	Iron Bark 400m Sth of Crk Possible Flower Structure in Christmas Crk, Top of FS Joint Bottom of FS Nuga Nuga Syncline, Nth of Christmas Crk, 400m frm Crk Joint Photo of Joint Photo of Out Crop 100m frm Crk Sth of Crk, 100m	660053	7258260	1 1
56 86 74 294 105 62 4 88 28 56 102 30 10 84 19	14 14 10 89 14 32 6 78 78 11 9 13 9 22 22	Rewan 9 Clematis Ss 10 Clematis Ss	Iron Bark 400m Sth of Crk Possible Flower Structure in Christmas Crk, Top of FS Joint Bottom of FS Nuga Nuga Syncline, Nth of Christmas Crk, 400m frm Crk Joint Photo of Joint Photo of Out Crop 100m frm Crk Sth of Crk, 100m Iron Bark	660053	7258260	1 1
56 86 74 294 105 62 4 88 28 56 102 30 10 84 19 10 41 86	14 14 10 89 14 32 6 78 11 9 13 9 22 22 6 8	Rewan 9 Clematis Ss 10 Clematis Ss	Iron Bark 400m Sth of Crk Possible Flower Structure in Christmas Crk, Top of FS Joint Bottom of FS Nuga Nuga Syncline, Nth of Christmas Crk, 400m frm Crk Joint Photo of Joint Photo of Out Crop 100m frm Crk Sth of Crk, 100m Iron Bark Photo of X&Trough Bedding 400m frm Crk	660053	7258260	1 1
56 86 74 294 105 62 4 88 28 56 102 30 10 84 19 10 41 41 86 40	14 14 10 89 14 32 6 78 78 11 9 22 22 6 8	Rewan 9 Clematis Ss 10 Clematis Ss	Iron Bark 400m Sth of Crk Possible Flower Structure in Christmas Crk, Top of FS Joint Bottom of FS Nuga Nuga Syncline, Nth of Christmas Crk, 400m frm Crk Joint Photo of Joint Photo of Out Crop 100m frm Crk Sth of Crk, 100m Iron Bark Photo of X&Trough Bedding 400m frm Crk West Rewan Syncline, Clematis Ss, Nth of Crk, 400m frm Crk	660053	7258260	1 1
56 86 74 294 105 62 4 88 28 56 102 30 10 84 19 10 41 46 40 60	14 14 10 89 14 32 6 78 78 11 9 22 22 26 8 18	Rewan 9 Clematis Ss 10 Clematis Ss	Iron Bark 400m Sth of Crk Possible Flower Structure in Christmas Crk, Top of FS Joint Bottom of FS Nuga Nuga Syncline, Nth of Christmas Crk, 400m frm Crk Joint Photo of Joint Photo of Joint Photo of Out Crop 100m frm Crk Sth of Crk, 100m Iron Bark Photo of X&Trough Bedding 400m frm Crk West Rewan Syncline, Clematis Ss, Nth of Crk, 400m frm Crk Rough Brk Grey Gum & Spotted	660053	7258260	
56 86 74 294 105 62 4 88 28 56 102 30 10 84 19 10 41 86 40 60 102	14 14 10 89 14 32 6 78 78 11 9 22 22 22 8 8 18 18	Rewan 9 Clematis Ss 10 Clematis Ss 13 Clematis Ss	Iron Bark 400m Sth of Crk Possible Flower Structure in Christmas Crk, Top of FS Joint Bottom of FS Nuga Nuga Syncline, Nth of Christmas Crk, 400m frm Crk Joint Photo of Joint Photo of Out Crop 100m frm Crk Sth of Crk, 100m Iron Bark Photo of X&Trough Bedding 400m frm Crk West Rewan Syncline, Clematis Ss, Nth of Crk, 400m frm Crk	660053	7258260	
56 86 74 294 105 62 4 88 28 56 102 30 10 84 19 10 41 86 40 60 00 102 80	14 14 10 89 14 32 6 78 78 11 9 22 22 6 8 18 18	Rewan 9 Clematis Ss 10 Clematis Ss 13 Clematis Ss	Iron Bark 400m Sth of Crk Possible Flower Structure in Christmas Crk, Top of FS Joint Bottom of FS Nuga Nuga Syncline, Nth of Christmas Crk, 400m frm Crk Joint Photo of Joint Photo of Joint Photo of Out Crop 100m frm Crk Sth of Crk, 100m Iron Bark Photo of X&Trough Bedding 400m frm Crk West Rewan Syncline, Clematis Ss, Nth of Crk, 400m frm Crk Rough Brk Grey Gum & Spotted	660053	7258260	
56 86 74 294 105 62 4 88 56 102 30 10 84 19 10 41 86 40 60 102 89 39	14 14 10 89 14 32 6 78 78 11 9 22 22 6 8 18 18 90 24	Rewan 9 Clematis Ss 10 Clematis Ss	Iron Bark 400m Sth of Crk Possible Flower Structure in Christmas Crk, Top of FS Joint Bottom of FS Nuga Nuga Syncline, Nth of Christmas Crk, 400m frm Crk Joint Photo of Joint Photo of Joint Photo of Out Crop 100m frm Crk Sth of Crk, 100m Iron Bark Photo of X&Trough Bedding 400m frm Crk West Rewan Syncline, Clematis Ss, Nth of Crk, 400m frm Crk Rough Brk Grey Gum & Spotted	660053	7258260	
56 86 74 105 62 4 88 28 56 102 30 10 84 19 41 86 60 102 80 93 76	14 14 10 89 14 32 6 78 78 11 9 13 9 22 22 6 8 8 18 18 90 24	Rewan 9 Clematis Ss 10 Clematis Ss	Iron Bark 400m Sth of Crk Possible Flower Structure in Christmas Crk, Top of FS Joint Bottom of FS Nuga Nuga Syncline, Nth of Christmas Crk, 400m frm Crk Joint Photo of Joint Photo of Out Crop 100m frm Crk Sth of Crk, 100m Iron Bark Photo of X&Trough Bedding 400m frm Crk West Rewan Syncline, Clematis Ss, Nth of Crk, 400m frm Crk Rough Brk Grey Gum & Spotted Joint	660053	7258260	
56 86 74 105 62 294 105 62 4 88 88 28 56 102 84 19 10 10 41 86 60 102 80 93 3 76 3	14 14 10 89 14 32 6 78 78 11 9 22 22 6 8 18 18 90 24 18	Rewan 9 Clematis Ss 10 Clematis Ss 13 Clematis Ss	Iron Bark 400m Sth of Crk Possible Flower Structure in Christmas Crk, Top of FS Joint Bottom of FS Nuga Nuga Syncline, Nth of Christmas Crk, 400m frm Crk Joint Photo of Joint Photo of Out Crop 100m frm Crk Sth of Crk, 100m Iron Bark Photo of X&Trough Bedding 400m frm Crk West Rewan Syncline, Clematis Ss, Nth of Crk, 400m frm Crk Rough Brk Grey Gum & Spotted Joint	660053	7258260	1 10
56 86 74 294 105 62 4 88 88 28 102 30 10 41 19 10 60 102 80 93 76 63 64	14 14 10 89 14 32 6 78 78 11 9 22 22 22 6 8 18 90 24 4 18 32 72	Rewan 9 Clematis Ss 10 Clematis Ss 13 Clematis Ss	Iron Bark 400m Sth of Crk Possible Flower Structure in Christmas Crk, Top of FS Joint Bottom of FS Nuga Nuga Syncline, Nth of Christmas Crk, 400m frm Crk Joint Photo of Joint Photo of Out Crop 100m frm Crk Sth of Crk, 100m Iron Bark Photo of X&Trough Bedding 400m frm Crk West Rewan Syncline, Clematis Ss, Nth of Crk, 400m frm Crk Rough Brk Grey Gum & Spotted Joint Joint West Rewan Syncline	660053	7258260	1
56 86 74 105 62 294 105 62 28 56 102 84 19 10 10 10 10 10 10 2 80 93 3 76 3	14 14 10 89 14 32 6 78 78 11 9 22 22 22 6 8 18 90 24 4 18 32 72	Rewan 9 Clematis Ss 10 Clematis Ss 13 Clematis Ss	Iron Bark 400m Sth of Crk Possible Flower Structure in Christmas Crk, Top of FS Joint Bottom of FS Nuga Nuga Syncline, Nth of Christmas Crk, 400m frm Crk Joint Photo of Joint Photo of Out Crop 100m frm Crk Sth of Crk, 100m Iron Bark Photo of X&Trough Bedding 400m frm Crk West Rewan Syncline, Clematis Ss, Nth of Crk, 400m frm Crk Rough Brk Grey Gum & Spotted Joint Joint West Rewan Syncline	660053	7258260	1 10
56 86 74 294 105 62 4 88 88 28 102 30 100 41 41 9 60 60 93 76 80 93 76	14 14 10 89 14 32 6 78 78 71 11 9 22 22 6 8 8 18 18 90 24 18	Rewan 9 Clematis Ss 10 Clematis Ss 13 Clematis Ss	Iron Bark 400m Sth of Crk Possible Flower Structure in Christmas Crk, Top of FS Joint Bottom of FS Nuga Nuga Syncline, Nth of Christmas Crk, 400m frm Crk Joint Photo of Joint Photo of Out Crop 100m frm Crk Sth of Crk, 100m Iron Bark Photo of X&Trough Bedding 400m frm Crk West Rewan Syncline, Clematis Ss, Nth of Crk, 400m frm Crk Rough Brk Grey Gum & Spotted Joint Joint West Rewan Syncline	660053	7258260	1 10
56 86 74 294 105 62 4 88 88 28 30 10 84 19 10 10 86 40 10 28 80 80 80 80 80 80 80 80 80 80 80 80 80	14 14 10 89 14 32 6 78 78 11 9 22 22 6 8 18 18 90 24 18 32 27 24	Rewan 10 Clematis Ss 13 Clematis Ss	Iron Bark 400m Sth of Crk Possible Flower Structure in Christmas Crk, Top of FS Joint Bottom of FS Nuga Nuga Syncline, Nth of Christmas Crk, 400m frm Crk Joint Photo of Joint Photo of Out Crop 100m frm Crk Sth of Crk, 100m Iron Bark Photo of X&Trough Bedding 400m frm Crk West Rewan Syncline, Clematis Ss, Nth of Crk, 400m frm Crk Rough Brk Grey Gum & Spotted Joint Joint West Rewan Syncline	660053	7258260	
56 86 74 294 105 62 4 88 88 28 86 102 30 10 41 86 60 102 28 93 76 63 84 93 88 93 88 93 88 94	14 14 10 89 14 32 6 78 78 11 9 22 22 22 22 22 22 22 22 22 22 22 22 2	Rewan 9 Clematis Ss 10 Clematis Ss 13 Clematis Ss	Iron Bark 400m Sth of Crk Possible Flower Structure in Christmas Crk, Top of FS Joint Bottom of FS Nuga Nuga Syncline, Nth of Christmas Crk, 400m frm Crk Joint Photo of Joint Photo of Out Crop 100m frm Crk Sth of Crk, 100m Iron Bark Photo of X&Trough Bedding 400m frm Crk West Rewan Syncline, Clematis Ss, Nth of Crk, 400m frm Crk Rough Brk Grey Gum & Spotted Joint Joint West Rewan Syncline	660053	7258260	1 10
56 86 74 294 105 62 4 88 56 102 10 84 11 91 10 80 93 3 64 88 88 88 88 88 88	14 14 10 89 14 32 6 78 78 71 11 9 22 22 6 8 8 18 18 19 24 18 24 18 24 18 24 18 24 18 24 18 24 24 25 26 26 27 27 27 27 27 27 27 27 27 27 27 27 27	Rewan 9 Clematis Ss 10 Clematis Ss 13 Clematis Ss	Iron Bark 400m Sth of Crk Possible Flower Structure in Christmas Crk, Top of FS Joint Bottom of FS Nuga Nuga Syncline, Nth of Christmas Crk, 400m frm Crk Joint Photo of Joint Photo of Out Crop 100m frm Crk Sth of Crk, 100m Iron Bark Photo of X&Trough Bedding 400m frm Crk West Rewan Syncline, Clematis Ss, Nth of Crk, 400m frm Crk Rough Brk Grey Gum & Spotted Joint Joint West Rewan Syncline Joint	660053	7258260	1 10
56 86 86 86 86 86 86 86 86 86 86 86 86 86	14 14 10 89 14 32 6 78 78 11 9 22 22 6 8 18 18 90 24 18 32 72 72 72 14 22 72 72	Rewan 9 Clematis Ss 10 Clematis Ss 13 Clematis Ss	Iron Bark 400m Sth of Crk Possible Flower Structure in Christmas Crk, Top of FS Joint Bottom of FS Nuga Nuga Syncline, Nth of Christmas Crk, 400m frm Crk Joint Photo of Joint Photo of Out Crop 100m frm Crk Sth of Crk, 100m Iron Bark Photo of X&Trough Bedding 400m frm Crk West Rewan Syncline, Clematis Ss, Nth of Crk, 400m frm Crk Rough Brk Grey Gum & Spotted Joint Joint West Rewan Syncline Joint	660053	7258260	1

Table 3 Dip and Strike measurements from ground truthing field trip

Rewan Syncline joining up with Christmas Creek cutting across the Warrinilla Anticline and finally transecting the Nuga Nuga Syncline some 45 kms to the north east from it's start. The results were plotted on rose diagrams and stereos plots using the Georient software package some of the results are shown in Figure 10.1.1



FIGURE 10.1.4 STANDARDISED DIFFERENCE IMAGE OF REIDS DOME – BAND4/7,4,6 AS B,G,R -AVG BANDS 1TO 7 NO BAND 6.

While the lineament analysis for this study was carried out on a three band false color image (Refer to Figure 3.1.2) the more traditional method is to use a grey scale image of a single band containing maximu variation such as PC 1 or Landsat Band 5.

The image is then sun shaded from different directions and lineaments are interpreted. Short interpretation times are used and only fully connected lineaments are interpreted. This is to avoid connecting linear segments together across gaps which can lead to interpreting imaginary lineaments.

This best practise was ignored due to the obviousness of the structural offsets and the need to focus on and highlight the 70 degree trending postulated deformation zones. Possible additional lineament work on the study area could involve following the above mentioned single band sun shaded methodology.

10.3 A GENERALISED REMOTE SENSING METHODOLOGY FOR GEOLOGICAL IDENTIFICATION OF THE SURFACE

By summarising the methodology used in this study, a generalised procedure for the geological identification of the surface using remotely sensed data can be stated as a guide for other studies in a similar geological setting.

- Initial field trip to familiarise with the geomorphic relationships and to view easily accessible outcrop of the area to be studied. This step can also be used to select a small pilot area to investigate first.
- 2. Obtain existing Geological outcrop data of the area to be studied in a digital format for use as a template.
- Selection of the most appropriate Satellite imagery depending on availability, local topography, ground cover, geobotonical associations and degree of surficial cover of outcrop.
- 4. Acquisition of appropriate satellite imagery during the appropriate time of the year in terms of the areas vegetation cover and rainfall. This will depend on whether the area has a geobotanical association or if the vegetation is merely a cover masking the true nature of the geological outcrop.
- 5. Processing of imagery including atmospheric compensation, topographic compensation, noise reduction, image enhancement, principal component analysis, standardization and georeferencing.
- 6. Intermediate ground truthing and collection or verification of georeferencing points with GPS or preexisting survey points.
- 7. Creation of a digital terrain model of the area to aid in visualising the area by combining with the imagery.

- 8. Creation of spectral signatures for each formation to be mapped by plotting data from each band or principal component on a formation by formation basis in a spreadsheet. This should highlight the most relevant bands for each formation.
- 9. Second processing phase focusing on the most relevant bands of data to be included in a directed principal component analysis, an unsupervised spectral classification and a context classification.
- 10. Interpretation of classified data with existing geological vector overlay as a template.
- 11. Lineament analysis of the area utilising rose diagrams and stereoplots to confirm structural interpretation of the area from the imagery and previous geological studies
- 12. Final ground truthing of area to confirm lineaments and classification of imagery to geology and not to agricultural variation in the area.
- 13. Refinement of the interpretation based on ground truthing and directed supervised classification of the imagery focusing primarily on those bands of data and their derivatives shown to highlight the geology. Followed by a write up of the study.
- 14. If time and budget permits, the above methodology can initially be carried out over a small pilot area which is deemed to have the best chance of succeeding prior to investing the time and money into a larger study which might not bare results.

The work flow used in this study is a modification Taylor's (1991) preferred methodology. The main differences are the addition of a standardization step—for the image processing which Taylor only alludes to in compensting for topographic effects, the use of the digital terrain map as an additional band of data, the use of a texture or context classification step after the spectral classification and a supervised classification step to derive statistics for comparing each band of data with each geological outcrop. This last step allows for additional refinement processing using a directed or selective principal component analysis or supervised classification approach.

11.0 RESULTS AND CONCLUSIONS

The "Structural and Stratigraphic Interpretation of the Central Denison Trough Using Remotely Sensed Data" Project resulted in the following:

An approximate classification of the landscape of the study area based on elevation, slope, and convexity and dip angle.

Spectral signatures for the outcropping Permian and younger aged sediments were created using normal imagery and imagery processed trough a Principal Component Analysis (PCA). The PCA of the data followed the removal of atmospheric and albedo effects from the data.

Suggestions for modification of the digital version of the Bowen Basin Solid Geology Map provided by the Queensland Department of Mines and Energy (Beta Version) as an overlay, have been made based on this study.

The identification of possible inter-grabenal shear zones or Transfer Corridors on satellite imagery, airphotos, seismic sections and aeromag maps.

Sharp deflections in the drainage pattern were used to identify possible subsurface structuring. These possible zones of deformation if real, could have significance to hydrocarbon migration and accumulation in the area.

A predominantly dendritic to incised meandering drainage pattern was found over the project area. The study area was divided into six drainage basins for the calculation of bifurcation ratios. The drainage cell containing Reid's Dome had the highest bifurcation ratio of the drainage cells, which may indicate a higher level of deformation than the surrounding cells.

It is felt that the ground work has been laid for further remote sensing based geological study in the Central Denison Trough. The further refinement of the spectral signatures characteristic to each Permian aged outcrop could be enhanced and applied to the surrounding area to either confirm or modify the existing geological interpretation.

The image processing methodology developed for this study has already been applied to 3D seismic data and most recently to a 3D seismic volume on the North West Shelf to map depositional environments using seismic stratigraphic techniques. Preliminary results of the study were presented at an Advanced Interpretation Workshop held by Shell Oil in the Haag, 1998.

Possible follow on work from the study includes construction of a 3D volume from seven bands of Landsat TM data. This would allow the use of seismic body tracking software to correlate and visualise the continuity of the data in a three dimensional sense.



The Mineral Potential of the Central Denison Trough using modern ASTER, Sentinel-2, Landsat-9 and USGS Hyperion Hyperspectral Imagery

Master of Philosophy Thesis for the

Earth Sciences Department, University of Queensland

By Robert J. Cornect

Jan 1, 2025

Supervised by Dr Tony Webster

Statement of Sources

I hereby declare that the work presented in this thesis, to the best of my knowledge and belief, is original work, except as acknowledged in the text, and that the material has not been submitted, either in whole or in part, for a degree at this or any other university.

Robert J. Cornect Jan 1, 2025

II.1 Introduction

After 25 years in Care and Maintenance, it was decided to revisit the Denison Trough Geology Thesis area using modern satellite imagery, and compare and contrast any new observations with the original study. A secondary objective is to highlight any Mineral potential of the study area capitalising on recent techniques used in the Iron Ore and Critical Minerals exploration in the Pilbara and Yilgarn cratons in WA.

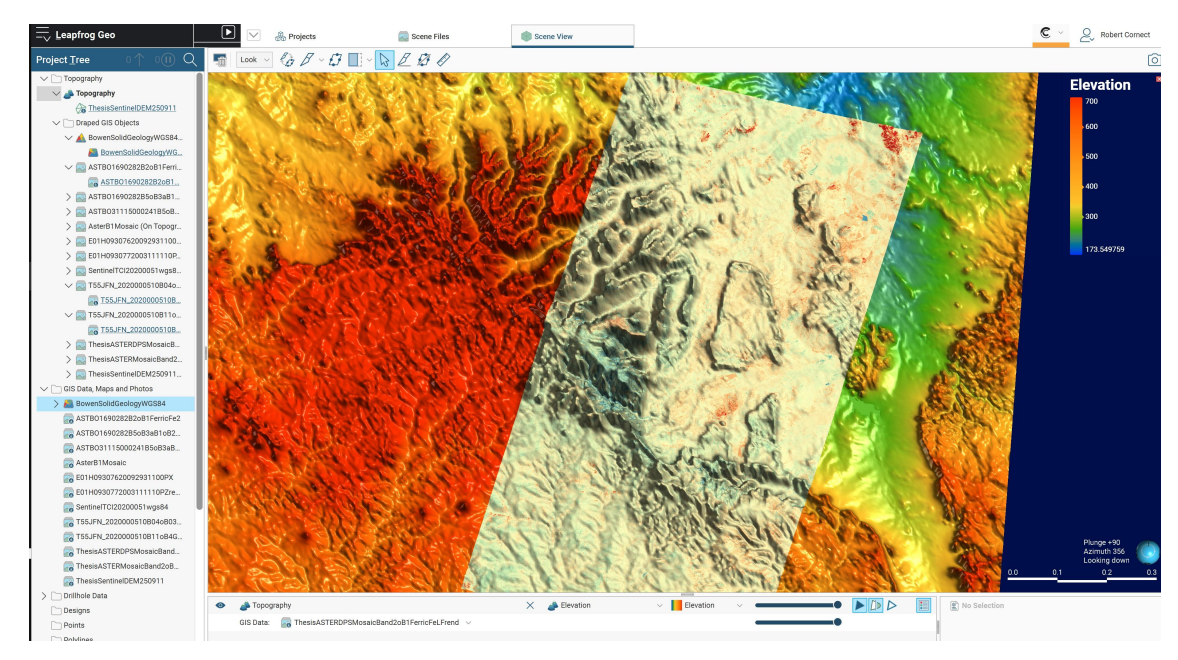


Figure II.1 Thesis area Ferric Fe ASTER Mosaic Band 3 /Band 1 Ratio Draped over DEM

The original study used primarily a 7 band Landsat 5 Thematic Mapper data set with a 30 m resolution and spectral response ranging from optical blue to thermal infrared the later of which had only 120m x120 m pixels.

ASTER Instrument Characteristics

Characteristic	VNIR	SWIR	TIR
Spectral Range	Band 1: 0.52 - 0.60 µm Nadir looking	Band 4: 1.600 - 1.700 μm	Band 10: 8.125 - 8.475 μm
	Band 2: 0.63 - 0.69 µm Nadir looking	Band 5: 2.145 - 2.185 μm	Band 11: 8.475 - 8.825 μm
	Band 3: 0.76 - 0.86 µm Nadir looking	Band 6: 2.185 - 2.225 μm	Band 12: 8.925 - 9.275 μm
	Band 3: 0.76 - 0.86 µm Backward looking	Band 7: 2.235 - 2.285 μm	Band 13: 10.25 - 10.95 μm
		Band 8: 2.295 - 2.365 µm	Band 14: 10.95 - 11.65 µm
		Band 9: 2.360 - 2.430 μm	
Ground Resolution	15 m	30m	90m
Data Rate (Mbits/sec)	62	23	4.2
Cross-track Pointing (deg.)	±24	±8.55	±8.55
Cross-track Pointing (km)	±318	±116	±116
Swath Width (km)	60	60	60
Detector Type	Si	PtSi-Si	HgCdTe
Quantization (bits)	8	8	12
System Response	VNIR Chart	SWIR Chart	TIR Chart
Function	VNIR Data	SWIR Data	TIR Data
AST	ER bands superimpo	sed on model atmosph	nere

Figure II.1 ASTER Image Characteristics, Resolution and Spectral Response

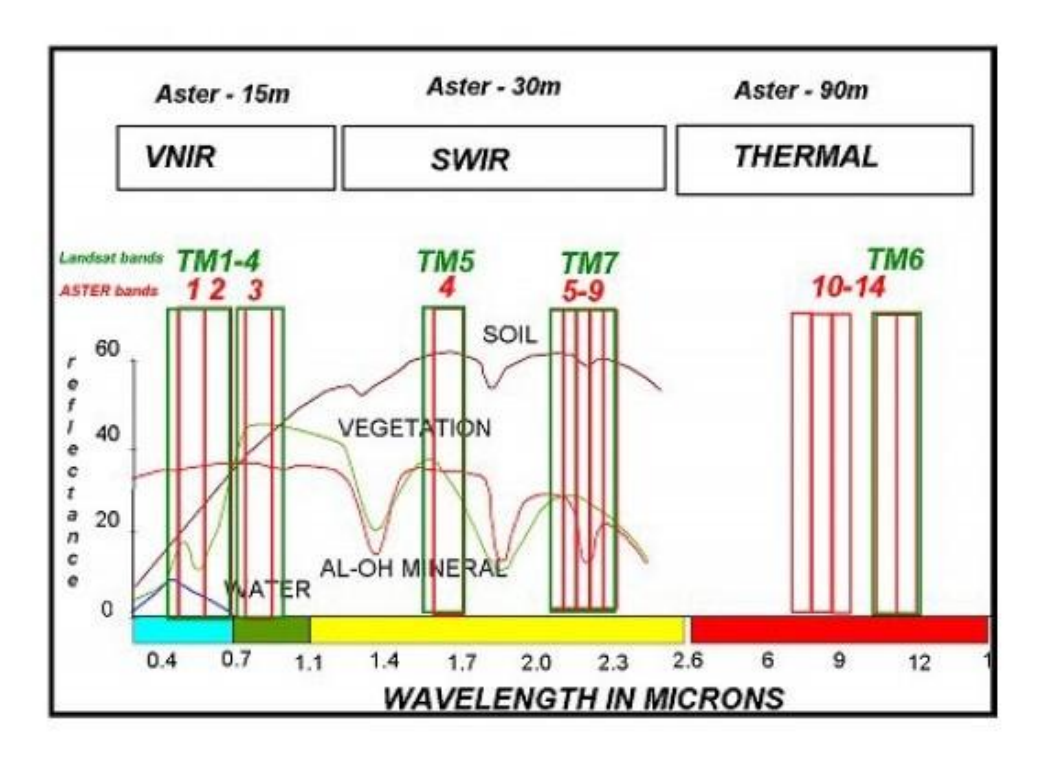


Figure II.2 Comparison of the electromagnetic response for each data band in both Landsat and ASTER

II.2 ASTER Data

The current study utilizes 2 scenes of ASTER imagery mosaiced together along with imagery from the Sentinel-2, USGS Landsat-9 OLI and Hyperion EO-1 hyperspectral satellites. The figure II.1 above shows the 14 band ASTER Instrument Characteristics but essentually comprises 4 bands of visual data from green to near Infra-red at 15x15m resolution, 6 bands of Short Wave infrared (SWIR) data at 30x30m resolution and 5 bands of Thermal infrared (TIR) data at 90x90m resolution. A mosaic of the SWIR band 8 is shown below generated in QGIS.

The spectral response for the various data bands in both the Landsat and ASTER satellites shown in figure 2.11.2 allows for a like for like comparison in any bands of similar wavelength coverage. This should help in comparing results from the original thesis which used Landsat 5 imagery and this current Part II study which utilizes the newer generation ASTER, Sentinel, Landsat-9 OLI and Hyperion EO-1 satellite data.

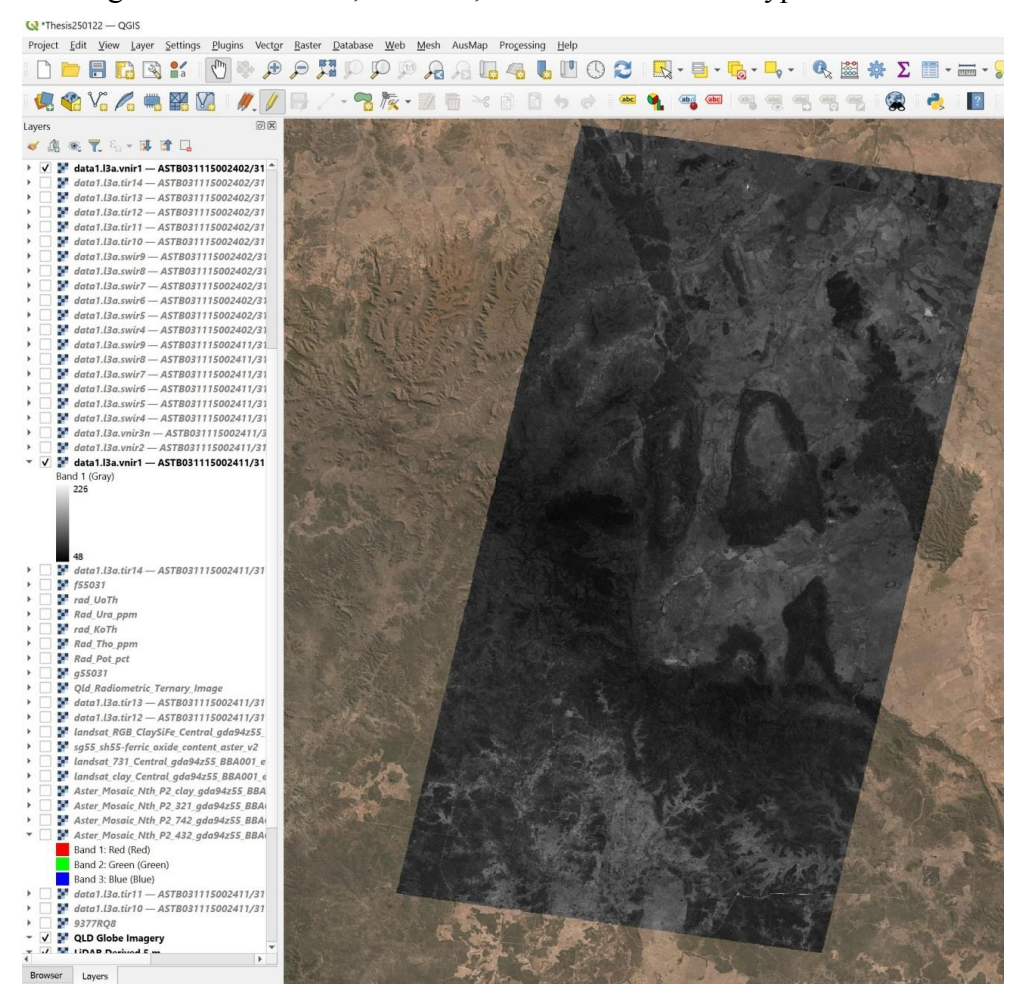


Figure II.3 ASTER Band 1 Visible Green Light Grey Scale Mosaic over Thesis area

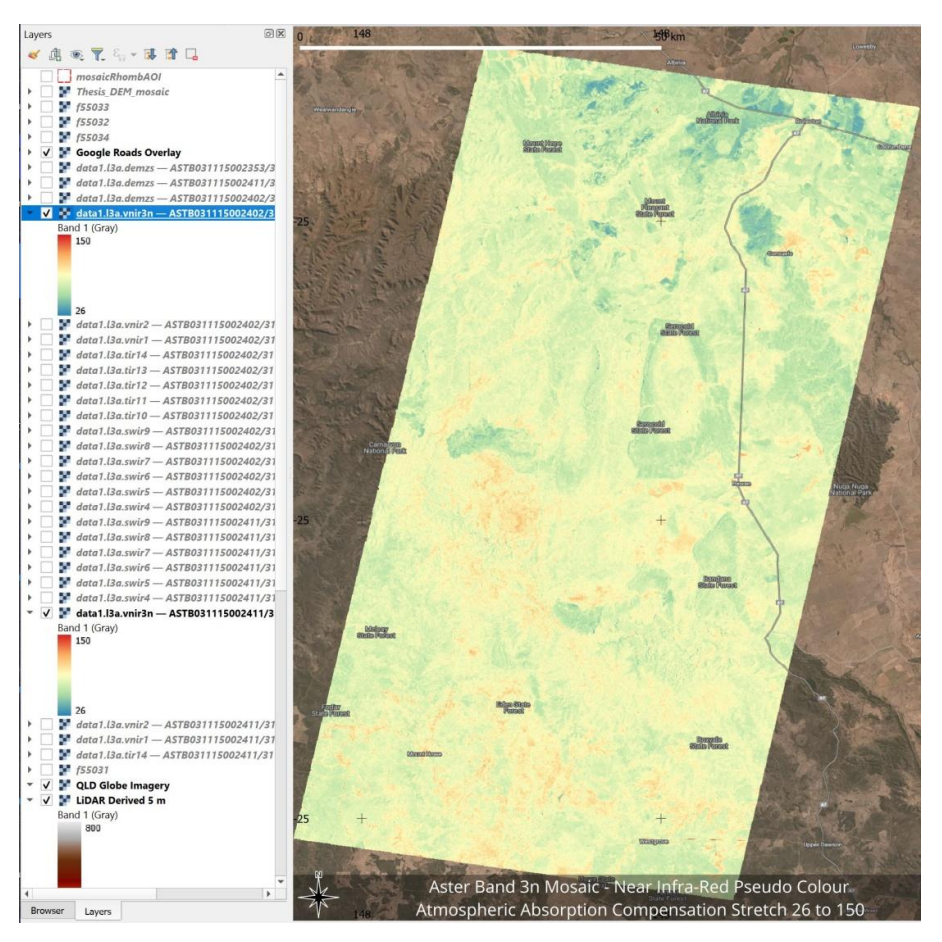


Figure II.4 Aster Band 3n Near Infra-Red Pseudo Colour Mosiac Corrected for Atmospheric Absortion

The pseudo colour mosaic of the near infra-red Band3n in figure 11.4 is corrected for atmospheric absorption by stretching the top tile to the darkest pixel and repeating values for the lower tile. See original thesis processing for a more detailed explanation (section 7.0 Data Processing, Dark Pixel Subtraction and Data Stretch). These two processes were combined and has a secondary effect of reducing the tiling effect or abrupt data change across the mosaic at tile boundaries. Low values are displayed as blue with hotter/higher values displayed as red.

The CSIRO has put together a series of Australia wide maps and suggested ratios from the ASTER data set which highlight various minerals based on their reflective or absorption properties for various ASTER bands. This has been extended to include the equivalent band ratios from this current study for Sentinel-2A, Landsat 8/9 and the hyperspectral Hyperion-EO1 satellites (see table 2.2 below).

Mineral Proxy Ratios	ASTER	Sentinel-2	Landsat 5/8/9	Hyperion EO-1	Reference
Iron Minerals					
Ferric Fe	B2/B1	B4/B3	B3/B1, B4/B3	B23/B13	Rowan CSIRO
Ferrous Iron	(B5/B3 + B1/B2)	(B3+B12)/(B4+B8),B12/B8+B3/B4	B5/B4, (B3+B7)/(B4+B5)		Rowan , Kalinowski & Olive, Carvalho
Laterite	B4/B5	B11/B12			Bierwith, Kalinowski
Gossan	B4/B2	B11/B4	B4/B2		Volesky, Kalinowski
Ferrous Silicates (Cu/Au Alteration)	B5/B4	B12/B11	B6/B5		CSIRO, Kalinowsski, Osinowo
Iron Oxides	B4/B3	(B4-B2)/B4+B2), B11/B8	B4/B2	B36/B9	CSIRO, Kalinowski, Ahmed, Vincent, NASA
Granite Type Oxidation Index	(B2/B1)/(B5/B3+B1/B2)	(B4/B3)/((B12/B8)+(B3/B4))	(B3/B1)/(B5/B4)		Proposed Chappell&White 1974/2001
Carbonates/ Mafic Minerals					
Carbonate/Chlorite/Epidote	(B7+B9)				Rowan
Epidote/ Chlorite/Amphibole	(B6+B9)/B8				CSIRO
Amphibole/MgOH	(B6+B9)/B8				Hewson
Amphibole	B6/B8				Bierwith
Dolomite	(B6+B8)/B7				Rowan, USGS
Carbonate	B13/B14				Bierwith, CSIRO, Nimoyima
Silicate Phyllic Alteration Minerals					
Sericite/Muscovite/Illite/Smectite	(B5+B7)/B6	B11/B12			Rowan, Hewson, Kalinowski
Alunite/Kaolinite/Pyrophyllite	(B4+B6)/B5				Rowan, USGS
Phengitic	B5/B6				Hewson
Muscovite	B7/B6				Hewson
Kaolinite	87/85				Hewson
Clay	(B5xB7)/(B6xB6)	B11/B12	B6/B7	B188/B185, (B134xB138)/(B148xB148)	Bierwith, Ahmed, Vincent, Bouzidi
Hydrothermal Alteration	84/85	B4/B2+B6/B11+B11/B12	B4/B2+B6/B5+B6/B7		Volesky, Sabin
Host Rock	B5/B6				Volesky
Silica Minerals					02177270
Quartx rich rocks	B14/B12				Rowan
Silica Index	(B11xB11)/B10/B12	B11/B4	B5/B4	B207/B205	Bierwith, Vincent, NASA
Basic Degree index (gnt,cpx,epi,chl)	B12/B13				Bierwith, CSIRO
SiO2	B13/B12				Palomera
Siliceous rocks	(B11xB11)/(B10/B12)			B26/B20, B207/B205	Nimoyima, Vincent, NASA
Silica	B11/B10				CSIRO
Silca	B11/B12				CSIRO
Silca	B13/B10				CSIRO
Lithium Minerals					
Spodumene		B1/B3			Cardosa-Fernandes
Petalite		B7/B6			Cardosa-Fernandes
Petalite		B13, B14			Cardosa-Fernandes
Vegetation					
NDVI	(B3-B2)/(B3+B2	(B8-B4)/(B8+B4)	(B4-B3)/B4+B3)		USGS,
Vegetation	B3/B2	88/84			USGS, Kalinowski

Table II.2 Mineral Band Ratios modified from CSIRO, Kalinowski et al for ASTER, Sentinel-2A, Landsat 8/9&Hyperion EO-1 The following figures show spectral response of the studied Satellite Platforms against generic Minerology/Vegetation using the USGS Spectral Viewer software for the satellites used in this study.

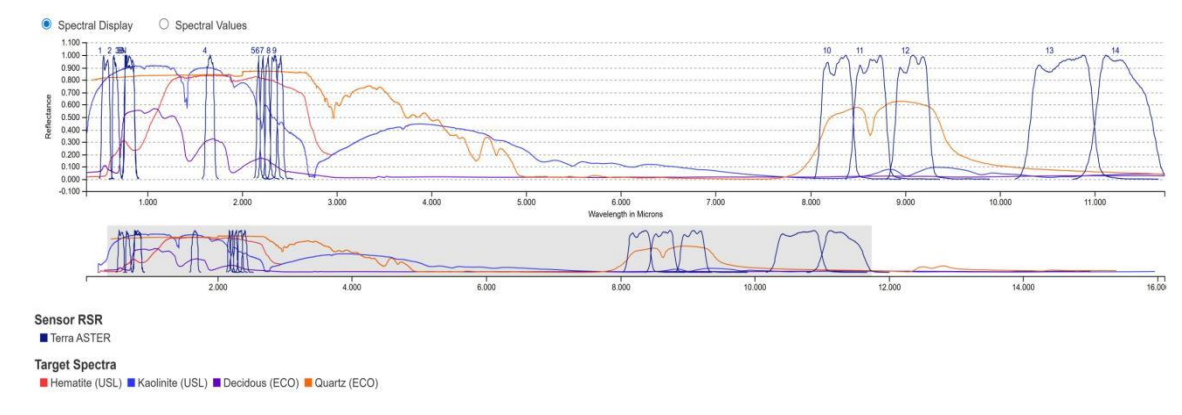


Figure II.5 Spectral Response of ASTER Data with Target Minerology/Vegetation

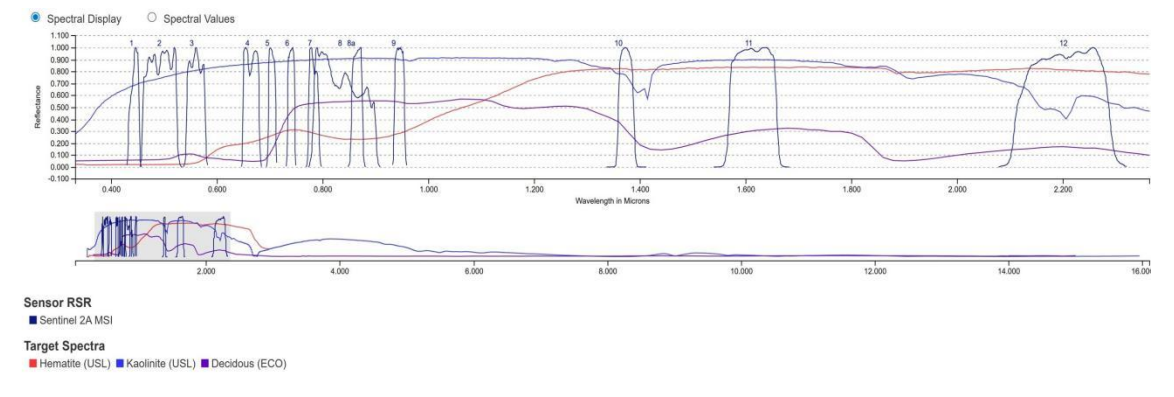


Figure II.6 Spectral Response of Sentinel-2A Data with Target Minerology/Vegetation

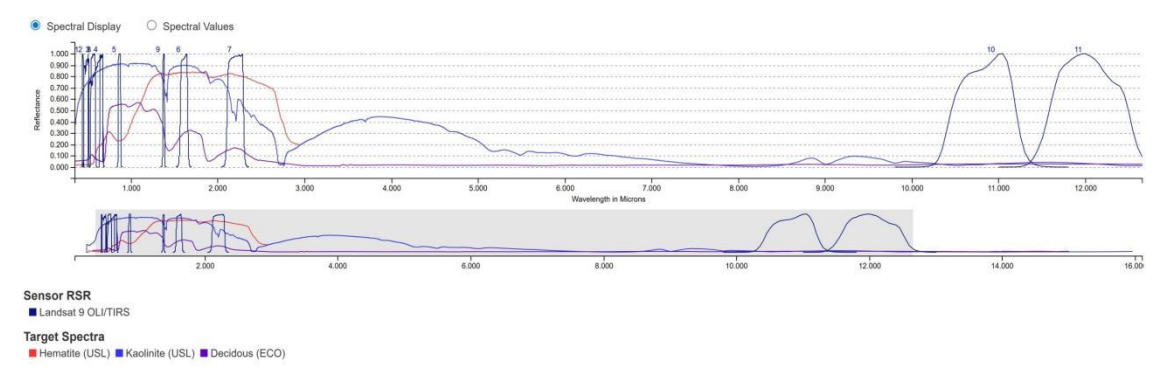


Figure II.7 Spectral Response of Landsat 8/9 OLI Data with Target Minerology/Vegetation

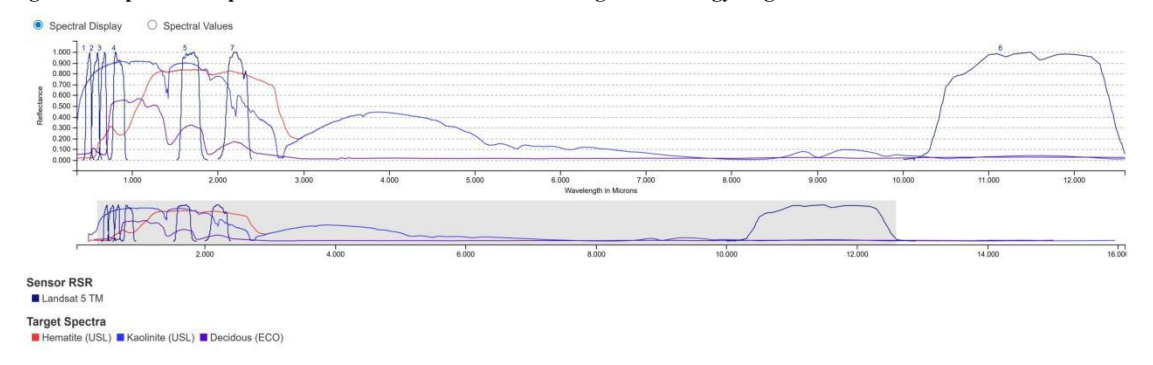


Figure II.8 Spectral Response of Landsat 5 TM Data with Target Minerology/Vegetation

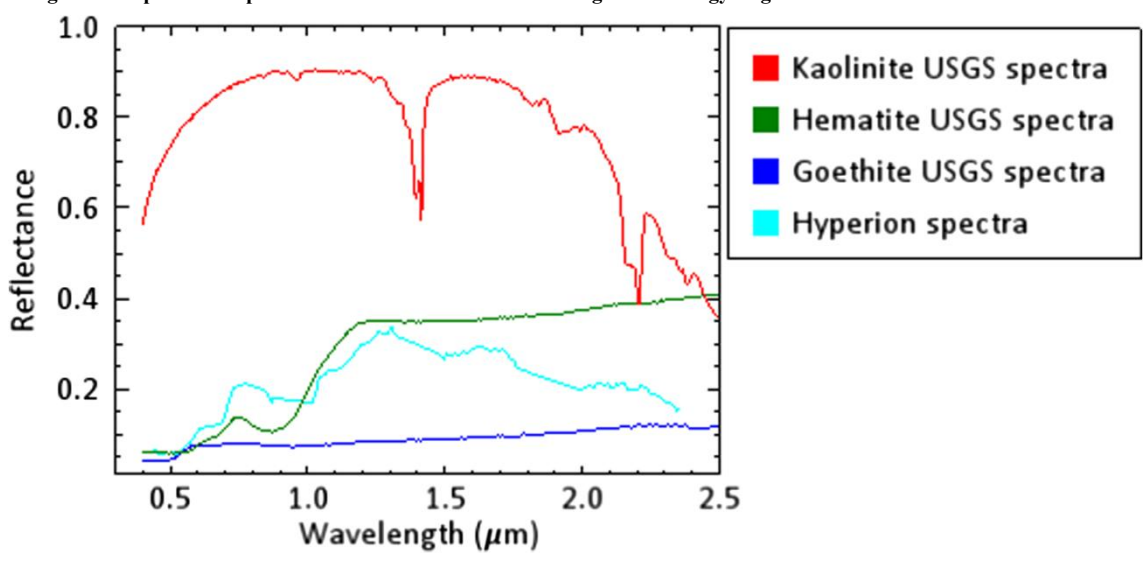


Figure II.9 Spectral Response of Hyperion EO-1 Hyperspectral Satellite Data with Target Minerology/Vegetation

II.3 Sentinel-2A Satellite Data

The Sentinel-2A data is part of the European Space Agency Copernicus

Program with the data freely available to the public and can be downloaded here; https://browser.dataspace.copernicus.eu/

A superior data set resolution wise with 10m resolution for the VNIR bands) and in size covering 110x110 kms compared to the ASTER tile size of 60x 60 kms. It does how ever lack the important thermal bands of ASTER and the Landsat 5 and Landsat 9.

II.4 Landsat 9 OLI

The Landsat 9 satellite data is the latest version of the USGS satellite with improved resolution down to 15m over the Landsat 5 30m pixels. It also possesses a second thermal band covering a similar range to the older Band 6 essentially dividing it in two (see figures II-7 and II.8) the zone between 10 and 13 microns. This data along with the legacy satellites and the Hyperion EO-1 hyperspectral data is available free of charge at the USGS Earth Explorer website here: https://earthexplorer.usgs.gov

II.5 Hyperion EO-1 Hyperspectral Data

The Hyperion EO-1 data set is comprised of some 242 spectral bands of 10 nanometer resolution compared to the usual 100m+ bandwidth of the other satellites in this study, for a higher fidelity approach at targeting the various emission and absorption peaks and troughs for various mineral responses (see figures II.5 to II.9 above). This data set however suffers from signal to noise issues due to it's smaller bandwidth and also a lack of coverage with only 2 relevant data strips over the study area. The Hyperion EO-1 data is included mainly as a comparison to what additional information can be gleaned from the higher fidelity targeting over the more traditional satellite bandwidths.

Discontinued in the early 2000's the hyperspectral data was a proof of concept platform which paved the way for a host of modern commercial hyperspectral satellite such as those offered by Esper Satellite Co (website here: https://www.espersatellites.co) which continue to launch newer and improved satellites as recently as Sept 2025.

II.6 S/I Granite Type from Fe Oxidation Index

In 1974 Chappell and White proposed a scheme of dividing granites into S-type (sedimentary derived) and I-type (igneous derived) based on the rocks that

were partially melted by the upwelling magma. Using the ratio of the more oxidised Fe minerals to the less oxidised Fe minerals from mapping and geochemical analysis of rock samples from the SE corner of Australia from Canbarra ACT to Lakes Entrance Victoria, they were able to draw an I/S demarcation line with the ratio of 0.31 FeO3/FeO2 line seperating the more oxidised granites to the east from the lesser oxidised granites to the west. The theory was that partial melting of the more carbon rich sedimentary rocks resulted in more Sn/W deposits forming in S-type granites with the more reduced igneous I-type granites resulting in more Cu/Mo deposits east of the line. This schema was widely adopted and in a paper 25 years later after more studies by Chappell and White and others in the Lachlan Fold Belt, the earlier work was substantiated in a follow up paper by the authors, "Two Contrasting Granite types: 25 years later". A further subdivision of the I-type granites into high and low temperature derived batholiths was also proposed. This I/S line is shown below superimposed on modern Landsat 9 satellite imagery. According to the table of Band Proxies above in TableII.2 it was investigated whether this I/S line could be recreated using Satellite imagery band ratios for calculating mineral proxies of Ferric Iron (Fe03) and the less oxidised Ferrous Iron (FeO2). After trying ASTER and Sentinel data with limited success it was eventually reproduced using the more recent Landsat 9 OLI data shown in figure II.10. The results were distorted by changing vegetation coverage across the area with it's high reflectivity in the NIR bands also used for the Fe mineral proxies thus requiring the generation of a vegetation mask to exclude these areas. The vegetation mask was easily created using an NDVI ratio of NIR to Visible red light showing higher values for more vigourous vegetated areas. While this ratio was no where near 0.31 Ferric to Ferrous Fe, it is proposed it could be used to broadly classify green field exploration areas into more and less oxidised regions which could in turn be used to guide exploration for one mineral type over another, so concentrate any Cu/Au/Mo exploration in the more oxidised areas with any Sn/W/Li exploration in the more S-type regions. There are of course lots of caveates and overlap between the S/I type areas and the need to calibrate the areas to detailed assay data from drilling, field mapping and lab work.

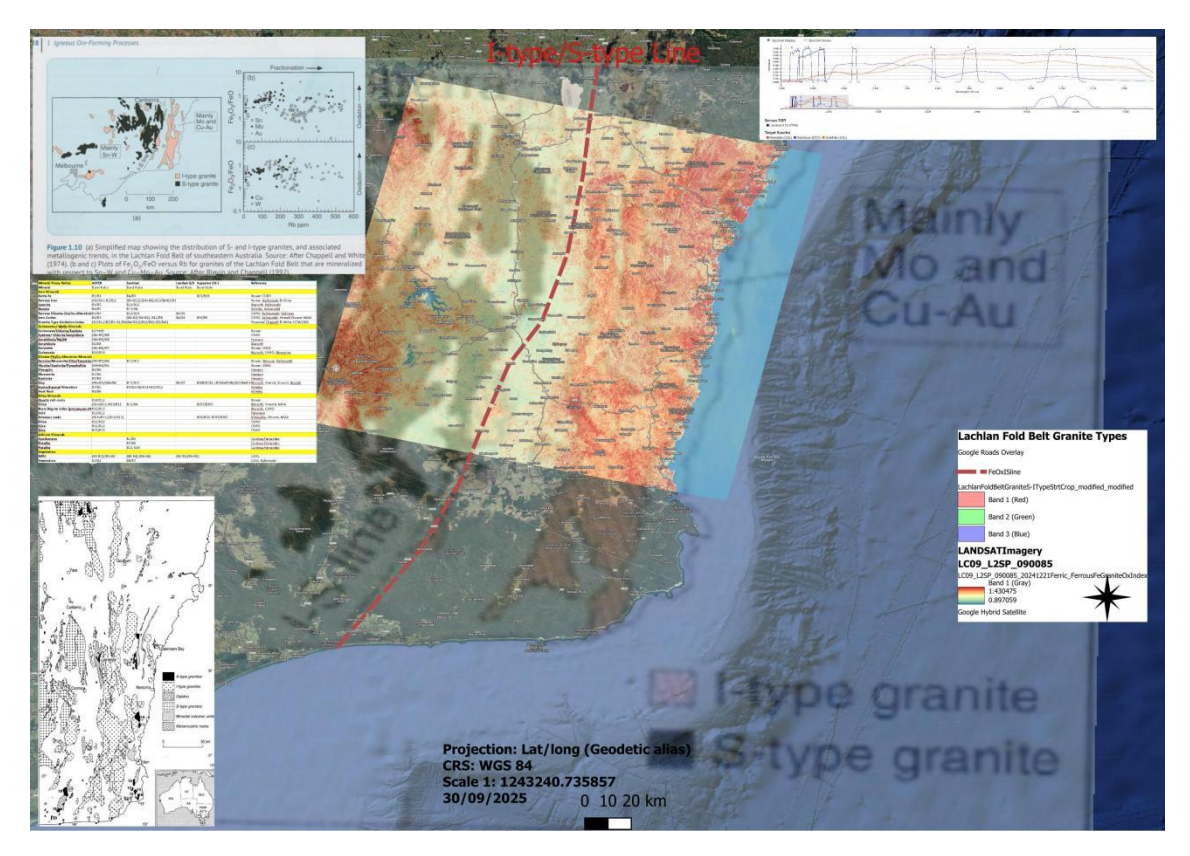


Figure II.10 Proposed Granite Fe Oxidation Index from Chappell & White 1974, 2001. Red = Higher Oxidation ratio

While the best result was derived from the Landsat 9 data which is corrected for atmospheric absorption. The Sentinel-2A data also seemed to be adaquately corrected however the ASTER data as downloaded seemed to only be partial corrected for atmospheric absorption and a further Dark Pixel Subtraction step had to be processed in order to get the correct West to East increasing oxidation trend (see Thesis Part I for dark pixel processing step)as mapped by Chappell and White et al.

Bibliography

E.A. Beaumont and N.H. Foster, (1992). *Remote Sensing*. Treatise of Petroleum Geology Reprint Series, No. 19, American Association of Petroleum Geologists.

H. Blatt, G. Middleton and R. Murray, (1980). *Origin of Sedimentary Rocks*. Prentice-Hall Inc.

K. Watkins and R.D. Regan, (1983). *Remote Sensing*. Geophysics Reprint Series, No.3, Society of Exploration Geophysicists.

ERA Maptec Australia, (1995). Structural Interpretation of Aeromagnetic and Satellite Imagery over ATP 267P/577P in the Eromanga Basin, South West Queeensland, Unpublished.

References

- T.E. Avery, and G.L. Berlin, (1992). *Fundamentals of Remote Sensing and Airphoto Interpretation Fifth Edition*. pp 405-466, Macmillan Publishing Company, where.
- J.C. Baker, C.R. Fielding et al, (1993). *Permian Evolution of Sandstone Composition in a Complex Back-Arc Extensional to Foreland Basin: The Bowen Basin, Eastern Australia*. Department of Earth Sciences, The University of Queensland. Journal of Sedimentary Petrology, Volume 63, No 5.
- P.E. Balfe, (1982). *Permian Stratigraphy of the Springsure Arcturus Downs Area*. Queensland Government Mining Journal.
- L. Cronin, (1997). Key Guide to Australian Trees, Reed Books, Australia.
- Z. Berger, (1994). Satellite Hydrocarbon Exploration. Springer-Verlag.
- R.S. Brown et al, (1983). Recent Exploration and Petroleum Discoveries in the Denison Trough, Queensland. APEA Journal, pp120-135.
- R.J. Chorley et al, (1972). *Spatial Analysis in Geomorphology*. British Geomorphological Research Group, Harper and Row Publishers.
- J.J. Draper, (1985). Summary of the Permian Stratigraphy of the Bowen Basin. Bowen Basin Coal Symposium, November 1985.
- L.G. Elliott, (1973). *Geology of the Springwood Area, Denison Trough, East Central Queensland*. Honours Geology Thesis, University of Queensland.
- L.G. Elliott, (1993). *Post Carboniferous Tectonic Evolution of Eastern Australia*, APEA Journal 1993, pp 215-236.

- C.R. Fielding et al, (1990). *Permian and Triassic Depositional Systems in the Bowen Basin*. Bowen Basin Symposium 1990.
- A.J. Glikson, (1997). *Mineral Mapping in the North Pilbara Craton*. Research Newsletter, Australian Geological Survey Organisation, Number 26, May 1997.
- I.D. Goodwin, (1984). An Evaluation of the Application of Digitised 70mm Colour Infrared Aerial Photography to Vegetation Studies. Third Australasian Remote Sensing Conference Queensland, 1984.
- R.L. Hammond, (1988). *The Bowen Basin, Queensland, Australia: an Upper Crustal Extension Model for its Early History*. CSIRO Division of Geomechanics.
- C.L.Horsfall et al, (1986), *Visible, Near Infrared and Short-Wavelength Infrared Spectra of Rock and Soil Samples from a Gold Prospect at Bardoc W.* AMIRA Project 82/P168 Spectral Properties of Australian Terrain. CSIRO Institute of Energy and Earth Resources, Division of Mineral Physics and Minerology
- B.H. Johns, and C.R. Fielding, (1993). *Reservoir Potential of the Catherine Sandstone, Denison Trough, East Central Queensland.* APEA Journal 1993.
- J.P. Le Roux and B.G. Jones, (1994). *Lithostratigraphy and Depositional Environment of the Permian Nowra Sandstone in the Southwestern Sydney Basin, Australia*. Australian Journal of Earth Sciences, Volume 41, pp??.
- S. McLoughlin, (1988). *Geology of the Inglis Dome, Denison Trough, Central Queensland*. Paper, Department of Geology, University of Queensland.
- R.G. Mollan et al, (1969). *Geology of the Springsure 1:250,000 Sheet Area, Queensland*. Geological Survey of Queensland.
- C.G. Murray, (1990). *Tectonic Evolution and Metallogenesis of the Bowen Basin*. Bowen Basin Symposium.

- T.W. Offield et al, (1983). Structure Mapping of Enhanced Landsat Images of Southern Brazil: Tectonic control of Mineralisation and Speculations on Metallogeny,
- C.I. Pattison et al, (1988). *The Intrusive History of the Northern Bowen Basin Tectonic Implications*. Queensland Institute of Technology, CSIRO Division of Geomatics
- C.I. Pattison, R.L.Hamond et al, (1986). *The Intrusive History of the Northern Bowen Basin Tectonic Implications*. Queensland Institute of Technology, CSIRO Division of Geomechanics.
- A.J. Richards and A.K. Milne, (1984). *Mapping Fire Burns and Vegetation Regeneration by Classification of Multitemporal Landsat MSS Image Data*. Third Australasian Remote Sensing Conference Queensland.
- V. Singhroy, (1996). *Environmental and Geological Site Characterisation in Vegetated Areas: Image Enhancement Guidelines*. ASTM STP 1279, American Society for Testing and Materials, pp.5-16.
- P.J. Stanmore and R.J. Cornect, (1993). *Dunellen-1Well Proposal*. Unpublished Company Report, Santos Ltd.
- A.H. Strahler and X. Li, (1984). *Spatial/Spectral Modelling of Conifer Forest Reflectance*. Third Australasian Remote Sensing Conference Queensland.
- G R Taylor et al, (1991). A Methodology for the Interpretation of Landsat Thematic Mapper Imagery in the Mapping of Sedimentary Basins", Unpublished.
- X. XXXXX, "Remote Sensing Principles and Interpretation, Chapter 5; Thermal Infrared Images", pp. 135-173.
- J.B. Wolley, (1943). *Report on the Geology of the Carnarvon Area*. Geological Report 9 for Shell (Queensland) Development Pty Ltd.

V. Ziolkowski and R. Taylor, (1985). *Regional Structure of the North Denison Trough*. Bowen Basin Coal Symposium.

Glossary of TermsABC Map: A seismic stratigraphic term where A B / C represents a seismically definable sequence's A - Top Boundary Expression, B - Bottom Boundary Expression written over the C - Internal Configuration. ABC maps are used to define seismically definable depositional packages.

Aldebaran Formation: A Permian aged fluvial sandstone dominated reservoir rock of the Denison Trough. The top of the formation forms a regional (at times) angular unconformity with the transitional Freitag formation. Found in out crop with a characteristic orange barked gum tree (Eucalyptus melliodora) as ground cover, which can be used to map the formation in between outcrop.

Angular Field of View: The angle subtended between the imaging sensor and the edges of the image's ground swath or left to right edges.

Asymmetric Cross Stream Profile: Possibly indicating sudden neotectonic movement in the stream valley.

Bandanna Formation: A coaly facies marking at the top of the Permian section in the Central Denison Trough

Basement Warp Structure: A topographic feature resulting from the drape or uplift of the surface by an underlying metamorphic basement structure such as a horst block.

Bifurcation Ratio: Used in drainage studies to indicate the ratio of the number of streams of one order with another, i.e. # 1st order streams / # 2nd order streams.

Catherine Sandstone: Permian aged coastal and inner marine shelf sandstones, reservoir quality of the Denison Trough. Densely populated by white spotted gum (Eucalyptus maculata) ground cover.

Clay Ratio Image: The image formed by dividing the same pixels from band 5(near IR) by band 7(far IR) in Landsat TM data. Usually indicative of clay content in the pixels ground cover.

Clematis Sandstone: A Triassic aged highly erosion resistant predominantly sandstone facies, which forms many of the ridges and high ground of the Central Denison Trough. The Clematis Sandstone bounds the "A" shaped Rewan syncline where it is preserved and densely treed.

Clustering: The grouping together of pixels in an image with similar density values. Clustering can be either hierarchical or non hierarchical. Context (Co-Occurrence)

Classification: A statistical cluster analysis perform on a spectrally classified image which takes into account the density values of the surrounding pixels in a 3x3 or 5x5 pixel (usually) kernel as opposed to a spectral classification which operates on a single pixel. The resulting classification results in colour assigning like areas or classes of an image.

Contrast Stretch: Usually expressed in terms of a percentage such as a 1-99% stretch, it increases the dynamic range of an image by clipping pixel density values below 1% and above 99% and redistributes the remainder over the full display range, 0 to 255 for 8 bit data. This results in a sharper image displaying more detail.

$$Dn'(x,y) = a Dn(x,y) + b$$

where Dn represents Pixel Density Value, a and b are coefficients chosen to expand Dn range over full dynamic range of data size

Covariance: The cross correlation of two pixels or classes of pixels. COVAR = 1/n * SUM {(SDEVj - MEAN) * (SDEVj+1 - MEAN)} Provides a measure of interband correlation

Convexity: Curvature of the ground. The second horizontal derivative of the digital terrain model (altitude).

Dark Pixel Subtraction: A processing step, which compensates for differential atmospheric absorption of data bands of differing wavelength. The darkest pixel's value in the entire image is subtracted from all pixels in that band, shifting its histogram to the left. The value is highest for blue light and reduces as the wavelength for each successive band increases. Dark Pixel subtraction is performed prior to the generation of band ratios and principle component analysis.

Dendritic Drainage Pattern: A branching tree like drainage pattern observed in creeks cutting across homogenous soil or country rocks which has minimal structural control. The closer the spacing of the branches, the softer the material being eroded.

Digital Terrain Model (DTM): Also called digital elevation model (DEM), is a digital grid of an area's elevation usually derived from digitising elevation contours or created from radar interferometry or airphoto stereo pairs.

Erosion: From the Latin "erodere" to gnaw or eat away. The processes that wear away the Earth's surface.

ERS-1 & 2: Two synthetic aperture radar satellites launched by the European Space Agency in 1991 and 1995. The acronym stands for "European Remote Sensing Satellite". Each satellite collects one band of 30x30m imagery.

Ferric Oxide Ratio: The ratio of Landsat TM band 3 / band 1. Measures ferric oxide content of ground cover due to its high reflectance in bands 1 (visible blue) and high absorption in band 3 (visible red).

Ferrous Minerals Ratio: The ratio of Landsat TM band 5 / band 4. Measures ferrous minerals content of ground cover.

Freitag Formation: A Permian aged transitional siltstone/Sandstone formation between the fluvial sandstone dominated Aldebaran Formation and the marine siltstone dominated Ingelara Formation. The formation top is a maximum flooding surface and the Freitag sandstone where present make excellent reservoirs.

Georeferencing: Rectification of imagery to fit a specific datum and projection. Usually requiring a minimum of four pixels, line and x, y ground control point pairs.

Ground Cover Texture: The texture units comprising a ground cover type, ie eucalypt and pine for Dry Sclerophyll Forest.

Ground Truthing: The field investigation of ground cover types, usually to confirm unsupervised classifications of imagery made in the office.

Hypsometric Curve: The cumulative frequency plot of the altitude.

Error Matrix: Also known as Confusion Matrix, is a method of accuracy assessment for classified images where the image is sampled and a table prepared showing the correctly classified areas and the errors of omission or exclusion and commission or inclusion. For example if an area of sandstone is classified as shale, it is an error of omission in a sandstone table with shale classified as sandstone a commission error in the same table.

Geomorphology: The study of the form and deformation of the landscape with reference to its neotectonic history and environmental setting.

Himalayas: A mountain range stretching from Pakistan to China resulting from the collision of the Indian Subcontinent Plate with Asia. Contains Mt Everest and many of the world's highest peaks.

Hierarchical Clustering: The similarity of an image cluster is evaluated using a distance measure between clusters. The process is iterative so that from an initial number of groupings, clusters are merged, usually according to the minimum distance between their centre of gravities, until a threshold number of classes are reached.

Index of Articulation or Dissection: The (average altitude - lowest altitude) divided by (maximum altitude - lowest altitude).

Ingelara Formation: A Permian aged marine mudstone of the Denison Trough. An easily eroded formation with a typical burr, spear grass and sparsely wooded black Iron Bark gum tree (Eucalyptus siderphloia) ground cover.

JERS-1: A synthetic aperture radar satellite launched by Japan in 1992, standing for The Japanese Earth Resources Satellite.

Landsat TM: Landsat Thematic Mapper, referring to the Landsat 4, 5 and (the lost) 6 satellites or their imagery. A Landsat Tm Scene covers 185x170 km at 30x30m pixel resolution and is comprised of 6 reflected bands ranging from visible blue to the mid infrared and one 120x120m pixel resolution band of emitted thermal infrared. All seven bands are recorded as 8 bit data ranging from 0 to 255 in density value.

Laterization: The dissolving of silicate under conditions of heavy leaching with the accumulation of insoluble minerals such as alumina or ferric oxide in the upper part of the weathering profile forming a weathering crust.

Lineament: Large-scale linear features observed on the earth's surface usually resulting from reactivated basement faults or zones of crustal weakness. A lineament analysis may involve the plotting of lineament vectors on a Rose diagram, which can relate to fracture directions observed in subsurface well cores.

Mantuan Formation: A fluvio-deltaic sandstone and siltstone sequence bound at the top by the Matuan Productus Beds. The top of the formation is a semi regional flooding surface containing the shore-face Productus fossil deposits in outcrop and a coaly facies starting from the northern edge of the study area becoming better developed in a north westerly direction. The Permian aged Mantuan Formation Sandstone is a marginal hydrocarbon reservoir in the central Denison trough.

Mass Movement: The down-slope migration of rock waste and the displacement of bedrock

Maximum Likelihood Classifier: A commonly used classification method in which a pixel is placed in the class in which it's position on a probability density plot for a

band, has the highest corresponding value or in statistical terms, the highest posterior probability of belonging to. It has various strengths and weaknesses but gives poor results in cases of strong correlation between bands or the ground truth data is homogenous. The likelihood can equal the Euclidean distance in the case of a symmetric variance-covariance matrix.

Minimum Distance Classifier: Used to classify the pixels in an image to clusters which minimise an individual pixel values distance to the central value of a class in multifeature space. The distance is defined as an index of similarity so that the minimum distance corresponds to the maximum similarity. A common distance type used for data with little correlation between bands is Euclidean distance.

 $Dt = sqrt\{(pixel value - class mean)t \times (pixel value - class mean)\}$

Mixel: The term used to describe the mixed origins resulting in the averaged reflectance value for an image pixel. This is because of the variety of ground cover present in the area covered (i.e. 80x80m for MSS) in some images.

MSS: Multispectral Scanner, referring to electro optical scanner used in Landsats 1,2 & 3 or the satellites and their imagery. An MSS scene covers 185x170km of 79x59m (usually sampled to 80x80m) pixel resolution. The data was recorded at 64 levels of intensity and is comprised of four reflected bands spanning visible green (band 4) to near infrared (band 7).

Multitemporal Classification: As the name implies, involves the use of a repeat data set in a classification as if they were simply additional data bands. This method while more expensive is ideal for change detection in an area. It also allows for the use of much lower order components when processing the image trough a principal component analysis. This process is mentioned here only out of completeness as having only one image for the study area did not allow it to be carried out.

Nadir: The line of traverse on the ground directly below a satellite or aircraft.

NDVI: Normalised Difference Vegetation Index is used to monitor vegetation vigour, with light tones indicating dense vegetation and biomass. The denominator

compensates for changing illumination conditions. NDVI= (near IR - red)/(nearIR + red) for Landsat TM use band 4 for nearIR and band 3 for red.

Nearest Neighbour: A method of resampling during image rectification or subsampling where to density value of the closest old pixel to the new transformed pixel is used. Gives the highest spectral integrity to the new pixel but can result in repeat pixels and a chunky appearance in the new image.

Nominal Data: Class ID-numbers are nominal data as opposed to the actual 0 to 255 density values of the pixels that where grouped into classes 1 to n.

Non-Hierarchical Clustering: An initial number of clusters are chosen at the start of the processing. The density values of the pixels within each cluster are compared according to pre-specified parameters or distance and are then reassigned to more appropriate clusters of higher separability.

Parallelepiped Classifier: Starts with the line dividing each axis in multispectral feature space, i.e. the x,y,z axis for a three band classification, then assigns a minimum and maximum density value in each axis for each cluster. The result viewed schematically for a three band case would resemble a series of boxes, one for each cluster with the sides of each box having the measurements of the max - min value of the cluster's pixels in each band. Pixel: The smallest element or cell of an image, having a numeric or density value from 0 to 255 for 8 bit data Range Land: Rough, hilly forested terrain.

Peawaddy Formation: A fluvio-lacturine predominantly siltstone sequence which progrades across the Central Denison Trough area in an easterly manner. The top of the formation forms a sometimes angular sequence boundary with the more sand prone Mantuan Formation. Typically possessing spear grass and black Iron Bark gum tree (Eucalyptus siderophloia) sparse ground cover.

Principal Component Analysis: A principal component analysis involves performing a cluster analysis on an image in much the same way as a

spectral analysis only that the data axis is rotated so that the new x or first principle axis PC1 is along the line of best fit for the data. This component contains the most information or variation. Each additional component is oriented orthogonal to the first in a sucessive order of variation and information content.

Relief Ratio: For a drainage basin, the Total Basin Relief (summit to basin mouth) divided by the Total Basin Length.

Scarplets: Very low relief scarps (cliffs) indicating recent movement of up to a few meters.

Sclerophyll Forest: Australian native (eucalypt dominated) open forest, either wet or dry.

Slash Pine: Pinus Elliotti an introduced conifer common in pine plantations in Queensland, taking about 30 years to reach maturity. Favoured for its straight nongnarly trunk, which makes it ideal for soft wood timber.

Spatial Resolution: The actual ground coverage for an individual pixel element in an image, ie 30x30m for Landsat TM data, 79x59m (resampled to 80x80m) for MSS imagery.

Spectral Resolution: The frequency bandwidth of a sensors particular channel, i.e. 0.5 to 0.6 micrometers for visible green light in band 4 for MSS data, expressed in wavelength.

SPOT: The satellites or their imagery recorded by the French System Pour l'Observation de la Terre platforms. SPOT 1& 2 record a monochromatic 10x10m band and three 20x20m spectral bands, visible green, red and a near infrared. The imagery is recorded by a pushbroom charged couple device array of 3000 sensors for spectral channels and 6000 for the panchromatic band. This alleviates the side to side motion of the whisk broom electro optical devices used on the Landsat satellites, eliminating scan line noise or streaking.

Structural Control: Influence of the landform development by the underlying geologic structure.

Subsequent Stream: One, which is formed along zones of structural or lithological weakness.

Supervised Classification: A spectral or context classification of an image utilising predetermined spectral signatures for specific ground cover training sites.

Texture: The spatial distribution of pixel density values caused by similar distribution of reflecting ground cover. A measure of surface roughness. Smooth texture could imply cropland or a body of water while coarse texture could indicate a forest or lava flow.

Temporal Resolution: The time required for repeat measurements of an area by a sensor, i.e. 16 days for Landsat TM satellites. Tone: Reflective characteristics of an area in an image, ie dark or light.

Thermal Capacity: The ability of a material to store heat. The number of calories required to raise one gram of the material one degree celcius.

Thermal Diffusivity: Determines the rate at which temperature changes within a material. The ability of a material to transfer heat from the surface during the day to the interior and back to the surface at night.

Thermal Inertia: A measure of the thermal response of a material to change in temperature. Mainly dependent on the density of the material.

Transverse Stream: One, which cuts across the body of a Basement Warp Structure.

Unsupervised Classification: A spectral or context classification performed on a purely statistical basis of a cluster analysis of like pixel density values in an image.

Variance: The autocorrelation of a pixel or pixel class, measuring its periodicity within an image line. VAR=1/n x SUM sqrt [SDEVj - MEAN]

Appendix A - Rose Diagrams and Stereo Plots from Numbered Outcrop

Appendix B - Selected Airphotos from Study Area

Appendix C - Selected Structural and Vegetation Photos of Study Area

Appendix D - Well Logs from Study Area

Appendix E - Selected Satellite Imagery of Study Area

Appendix F - The Denison Trough Remote Sensing Study